



University of
Massachusetts
Amherst

Ordered phases in mesogen-containing polyurethanes/

Item Type	Dissertation (Open Access)
Authors	Stenhouse, Peter James
DOI	10.7275/c3z1-j288
Download date	2026-06-12 00:02:16
Link to Item	https://hdl.handle.net/20.500.14394/16938



312066008179106

ORDERED PHASES IN MESOGEN-CONTAINING POLYURETHANES

A Dissertation Presented

by

PETER JAMES STENHOUSE

Submitted to the Graduate School of the
University of Massachusetts in partial fulfillment
of the requirements for the degree of

DOCTOR OF PHILOSOPHY

February 1992

Department of Polymer Science and Engineering

© Copyright by Peter James Stenhouse 1992

All Rights Reserved

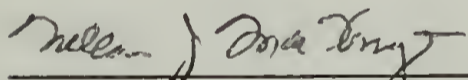
ORDERED PHASES IN MESOGEN-CONTAINING POLYURETHANES

A Dissertation Presented

by

PETER JAMES STENHOUSE

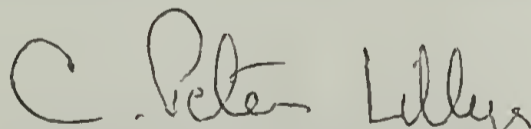
Approved as to style and content by:



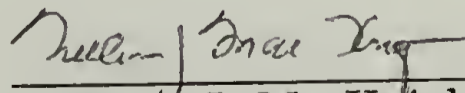
William J. MacKnight, Chair



Simon W. Kantor, Member



C. Peter Lillya, Member



William J. MacKnight,
Department Head
Polymer Science and Engineering

ACKNOWLEDGEMENTS

I would like to thank all of the colleagues, friends and family members who have helped make the task of obtaining a Ph.D. less difficult. I am especially indebted to my committee chairman, Professor William J. MacKnight, for his guidance and patience. My other committee members, Professors Simon W. Kantor and C. Peter Lillya, provided a great deal of valuable input.

The people who collaborated with me on this project – Enrique Vallés, Gerard Smyth, Steve Pollack, and Fotis Papadimitrakopoulos – helped considerably by discussing their ideas and listening to mine. My friends in Amherst and elsewhere – especially John and Brenda Reffner and Roberto Gregorius – provided emotional support and good advice when I needed them. Chris Salame of the PSE office was extremely helpful during my final year at UMass. The Center for UMass - Industry Research in Polymers (CUMIRP) provided funding for this research project.

Finally, I would like to thank my sisters, Elizabeth Stenhouse, Nancy Bieringer and Janet Polimer, and my parents, Robert and Dorothy Stenhouse, who have given me love and support for the past thirty years.

ABSTRACT

ORDERED PHASES IN MESOGEN-CONTAINING POLYURETHANES

FEBRUARY 1992

PETER JAMES STENHOUSE, B.A., BOSTON UNIVERSITY

Ph.D., UNIVERSITY OF MASSACHUSETTS

Directed by: Professor William J. MacKnight

Polyurethanes containing the biphenyl mesogen were synthesized and characterized by differential scanning calorimetry, wide-angle X-ray scattering and polarizing optical microscopy. One polyurethane (D6T24), which has an asymmetric structure, displays a monotropic smectic mesophase. The crystallization and mesophase-forming behavior of D6T24 is highly dependent on molecular weight. Another polyurethane (D6T26), which has a symmetrical structure, also displays a monotropic smectic mesophase. Because the crystalline unit cells of D6T24 and D6T26 are significantly different, combining the two polyurethanes in copolymers and blends suppresses crystallization, and in some cases produces enantiotropic systems. Blends of D6T24 and D6T26 containing more than 30% D6T24 by weight, and a random copolymer containing 47% D6T24 repeat units and 53% D6T26 repeat units, form enantiotropic smectic mesophases which do not crystallize. Annealing at high temperatures appears to transform the blends into copolymers, probably by means of transurethanification reactions.

TABLE OF CONTENTS

ACKNOWLEDGEMENTS.....	iv
ABSTRACT.....	v
LIST OF FIGURES.....	viii
Chapter	
1. INTRODUCTION	1
1.1 Objectives.....	1
1.2 Dissertation Overview.....	1
1.3 Literature Review	2
1.3.1 The Liquid-Crystalline State.....	2
1.3.2 Liquid-Crystalline Polymers.....	6
1.3.3 Monotropic Liquid-Crystalline Polymers.....	7
1.3.4 Liquid-Crystalline Polyurethanes.....	11
1.4 Experimental Methods.....	14
1.4.1 Preparation of Polymers and Polymer Blends.....	14
1.4.1.1 Starting Materials	14
1.4.1.2 Synthesis	15
1.4.2 Polymer Characterization.....	15
References.....	21
2. BHHBP: A MESOGENIC DIOL.....	26
2.1 Introduction	26
2.2 Synthesis and Purification	27
2.3 Properties.....	27
References.....	29
3. D6T24 AND D6T26: MESOGENIC POLYURETHANES.....	31
3.1 Introduction	31
3.2 D6T24: An Asymmetric Mesogenic Polyurethane.....	34
3.2.1 Synthesis of D6T24	34

3.2.2	Crystalline and Liquid-Crystalline Phases	36
3.2.3	Kinetics of Crystallization and Mesophase Formation	38
3.3	D6T26: A Symmetrical Variant of D6T24.....	45
3.3.1	Motivation for Studying D6T26	45
3.3.2	Synthesis and Solution Properties.....	46
3.3.3	Crystalline and Liquid-Crystalline Phases	47
	References.....	67
4.	BLENDS AND COPOLYMERS OF D6T24 AND D6T26	68
4.1	Motivation for Preparing Blends and Copolymers	68
4.2	Blends of D6T24 and D6T26.....	69
4.2.1	Preparation of Blends	69
4.2.2	Properties of Blends.....	69
4.3	C47: A Random Copolymer of D6T24 and D6T26	74
4.3.1	Synthesis of C47	74
4.3.2	Properties of C47.....	75
4.4	Annealing Studies of Copolymers and Blends.....	75
	References.....	91
5.	CONCLUSIONS AND FUTURE WORK.....	92
	BIBLIOGRAPHY.....	94

LIST OF FIGURES

1.1	Structures of cholesterol benzoate (above) and cholesterol (below).....	17
1.2	Types of liquid-crystalline phases: a) nematic; b) cholesteric; c) smectic A; d) smectic C.....	18
1.3	Schematic representation of the DSC scans of a typical enantiotropic liquid-crystalline polymer	19
1.4	Schematic representation of the DSC scans of a typical monotropic liquid-crystalline polymer.....	20
2.1	Structure of BHHBP.....	26
3.1	Structure of D6T24.....	50
3.2	DSC scans (10 °C/min) of low molecular weight D6T24 after cooling from the isotropic melt at 10 °C/min: a) heating; b) cooling.....	51
3.3	Texture of low molecular weight D6T24 seen in the polarizing optical microscope after cooling to below 132 °C	52
3.4	WAXS diffraction pattern of high molecular weight D6T24 in the crystalline state.....	53
3.5	WAXS diffraction pattern of D6T24 fibers drawn from the isotropic melt at 178 °C, before thermal treatment	54
3.6	WAXS diffraction pattern of D6T24 melt-drawn fibers after annealing 16.5 h at 174 °C.....	55
3.7	DSC scans (10 °C/min) of high molecular weight D6T24 after cooling from isotropic melt at 10 °C/min: a) heating; b) cooling.....	56
3.8	Texture of D6T24 seen in the polarizing optical microscope after annealing at 150 °C.....	57
3.9	DSC heating scans of low molecular weight D6T24 at various rates: a) 10 °C/min; b) 1.0 °C/min; c) 0.5 °C/min; d) 0.2 °C/min	58

3.10	DSC heating scans of high molecular weight D6T24 at various rates: a) 10 °C/min; b) 1.0 °C/min; c) 0.5 °C/min; d) 0.2 °C/min.....	59
3.11	DSC scans (10 °C/min) of low molecular weight D6T24, cooled from the isotropic melt to various temperatures and then immediately reheated.....	60
3.12	Structures of D6T24 and D6T26.....	61
3.13	DSC scans (10 °C/min) of D6T26 after cooling at 10 °C/min from isotropic melt: a) heating; b) cooling	62
3.14	WAXS diffraction pattern of a melt-drawn fiber of D6T26 (150 °C).....	63
3.15	WAXS diffraction pattern of a melt-drawn fiber of D6T26 (23 °C).....	64
3.16	DSC scans (10 °C/min) of D6T26, cooled from the isotropic melt to various temperatures and then immediately reheated.....	65
3.17	DSC heating scans of D6T26 at various rates: a) 10 °C/min; b) 5 °C/min; c) 2 °C/min; d) 1 °C/min; e) 0.5 °C/min.....	66
4.1	WAXS diffraction pattern (23 °C) of B60, as precipitated from solution.....	79
4.2	DSC scans (10 °C/min) of B60 after precipitation from solution: a) first heating; b) first cooling; c) second heating.....	80
4.3	WAXS diffraction pattern of B60, heated to 220 °C and cooled at 10 °C/min to 23 °C	81
4.4	DSC scans of B40, heated and cooled repeatedly between 40 °C and 200 °C at 10 °C/min: a) first heating after precipitation from solution; b) second heating; c) fourth heating; d) eighth heating.....	82
4.5	DSC heating scans (10 °C/min) of blends of D6T24 and D6T26: a) pure D6T24; b) B80; c) B60; d) B40; e) B20; f) pure D6T26.....	83
4.6	DSC scans (10 °C/min) of C47 after cooling at 10 °C/min from the isotropic melt: a) heating; b) cooling	84

4.7	WAXS diffraction pattern (23 °C) of a melt-drawn fiber of C47, before thermal treatment.....	85
4.8	DSC heating scans (10 °C/min) of: a) C47, cooled from the isotropic melt at 10 °C/min; b) C47, annealed 6.5 hours at 120 °C; c) B60, cooled from the isotropic melt at 10 °C/min; d) B60, annealed 6.5 hours at 120 °C.....	86
4.9	WAXS diffraction pattern (23 °C) of a melt-drawn fiber of C47 after annealing for 6.5 hours at 120 °C.....	87
4.10	WAXS diffraction pattern (23 °C) of a melt-drawn fiber of B60, before thermal treatment.....	88
4.11	WAXS diffraction pattern (23 °C) of a melt-drawn fiber of B60 after annealing for 6.5 hours at 120 °C.....	89
4.12	DSC heating scan (10 °C/min) of B60 after annealing for 8 h at 180 °C followed by 6.5 h at 120 °C.....	90

CHAPTER 1

INTRODUCTION

1.1 Objectives

Liquid-crystalline polyurethanes are a relatively new and unexplored class of polymers. For reasons pertaining to the chemical instability of the urethane group, and to its tendency to form strong intermolecular attractions, the attainment of a liquid-crystalline phase in polyurethanes is difficult. However, liquid-crystalline polyurethanes may prove to be very important materials from a practical standpoint. Segmented polyurethanes whose hard domains are capable of forming liquid-crystalline phases may have unique and desirable properties. Moreover, the effect of strongly interacting groups on the ability of polymers to form liquid-crystalline phases is interesting to study from a theoretical standpoint. The primary goal of this research project is to conduct a thorough study of a series of liquid-crystalline polyurethanes. The emphasis is on the kinetics of crystallization and mesophase formation, and how these properties relate to chemical structure.

1.2 Dissertation Overview

Most of Chapter 1 consists of a literature review on topics relating to this research project: the liquid-crystalline state; liquid-crystalline polymers; monotropic liquid-crystalline polymers; and liquid-crystalline polyurethanes. The experimental methods used in the project are outlined at the end of the chapter. Chapter 2 discusses the mesogenic

diol BHHBP, itself a low molecular weight liquid crystal, which was used in the synthesis of the polyurethanes. Chapter 3 reports the synthesis and properties of two mesogenic polyurethanes, D6T24 and D6T26, whose chemical structures differ from one another only in the placement of a methyl group. Chapter 4 discusses the consequences of combining D6T24 and D6T26 in blends and copolymers. Chapter 5 summarizes the results of the preceding chapters and provides suggestions for further research.

1.3 Literature Review

1.3.1 The Liquid-Crystalline State

In 1888, Reitnitzer¹ discovered that cholesterol benzoate formed an intermediate phase as it passed from the solid crystalline state to the isotropic melt. At 145 °C, the solid melted to yield a turbid liquid, which gave way to the isotropic melt at 179 °C. The newly discovered phase was given the name "liquid crystal." The degree of order in a liquid-crystalline phase, also called a **mesophase**, is intermediate between that of a three-dimensional crystal and an isotropic liquid.

A great many liquid-crystalline compounds have been reported.²⁻¹⁵ Most liquid crystals are characterized by a high axial ratio (the ratio between the length and the width of the molecule) and a high degree of rigidity. There are also examples of disc-shaped¹⁶⁻²³ and bowl-shaped²⁴⁻²⁸ liquid crystals.

Liquid-crystalline phases can be attained in solution or in the bulk state. Liquid-crystalline phases in solution are called **lyotropic**. When the concentration of the solution is raised above a critical level,

geometric constraints force the solute molecules into an anisotropic arrangement. Liquid-crystalline phases in the bulk are called **thermotropic**. In a thermotropic liquid crystal, the mesophase exists in the temperature range above the crystalline melting temperature (T_m) and below the **isotropization** or **clearing** temperature (T_i).

Generally speaking, strong intermolecular attractions hinder the formation of a mesophase because such interactions provide a strong driving force for crystallization. Cholesterol, for example, does not form a mesophase even though its chemical structure is quite similar to that of cholesterol benzoate (Figure 1.1). Cholesterol can form hydrogen bonds between adjacent hydroxy groups; cholesterol benzoate has no hydrogen-bonding ability.

Liquid crystals are classified into three major categories based on the type of ordering within the mesophase (Figure 1.2). A **nematic** phase (Figure 1.2a) exhibits orientational order but no positional order; i.e., the centers of gravity of the molecules are randomly located. The chain axes tend to align nearly parallel to one another. The vector corresponding to the average direction of the chain axes is called the **director** (\mathbf{n}). The degree of fluctuation of the orientation of the molecular axes from the director is expressed as the **order parameter** S , defined as follows:

$$S = 1/2 (3 \langle \cos^2\theta \rangle - 1) \quad (1.1)$$

where θ is the angle between a chain axis and the director and the brackets denote the mean value for all the molecules. $S = 1$ when all the

axes are exactly parallel to the director, and $S = 0$ when there is no orientational ordering.

A **cholesteric** liquid-crystalline phase consists of a helical stacking of nematic layers as shown in Figure 1.2b. Cholesterol benzoate falls into this category. The formation of a cholesteric phase requires a chiral center.

In a **smectic** phase (Figure 1.2c-d), orientational ordering is accompanied by the arrangement of the molecules into layers. Smectic phases are classified into several types according to the positional ordering of the molecules within the layers and the angle between the layers and the director. Smectic phases with no positional ordering within the layers are classified as smectic A if the layers are normal to the director, and smectic C otherwise. There are several known smectic phases which display positional ordering within the layers; some examples are smectic B (hexagonal ordering), smectic D (body-centered cubic ordering), and smectic E (orthorhombic ordering).

The principal techniques used to characterize liquid crystals are differential scanning calorimetry (DSC), polarized light optical microscopy (POM)²⁹⁻³¹, and wide-angle X-ray scattering (WAXS).³²⁻⁴⁰ DSC can measure the thermal energy gained or lost by the system as phase transitions occur. Crystal-to-liquid-crystal, liquid-crystal-to-isotropic, and liquid-crystal-to-liquid-crystal transitions are all first-order and therefore give rise to peaks in a DSC temperature scan. The enthalpy and entropy of each transition can be calculated from the peak areas.

POM is used to observe birefringent textures which result from spatial fluctuations of the director within the sample.²⁹ Nematic phases typically give rise to the so-called schlieren texture; smectic phases can produce several different types of textures, including schlieren, mosaic and fan-shaped textures.^{29,30}

WAXS measures the periodicity of electron density over a scale of about 4 Å - 40 Å. In a three-dimensional crystal, the WAXS diffraction pattern consists of many sharp reflections, indicating a high degree of order that persists over a long range. In a liquid crystal, the WAXS reflections are fewer and less sharp. Nematic phases show only a single reflection, at a spacing on the order of 4 - 5 Å, corresponding to the distance between the long axes of the molecules. The reflection is diffuse, indicating that the interchain distance is not uniform. Smectic phases show this reflection, plus an additional reflection at low angles, which corresponds to the spacing between layers. Ordering within the smectic layers can cause the outer reflection to sharpen and sometimes to resolve into two or more components.⁴¹ In samples that do not possess long-range orientation, the reflections are seen as rings; in oriented samples, the low-angle reflections are usually meridional spots or arcs and the high-angle reflections are usually equatorial arcs. Low molecular weight liquid crystals can be oriented by placing the sample in a magnetic field.⁴² Polymer liquid-crystalline phases can be oriented by uniaxial stretching.

1.3.2 Liquid-Crystalline Polymers

The discussion so far has been mainly restricted to low molecular weight liquid crystals. Polymers, of course, are also capable of forming liquid-crystalline phases. A necessary condition is a high degree of rigidity in the polymer structure. The polymer must be a rigid rod, or be composed of rigid units connected by flexible spacers.

Bawden and Pirie⁴³ in 1937 were the first researchers to report a polymer liquid-crystalline phase. They discovered that a tobacco mosaic virus solution formed an anisotropic phase above a critical concentration. Later, it was found that poly(γ -benzyl-L-glutamate) forms a cholesteric phase in chloroform.⁴⁴⁻⁴⁶ Many examples of synthetic lyotropic polymers were developed in the years that followed.⁴⁷⁻⁴⁹

Rigid-rod polymers are generally incapable of forming thermotropic mesophases because they decompose before melting. In order to lower the melting point, some flexibility must be incorporated into the polymer chain. DeGennes⁵⁰ predicted in 1975 that thermotropic liquid-crystalline polymers could be made by connecting rigid anisotropic moieties (**mesogens**) with flexible spacer groups. Many researchers have proven this to be correct. There are two major types of thermotropic liquid-crystalline polymers. In **main-chain** liquid-crystalline polymers, the mesogenic units are part of the polymer backbone; in **side-chain** liquid-crystalline polymers, the mesogens are located on pendent groups. Many examples of both types have been reported in the literature.⁵¹⁻⁶³

The first known thermotropic liquid-crystalline polymers, polyalkanoates of *p,p'*-dihydroxy- α,α' -dimethyl benzalazine, were

reported by Roviello and Sirigu in 1975.⁵¹ In 1976, Jackson and Kuhfuss⁵² modified poly(ethylene terephthalate) (PET) with p-hydroxybenzoic acid and discovered that the resulting copolymers formed anisotropic fluid phases. These nematic melts displayed two phenomena which are the basis for the technological importance of thermotropic main-chain liquid-crystalline polymers. First, the viscosity in the nematic state was found to be much lower than in the isotropic state, which facilitates melt processing of the polymer. Second, injection-molded samples showed a very high degree of orientation, which greatly enhances the tensile modulus. Du Pont's Kevlar[®], a polyamide, and Celanese's Vectra[®], a polyester, are two examples of main-chain liquid-crystalline polymers that can be processed into highly oriented, high-strength materials.

1.3.3 Monotropic Liquid-Crystalline Polymers

In the discussion of low molecular weight liquid crystals above, it was mentioned that thermotropic liquid-crystalline phases exist in the temperature range between T_m , the crystalline melting temperature, and T_i , the isotropization temperature. This is true under equilibrium conditions, but in practice the transition temperatures in polymers are dependent on non-equilibrium factors such as cooling rate and thermal history. It is observed in crystallizable polymers that the temperature at which the crystalline phase melts on heating is higher than the temperature at which the crystalline phase forms on cooling. This phenomenon is known as supercooling and is a result of the slowness of the crystallization process. The degree of supercooling depends on the

heating and cooling rates. It is therefore insufficient to assign a single, unambiguous value to T_m in a crystallizable polymer; it is necessary to specify the conditions under which T_m is measured.

Supercooling is also observed in mesophase-to-isotropic transitions in liquid-crystalline polymers, but the effect is much smaller. This is because the formation of a liquid-crystalline phase from the melt is a faster process than crystallization. The DSC scans obtained on cooling and heating a typical thermotropic liquid-crystalline polymer are illustrated in Figure 1.3. $T_{i\text{ eq}}$ is defined as the temperature at which the isotropic phase and the mesophase have the same free energy. Similarly, $T_{m\text{ eq}}$ is defined as the temperature at which the mesophase and the crystalline phase have the same free energy. Above $T_{i\text{ eq}}$, the isotropic phase has the lowest free energy. As the melt is cooled to below $T_{i\text{ eq}}$, mesophase formation becomes thermodynamically favored. The mesophase forms relatively quickly, as shown by an exotherm in the DSC scan. On further cooling, $T_{m\text{ eq}}$ is reached, and crystallization becomes thermodynamically favored. Crystallization, a slower process than mesophase formation, takes place at a temperature somewhat lower than $T_{m\text{ eq}}$. On reheating, the crystal-to-mesophase transition is seen at a temperature slightly higher than $T_{m\text{ eq}}$, and as $T_{i\text{ eq}}$ is surpassed, the clearing transition is seen.

In the example given above, the mesophase is thermodynamically stable (i.e., it is the phase with the lowest free energy) in the temperature range between $T_{m\text{ eq}}$ and $T_{i\text{ eq}}$. Thermotropic liquid-crystalline polymers which display such a mesophase are termed **enantiotropic**. There is another class of thermotropic liquid-crystalline polymers,

termed **monotropic**, in which the mesophase is not thermodynamically stable at any temperature. In monotropic liquid-crystalline polymers, $T_{m\text{ eq}}$ is higher than $T_{i\text{ eq}}$. Below $T_{m\text{ eq}}$, the crystalline phase has the lowest free energy; above $T_{m\text{ eq}}$, the isotropic melt has the lowest free energy. It is possible, however, to produce the mesophase under certain conditions, owing to the relative rates of crystallization and mesophase formation. The DSC scans of a typical monotropic liquid-crystalline polymer are shown in Figure 1.4. On cooling the isotropic melt to below $T_{m\text{ eq}}$, crystallization becomes thermodynamically favored, but if cooling is rapid enough, very little crystallization takes place. When $T_{i\text{ eq}}$ is reached, the sample is still mostly in the isotropic melt. At $T_{i\text{ eq}}$, the free energy of the mesophase becomes lower than that of the isotropic melt, and a transition from isotropic melt to mesophase takes place. Of course, the crystalline phase is still the phase with the lowest free energy. Further cooling results in a transition from the mesophase to the crystalline phase. On heating, the transition from the crystalline phase to the isotropic melt occurs slightly above $T_{m\text{ eq}}$, with no intermediate transition to the mesophase. The mesophase is observed only on cooling, not on heating.

The behavior of the monotropic liquid-crystalline polymer described above is produced by intermediate cooling and heating rates. If the polymer is cooled extremely slowly, crystallization from the isotropic melt may occur before $T_{i\text{ eq}}$ is reached, and the mesophase would therefore not be formed. If the polymer is cooled extremely rapidly, it may be possible to quench the polymer to below its glass transition temperature while it is still in the mesophase, thereby

preventing crystallization entirely and producing a supercooled mesophase.

Monotropic mesophases have been reported in low molecular weight liquid crystals¹²⁻¹⁵ as well as in liquid-crystalline polymers.⁶⁴⁻⁷⁴ Several methods have been used to modify monotropic systems to bring about enantiotropic behavior. In most cases, the key is to depress the crystalline melting temperature. Vogel et al.¹⁴ studied the effect of small amounts of impurities in cholesterol nonanoate, which in pure form displays an enantiotropic cholesteric phase and a monotropic smectic phase. It was found that the addition of the proper impurity could lower the crystalline-to-smectic transition temperature so that it was below the smectic-to-cholesteric transition temperature, thereby changing the smectic phase from monotropic to enantiotropic. The impurity destabilized the crystalline phase but left the mesophases relatively unchanged.

A similar effect can be achieved in polymeric systems by copolymerization. Percec et al.⁶⁴ studied random copolymers of two semiflexible polyethers, which differed only in the lengths of their flexible spacers. Homopolymers of both polyethers displayed monotropic mesophases, but copolymers with compositions near 50/50 displayed enantiotropic mesophases. Zhou et al.⁶⁵ studied random copolymers of an enantiotropic polyester and another polyester of similar structure which did not display a mesophase. All of the copolymers were found to be enantiotropic, including one which contained only 10 mol% of the former units and 90% of the latter units. T_m , which was approximately the same for each homopolymer, was depressed by copolymerization,

reaching a minimum near a copolymer composition of 50/50. T_i , by contrast, increased approximately linearly with increasing content of the enantiotropic comonomer. The authors extrapolated the T_i values of the copolymers to find a theoretical T_i for the non-enantiotropic homopolymer. This theoretical T_i was lower than the homopolymer's T_m , so it was hypothesized that the homopolymer was probably monotropic.

Another way to change a monotropic polymeric mesophase to an enantiotropic one is to increase the molecular weight of the polymer. Blumstein and coworkers⁶⁶⁻⁶⁸ noted that the nematic mesophase of model compounds and oligomers of poly(2,2'-dimethyl-4,4'-dioxiazobenzene dodecanedioyl) (DDA-9) changed from monotropic to enantiotropic as the molecular weight increased. The lowest molecular weight to display an enantiotropic phase was $M_n = 2,700$, which corresponds to approximately six repeating units per chain. Zhou et al.⁶⁹ and Percec et al.⁷⁰ reported similar phenomena in other systems.

Changing the length of flexible spacers can also effect a change from monotropic to enantiotropic behavior. Roviello and Sirigu⁷¹ noted that in a series of thermotropic polyesters, the mesophase was monotropic when the flexible spacers consisted of 12 methylene units and enantiotropic when the spacers were shorter.

1.3.4 Liquid-Crystalline Polyurethanes

Of the many thermotropic liquid-crystalline polymers that have been reported in the literature, only a few are polyurethanes. This is partly because of the chemical instability of the polyurethane functional

group at temperatures above 180 °C. Liquid-crystalline polyurethanes are of theoretical interest because of the strong tendency of polyurethanes to form hydrogen bonds. Ordered phases that incorporate hydrogen bonds are likely to gain thermodynamic stability from these interactions. This may have a profound effect on the structure and thermal behavior of mesophases in these polymers.

The first reported liquid-crystalline polyurethanes were synthesized by Imura et al.⁷⁵ from 3,3'-dimethyl-4,4'-biphenyldiyl diisocyanate (DBD) and α,ω -alkanediols. Liquid crystallinity was reported on the basis of DSC and optical microscopy data; the mesophases were not classified.

Tanaka and Nakaya reported main-chain thermotropic liquid-crystalline polyurethanes derived from 4,4'-bis(2-hydroxyethoxy)biphenyl (DHB)⁷⁶ and bis(p-oxyethylphenyl)terephthalate (BOPT)⁷⁷, each with four isocyanates: hexamethylene diisocyanate (HDI), dicyclohexylmethane-4,4'-diisocyanate (H₁₂MDI), cyclohexane-1,3-di(methylisocyanate) (H₆XDI), and 2,4-toluenediisocyanate (TDI). In the first series, the polyurethanes DHB/HDI, DHB/H₁₂MDI, DHB/H₆XDI, and DHB/TDI were reported on the basis of DSC and optical microscopy to display mesophases within temperature ranges of 188-203°C, 147-172°C, 135-193°C, and 151-193°C respectively. A polyurethane derived from DHB and 4,4'-diphenylmethanediisocyanate (MDI) decomposed before any thermal transitions took place. In the second series, mesophases were reported for BOPT/HDI, BOPT/H₁₂MDI, BOPT/H₆XDI, and BOPT/TDI; transition temperatures were 30 - 60 °C

higher than in the first series. All polyurethanes in both series had intrinsic viscosities between 0.10 and 0.20 dL/g.

Mormann⁷⁸ synthesized a series of poly(diesterurethane)s based on diisocyanatoesters and α,ω -alkanediols. Four of these polymers were reported to be liquid-crystalline. The mesophases were declared nematic on the basis of miscibility studies with low molecular weight nematogens. The crystalline melting temperatures were between 226 °C and 285 °C; clearing temperatures were all slightly above or below T_m . Mormann and Baharifar⁷⁹ studied semiflexible polyurethanes containing 4,4'-diisocyanatoazobenzene, itself a low molecular weight liquid crystal, as a mesogen. No liquid-crystalline behavior was detected in the polyurethanes.

Mormann and Bramm⁷³ synthesized a series of polyurethanes using mesogenic diisocyanates. The mesogenic units consisted of either two aromatic rings, or one aromatic ring and one cyclohexyl ring, connected by an ester linkage. Some of the aromatic rings contained methyl substituents, the purpose of which was to lower the transition temperatures of the polyurethanes by inducing structural irregularity and also by sterically hindering hydrogen bonding. Only the polyurethanes made from unsubstituted diisocyanates, however, showed liquid-crystalline phases. The mesophases were monotropic and nematic, with T_m close to 250 °C and T_i in the range 222-258 °C.

Kricheldorf and Awe⁸⁰ prepared a series of polyurethanes from various bipiperidines and 4,4'-biphenylene dichloroformate. Mesophases were observed (with accompanying decomposition) in the optical microscope at temperatures above 300 °C.

Jadhav and Kantor⁸¹ synthesized a series of biphenyl-containing polyurethanes. 2,4-TDI, MDI, and HDI were each combined with 4,4'-bis(6-hydroxyhexoxy)biphenyl (BHHBP) and 4,4'-bis(2-hydroxyethoxy)biphenyl (BHEBP), for a total of six polyurethanes. DSC heating scans showed two endotherms in all cases, and polarizing optical microscopy showed threaded textures indicative of mesophase ordering. Only two of the six polyurethanes were found to have transition temperatures below 200 °C. Not surprisingly, the polyurethanes with the greatest amounts of flexibility and structural irregularity have the lowest transition temperatures. Both of the MDI-based polyurethanes have crystalline melting temperatures above 250 °C; all three of the polyurethanes with only two methylene units in the flexible spacer have melting temperatures above 200 °C. The low transition temperatures of HDI/BHHBP arise from the high flexibility presented by the three hexamethylene spacers in each repeat unit. The less-flexible 2,4-TDI/BHHBP has even lower transition temperatures than HDI/BHHBP; it is likely that the transition temperatures are depressed by the asymmetric placement of the methyl group on the aromatic ring that connects the two urethane linkages. This dissertation represents a continuation of Jadhav's work.

1.4 Experimental Methods

1.4.1 Preparation of Polymers and Polymer Blends

1.4.1.1 Starting Materials

2,4-Toluenediisocyanate (2,4-TDI) was obtained from Fluka Chemical Corporation. Dioxane was obtained from Fisher Scientific.

All other starting materials were obtained from Aldrich Chemical Company.

Dimethylformamide (DMF), dimethylsulfoxide (DMSO), 1-butanol, 2,4-toluenediisocyanate, and 2,6-toluenediisocyanate were purified by vacuum distillation. All other starting materials were used as received.

1.4.1.2 Synthesis

Synthetic procedures are described in detail in the appropriate chapters, as follows:

BHHBP: Chapter 2.

Polyurethanes: Chapter 3.

Blends and copolymers of D6T24 and D6T26: Chapter 4.

The chemical structures of newly synthesized materials were confirmed by elemental analysis, ^1H NMR, and infrared spectroscopy. Elemental analysis for carbon, hydrogen and nitrogen was carried out by the Microanalytical Lab at the University of Massachusetts. ^1H NMR spectra were recorded on a Varian XL-200 Spectrometer, operating at 200 MHz, in perdeuterated DMSO. Tetramethylsilane (TMS) was used as a reference. Infrared spectroscopy measurements were made on an IBM Fourier Transform Infrared Spectrometer, using either solution-cast films or KBr pellets.

1.4.2 Polymer Characterization

Intrinsic viscosities were measured in a Ubbelohde viscometer in DMSO. The measurement temperature was 30.0 °C for D6T24, and 60.0 °C for D6T26. Size exclusion chromatography (SEC) of D6T24 was

performed on a Waters Model 590 gel permeation chromatograph (GPC) equipped with four Ultrastyrigel columns (500, 10^3 , 10^4 , and 10^5 Å), using DMF as eluent at 45 °C. A flux of 1 mL/min was maintained in all runs.

Differential scanning calorimetry measurements were done on a Perkin-Elmer DSC 7, using indium standards for temperature and enthalpy calibration. Dry nitrogen was circulated through the sample and reference cells at a rate of 20 mL/min. The peak temperatures were taken as the transition temperatures.

Wide-angle X-ray scattering patterns were obtained in a Statton X-ray camera using pinhole-collimated Cu-K α radiation ($\lambda = 1.542$ Å). Samples were placed in a 1.5-mm glass tube which was sealed and placed in the path of the X-ray beam in a heating chamber connected to an Omega thermocouple. The scattering patterns were recorded on photographic film.

Optical textures were studied on a Carl Zeiss Ultraphoto II polarizing optical microscope equipped with a Linkam Scientific Instruments TMS 90 temperature controller and a TMH 600 hot stage, which was calibrated with vanillin and potassium nitrate standards. The polymer sample was placed between glass slides and heated to the isotropic melt, and the slides were then removed from the hot stage and sheared to produce a thin layer of melted polymer. The sample was then returned to the hot stage and the desired thermal treatment was executed.

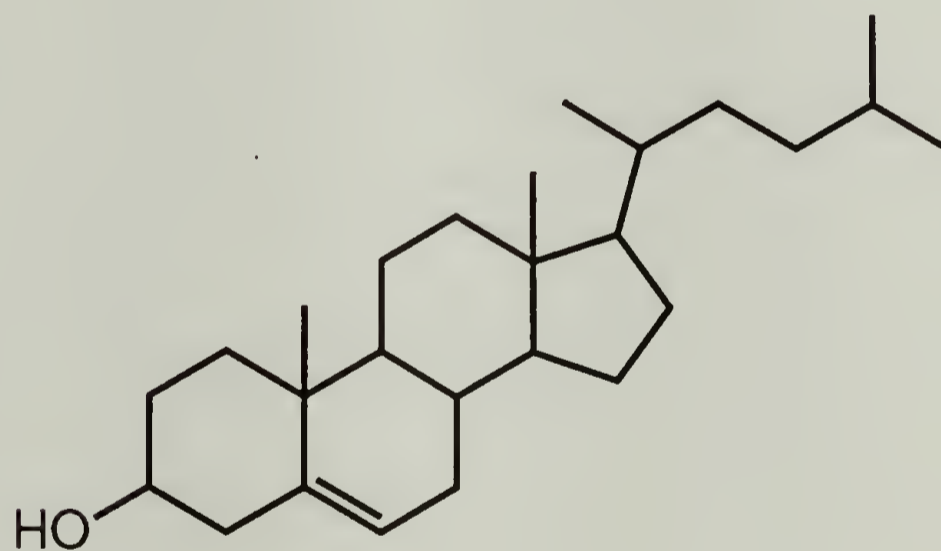
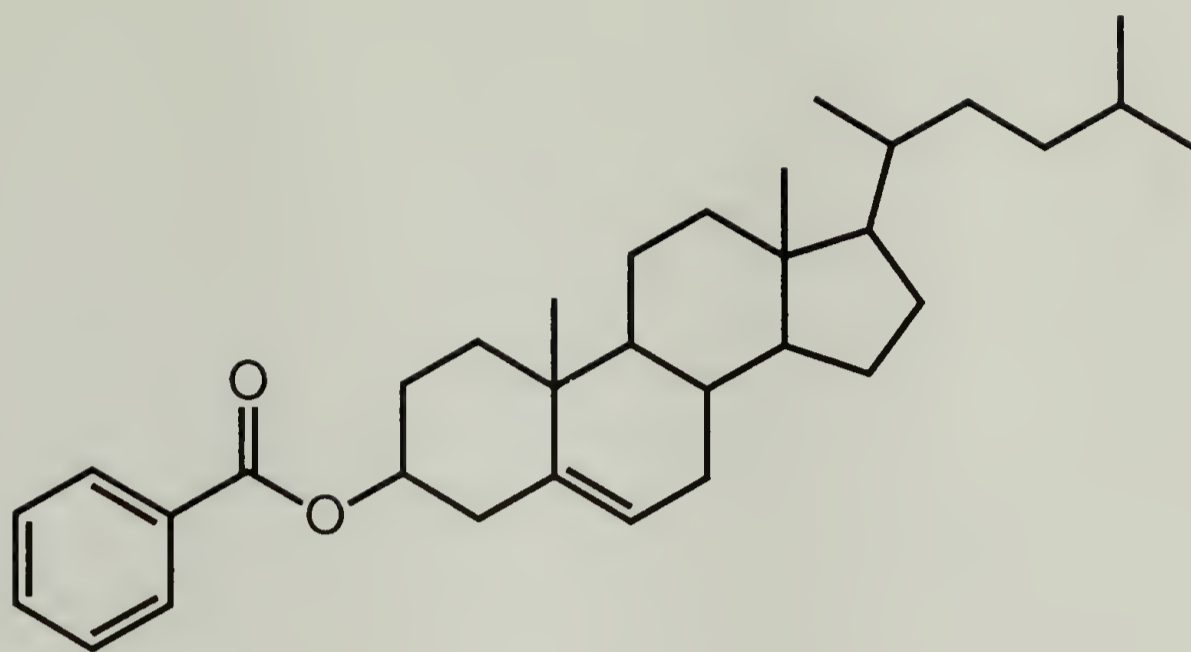
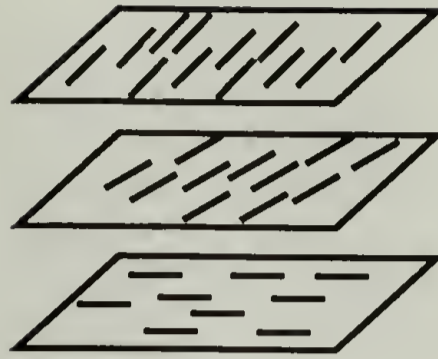


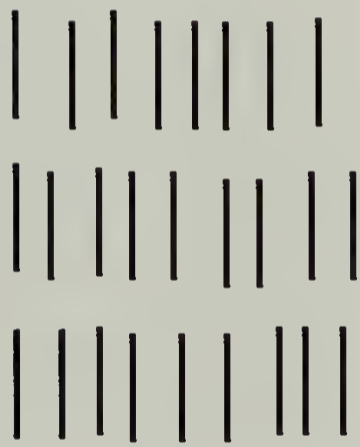
Figure 1.1. Structures of cholesterol benzoate (above) and cholesterol (below).



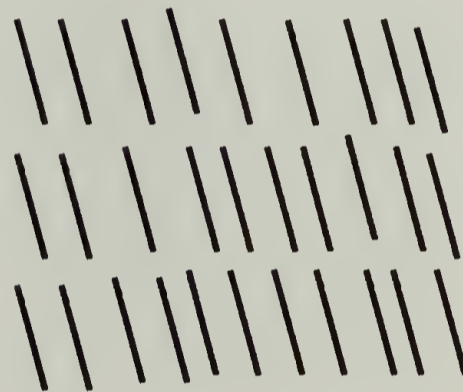
a



b



c



d

Figure 1.2. Types of liquid-crystalline phases: a) nematic; b) cholesteric; c) smectic A; d) smectic C.

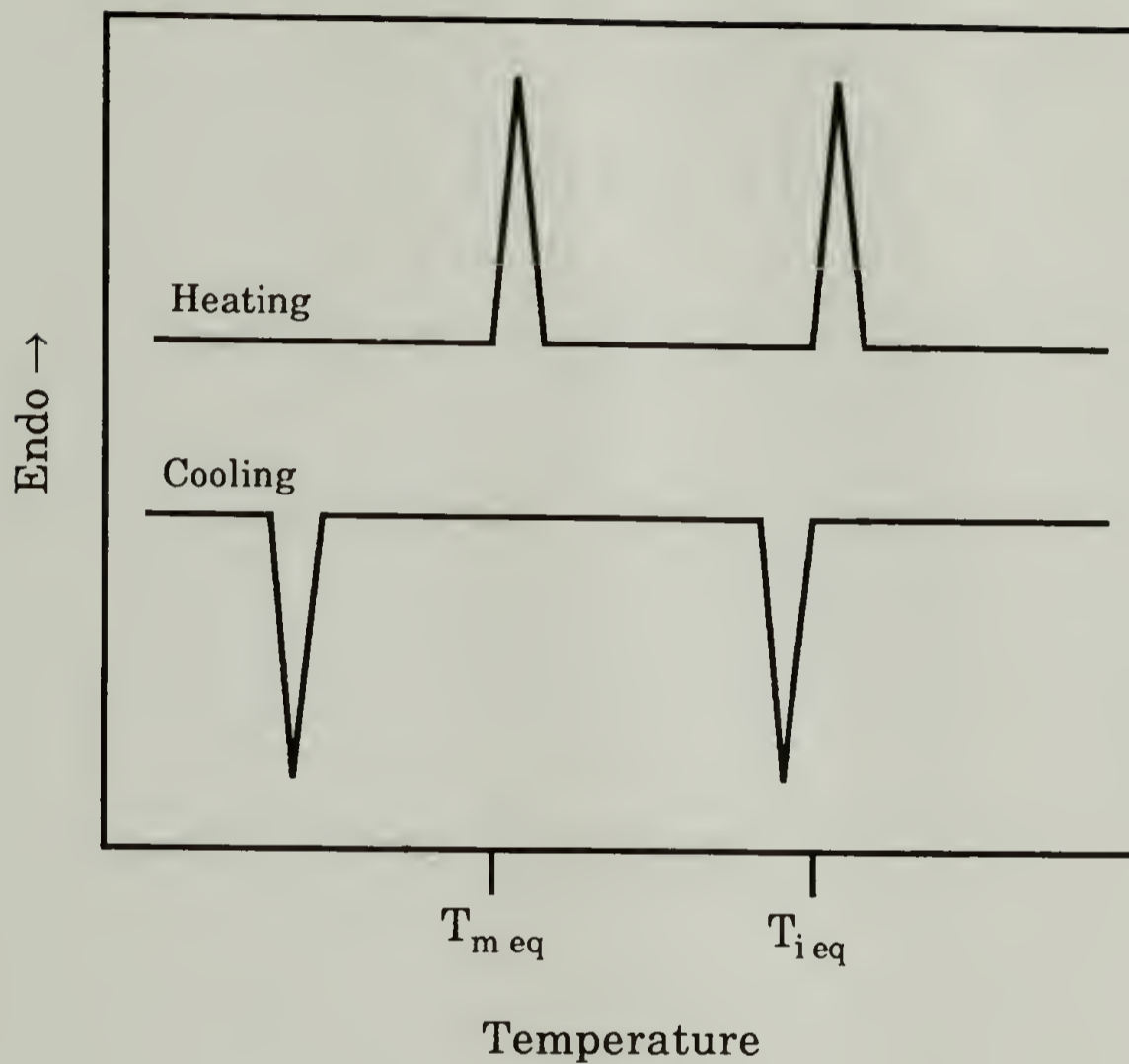


Figure 1.3. Schematic representation of the DSC scans of a typical enantiotropic liquid-crystalline polymer.

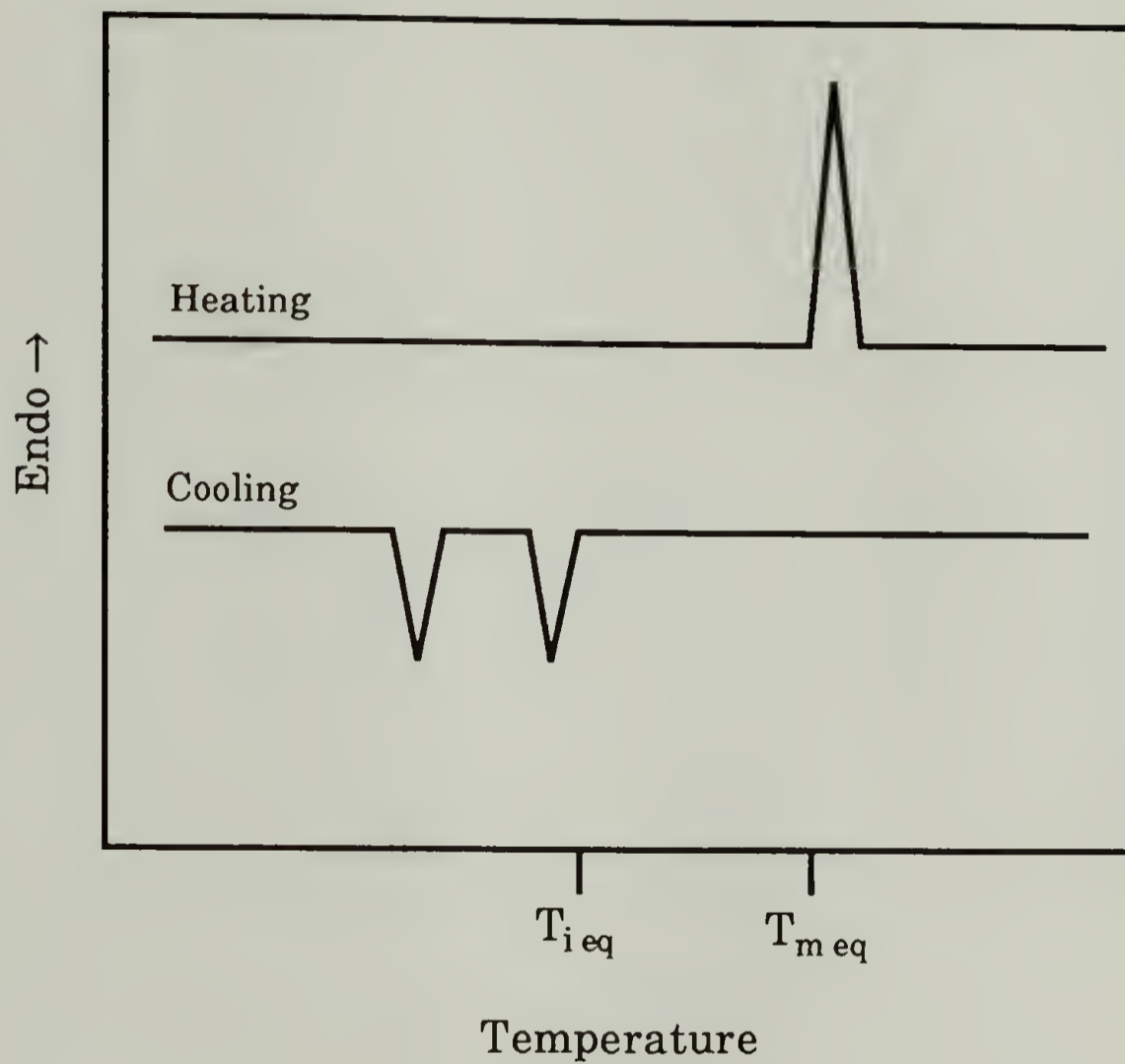


Figure 1.4. Schematic representation of the DSC scans of a typical monotropic liquid-crystalline polymer.

References

- (1) Reitnitzer, F. *Monatsh. Chem.* **1888**, 9, 421.
- (2) Freidel, E. *C. R. Acad. Sci.* **1925**, 180, 269.
- (3) Vorländer, D. *Z. Phys. Chem.* **1927**, A126, 449.
- (4) Arnold, H. *Z. Phys. Chem. (Leipzig)* **1964**, 226, 146.
- (5) Small, D. M., Bourgis, M. *Mol. Cryst.* **1966**, 1, 541.
- (6) Lawson, K. D., Flautt, T. J. *J. Am. Chem. Soc.* **1967**, 89, 5489.
- (7) Taylor, T. R., Arora, S. L., Ferguson, J. L. *Phys. Rev. Lett.* **1970**, 25, 722.
- (8) Demus, D., Diele, S., Klapperstück, M., Link, V., Zschke, H. *Mol. Cryst. Liq. Cryst.* **1971**, 15, 161.
- (9) Merret, W. G., Cole, G. D., Walker, W. W. *Mol. Cryst. Liq. Cryst.* **1971**, 15, 105.
- (10) McMillan, W. L. *Phys. Rev.* **1972**, A6, 936.
- (11) Gray, G. W. In *Liquid Crystals and Ordered Fluids*; J. F. Johnson and R. S. Porter, Ed.; Plenum: 1974; Vol. 2; p. 617.
- (12) Ennulat, R. D. In *Analytical Calorimetry*; R. S. Porter and J. F. Johnson, Ed.; Plenum Press: New York, 1968; p. 219.
- (13) Ennulat, R. D. *Mol. Cryst. Liq. Cryst.* **1969**, 8, 247.
- (14) Vogel, M. J., Barrall II, E. M., Mignosa, C. P. *Mol. Cryst. Liq. Cryst.* **1971**, 15, 49.
- (15) Jungbauer, D., Wendorff, J. H. *Mol. Cryst. Liq. Cryst.* **1989**, 170, 159.
- (16) Chandrasekhar, S., Sadashiva, B. K., Suresh, K. A. *Pramana* **1977**, 9, 471.
- (17) Sorai, M., Tsuji, K., Suga, H., Seki, S. *Mol. Cryst. Liq. Cryst.* **1980**, 80, 33.

- (18) Sorai, M., Suga, H. *Mol. Cryst. Liq. Cryst.* **1981**, 73, 47.
- (19) Sorai, M., Yoshioka, H., Suga, H. *Mol. Cryst. Liq. Cryst.* **1982**, 84, 39.
- (20) Chandrasekhar, S. *Philos. Trans. R. Soc. London, A* **1983**, 309, 93.
- (21) Levelut, A. M. *J. Chim. Phys.* **1983**, 80, 149.
- (22) Destrade, C., Foucher, P., Gasparoux, H., Tinh, N. H. *Mol. Cryst. Liq. Cryst.* **1984**, 106, 121.
- (23) Tinh, N. H., Foucher, P., Destrade, C., Levelut, A. M., Malthete, J. *Mol. Cryst. Liq. Cryst.* **1984**, 111, 277.
- (24) Zimmermann, H., Poupko, R., Luz, Z., Billard, J. Z. *Naturforsch* **1985**, 40a, 149.
- (25) Malthete, J., Collet, A. *Nouv. J. de Chemie* **1985**, 9, 151.
- (26) Levelut, A. M., Malthete, J., Collet, A. *J. Phys. (Paris)* **1986**, 47, 351.
- (27) Lei, L. *Mol. Cryst. Liq. Cryst.* **1987**, 146, 41.
- (28) Leung, K. M., Lei, L. *Mol. Cryst. Liq. Cryst.* **1987**, 146, 71.
- (29) Hartshorne, N. H. *The Microscopy of Liquid Crystals*; Microscope Publications Ltd.: London, 1974.
- (30) Demus, D., Richter, L. *Textures of Liquid Crystals*; Verlag Chemie: Weinheim, 1978.
- (31) Alderman, N. J., Mackley, M. R. *Faraday Discuss. Chem. Soc.* **1985**, 79, 149.
- (32) de Vries, A. *Mol. Cryst. Liq. Cryst.* **1970**, 10, 219.
- (33) de Vries, A. *J. Chem. Phys.* **1972**, 56, 4489.
- (34) Leadbetter, A. J., Norris, E. K. *Mol. Phys.* **1979**, 38, 669.
- (35) Azaroff, L. V. *Proc. Natl. Acad. Sci. U.S.A.* **1980**, 77, 1252.
- (36) Azaroff, L. V. *Mol. Cryst. Liq. Cryst.* **1980**, 60, 73.

- (37) Azaroff, L. V., Schuman, C. A. *Mol. Cryst. Liq. Cryst.* **1985**, 122, 309.
- (38) de Vries, A. *Mol. Cryst. Liq. Cryst.* **1985**, 131, 125.
- (39) Azaroff, L. V. *Mol. Cryst. Liq. Cryst.* **1987**, 145, 31.
- (40) Blackwell, J., Biswas, A., Gutierrez, G. A., Chivers, R. A. *Faraday Discuss. Chem. Soc.* **1985**, 79, 73.
- (41) Smyth, G., Pollack, S. K., MacKnight, W. J., Hsu, S. L. *Liq. Cryst.* **1990**, 7, 839.
- (42) Chistyakov, I. G., Chaikowsky, W. M. *Mol. Cryst. Liq. Cryst.* **1969**, 7, 269.
- (43) Bawden, F. C., Pirie, N. W. *Proc. R. Soc. London, Ser. B* **1937**, 123, 274.
- (44) Elliot, A., Ambrose, E. J. *Faraday Discuss. Chem. Soc.* **1950**, 9, 246.
- (45) Robinson, C. *Trans. Faraday Soc.* **1956**, 52, 571.
- (46) Robinson, C., Ward, J. C., Beevers, R. B. *Discuss. Faraday Soc.* **1958**, 25, 29.
- (47) Morgan, P. W. *Macromolecules* **1977**, 10, 1381.
- (48) Wong, C. P., Ohnuma, H., Berry, G. C. *J. Polym. Sci., Polym. Symp.* **1978**, 65, 173.
- (49) Panar, M., Beste, L. F. *Macromolecules* **1977**, 10, 1401.
- (50) de Gennes, P. *C. R. Acad. Sci. Paris, Ser. B* **1975**, 281, 101.
- (51) Roviello, A., Sirigu, A. *J. Polym. Sci., Polym. Lett. Ed.* **1975**, 13, 455.
- (52) Jackson, W. J., Jr., Kuhfuss, H. F. *J. Polym. Sci., Polym. Chem. Ed.* **1976**, 14, 2043.
- (53) Blumstein, A., Sivaramakrishnan, K. N., Clough, S. B., Blumstein, R. B. *Mol. Cryst. Liq. Cryst.* **1979**, 49, 255.
- (54) Roviello, A., Sirigu, A. *Eur. Polym. J.* **1979**, 15, 61.

- (55) Griffin, A. C., Havens, S. J. *J. Polym. Sci., Polym. Phys. Ed.* **1981**, *19*, 951.
- (56) Galli, G., Benedetti, E., Chiellini, E., Ober, C., Lenz, R. W. *Polym. Bull.* **1981**, *5*, 497.
- (57) Viney, C., Windle, A. H. *J. Mater. Sci.* **1982**, *17*, 2661.
- (58) Ringsdorf, H., Portugal, M., Happ, M., Finkelmann, H. *Makromol. Chem.* **1978**, *179*, 2541.
- (59) Shibaev, V. P., Platé, N. A., Smolyansky, A. L., Voloskov, A. Y. *Makromol. Chem.* **1980**, *181*, 1393.
- (60) Finkelmann, H., Rehage, G. *Makromol. Chem., Rapid Commun.* **1980**, *1*, 31.
- (61) Keller, P. *Macromolecules* **1984**, *17*, 2937.
- (62) Shilov, V. V., Tsukruk, V. V., Lipatov, Y. S. *J. Polym. Sci., Polym. Phys. Ed.* **1984**, *22*, 41.
- (63) Reck, B., Ringsdorf, H. *Makromol. Chem., Rapid Commun.* **1985**, *6*, 291.
- (64) Percec, V., Yourd, R. *Macromolecules* **1989**, *22*, 3229.
- (65) Zhou, Q.-F., Jin, J.-I., Lenz, R. W. *Can. J. Chem.* **1985**, *63*, 181.
- (66) Blumstein, R. B., Stickles, E. M. *Mol. Cryst. Liq. Cryst.* **1982**, *82*, 151.
- (67) Blumstein, R. B., Stickles, E. M., Blumstein, A. *Mol. Cryst. Liq. Cryst.* **1982**, *82*, 205.
- (68) Blumstein, R. B., Stickles, E. M., Gauthier, M. M., Blumstein, A., Volino, F. *Macromolecules* **1984**, *17*, 177.
- (69) Zhou, Q. F., Duan, X. L., Liu, Y. L. *Macromolecules* **1986**, *19*, 247.
- (70) Percec, V., Tomazos, D., Pugh, C. *Macromolecules* **1989**, *22*, 3259.
- (71) Roviello, A., Sirigu, A. *Makromol. Chem.* **1982**, *183*, 409.
- (72) Ober, C., Lenz, R. W., Galli, G., Chiellini, E. *Macromolecules* **1983**, *16*, 1034.
- (73) Mormann, W., Brahm, M. *Macromolecules* **1991**, *24*, 1096.

- (74) Papadimitrakopoulos, F., Hsu, S. L., MacKnight, W. J. Submitted for publication.
- (75) Iimura, K., Koide, N., Tanabe, H., Takeda, M. *Makromol. Chem.* **1981**, *182*, 2569.
- (76) Tanaka, M., Nakaya, T. *Kobunshi Ronbunshu* **1986**, *43*, 311.
- (77) Tanaka, M., Nakaya, T. *J. Macromol. Sci., Chem.* **1987**, *A24*, 777.
- (78) Mormann, W. *Polym. Prepr.* **1989**, *30(1)*, 291.
- (79) Mormann, W., Baharifar, A. *Polym. Bull.* **1990**, *24*, 413.
- (80) Kricheldorf, H. R., Awe, J. *Makromol. Chem.* **1989**, *190*, 2597.
- (81) Jadhav, J. Y., Kantor, S. W. Submitted for publication.

CHAPTER 2

BHHBP: A MESOGENIC DIOL

2.1 Introduction

The mesogenic diol used in all of the polyurethanes in this work is 4,4'-bis(6-hydroxyhexoxy)biphenyl (BHHBP) (Figure 2.1). BHHBP was first reported by Reck and Ringsdorf¹ in a study of liquid-crystalline polymers containing both main-chain and side-chain mesogens. A number of liquid-crystalline polymers have been reported¹⁻⁸ which contain BHHBP linkages; all of these polymers exhibit smectic phases. Many other liquid-crystalline polymers containing the biphenyl mesogen^{3,9-19} have been reported; some of these exhibit only nematic mesophases.

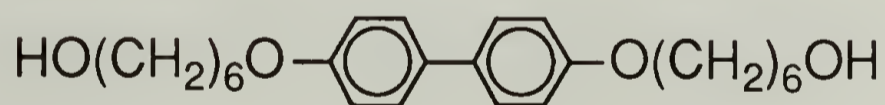


Figure 2.1. Structure of BHHBP.

This chapter reports the synthesis and purification of BHHBP. This is followed by a brief discussion of a study conducted by Smyth et al.²⁰ on its properties.

2.2 Synthesis and Purification

The synthesis of BHHBP was carried out as follows: Sodium hydroxide (32.00 g, 0.800 mol) and 4,4'-dihydroxybiphenyl (37.2 g, 0.200 mol) were added to 400 mL of ethanol. The mixture was heated to reflux with vigorous stirring, and 6-chloro-1-hexanol (120.2 g, 0.880 mol) was added dropwise at a rate of approximately 5 mL/min. The color of the reaction mixture changed from a faint yellow to a deep olive green as the reaction proceeded. After 24 hours under reflux, the mixture was poured into 4 L of distilled water, and the precipitated solid was collected by vacuum filtration.

Two recrystallization methods were used. The first method consisted of recrystallizing the crude product first from a 3:1 mixture of ethanol and DMF and then from 1-butanol. This procedure was time-consuming and required a large amount of solvent. A better method was to recrystallize two or three times from dioxane, using charcoal as a decolorizing agent. The second method resulted in higher purity and about the same percent yield as the first method. The yield ranged from 62% to 88%. The melting point of the final product was 176 ± 2 °C.

2.3 Properties

Smyth et al.²⁰ reported that BHHBP exhibits a smectic mesophase between 97°C and 179°C. WAXS revealed that positional ordering existed within the smectic layers. In both the crystalline phase and the mesophase, the chain axes are considerably tilted with respect to the layer normal. In the crystalline phase, the molecular axes form an

angle of 45-55° with the layer normal. The alkoxy chain is coplanar with the phenyl ring, and the alkyl chains are most likely in an all-trans conformation.

On the transition from crystal to mesophase, the molecule gains some positional disorder. The biphenyl moieties and the adjacent alkoxy carbons remain positionally and rotationally restricted, but the methylene carbons further out on the chain gain a considerable degree of mobility. Infrared spectroscopy reveals that hydrogen bonding becomes much weaker in the mesophase than in the crystalline phase. However, some hydrogen bonding does persist. The conformations of the alkyl linkages remain primarily trans, probably because conformational disordering is hindered by hydrogen bonding.

Smyth et al.²⁰ suggest that the mesophase of BHHBP should be associated with the tilted smectic J and K phases which Leadbetter²¹ terms "disordered crystals." In these phases, the molecules are orientationally disordered but are positionally ordered in three dimensions.

References

- (1) Reck, B., Ringsdorf, H. *Makromol. Chem., Rapid Commun.* **1985**, *6*, 291.
- (2) Reck, B., Ringsdorf, H. *Makromol. Chem., Rapid Commun.* **1985**, *6*, 691.
- (3) Sato, M., Nakatsuchi, K., Ohkatsu, Y. *Makromol. Chem., Rapid Commun.* **1986**, *7*, 231.
- (4) Reck, B., Ringsdorf, H. *Makromol. Chem., Rapid Commun.* **1987**, *7*, 389.
- (5) Pollack, S. K., Shen, D. Y., Wang, Q., Stidham, H. D., Hsu, S. L. *Macromolecules* **1989**, *22*, 551.
- (6) Stenhouse, P. J., Vallés, E. M., Kantor, S. W., MacKnight, W. J. *Macromolecules* **1989**, *22*, 1467.
- (7) Shen, D. Y., Pollack, S. K., Hsu, S. L. *Macromolecules* **1989**, *22*, 2565.
- (8) Smyth, G., Vallés, E. M., Pollack, S. K., Grebowicz, J., Stenhouse, P. J., Hsu, S. L., MacKnight, W. J. *Macromolecules* **1990**, *23*, 3389.
- (9) Asrar, J., Toriumi, H., Watanabe, J., Krigbaum, W. R., Ciferri, A., Preston, J. *J. Polym. Sci., Polym. Phys. Ed.* **1983**, *21*, 1119.
- (10) Blumstein, A., Sivaramakrishnan, K. N., Clough, S. B., Blumstein, R. B. *Mol. Cryst. Liq. Cryst.* **1979**, *49*, 255.
- (11) Kricheldorf, H. R., Awe, J. *Makromol. Chem.* **1989**, *190*, 2597.
- (12) Meurisse, P., Noel, C., Monnerie, L., Fayolle, B. *Br. Polym. J.* **1981**, *13*, 55.
- (13) Sagane, T., Lenz, R. W. *Macromolecules* **1989**, *22*, 3763.
- (14) Sato, M., Jadhav, J. Y., Mallon, J. J., Kantor, S. W. Submitted for publication.
- (15) Shaffer, T. D., Jamaludin, M., Percec, V. *J. Polym. Sci., Polym. Chem. Ed.* **1985**, *23*, 2913.

- (16) Shaffer, T. D., Percec, V. *J. Polym. Sci., Polym. Lett. Ed.* **1985**, *23*, 185.
- (17) Shaffer, T. D., Percec, V. *Makromol. Chem.* **1986**, *187*, 111.
- (18) Tanaka, M., Nakaya, T. *Kobunshi Ronbunshu* **1986**, *43*, 311.
- (19) Van Luyen, D., Strzelecki, L. *Eur. Polym. J.* **1980**, *16*, 303.
- (20) Smyth, G., Pollack, S. K., MacKnight, W. J., Hsu, S. L. *Liq. Cryst.* **1990**, *7*, 839.
- (21) Leadbetter, A. J. In *Thermotropic Liquid Crystals*; G. W. Gray, Ed.; John Wiley and Sons: Chichester, 1987; p. 1.

CHAPTER 3

D6T24 AND D6T26: MESOGENIC POLYURETHANES

3.1 Introduction

As mentioned in Chapter 1, very few liquid-crystalline polyurethanes have been reported. Moreover, most of those that have been reported have not been extensively characterized. The main reason for this is that in many cases, the mesophase exists only at temperatures at which the polyurethane functional group is chemically unstable. The formation of the mesophase is often accompanied by decomposition.

Jadhav¹ reported the transition temperatures of six biphenyl-containing polyurethanes, all of which showed multiple transitions in their DSC scans. The polyurethane with the lowest transition temperatures was the product of BHHBP and 2,4-toluenediisocyanate (2,4-TDI). This polyurethane is designated D6T24 and its structure is shown in Figure 3.1.

Because of its low transition temperatures, D6T24 was considered to be a very promising subject for further study. The DSC data indicated that all of the ordered phases, as well as the isotropic melt phase, of D6T24 existed at temperatures below 180 °C. Therefore, all of these phases could be studied extensively with little worry about decomposition. It was initially inferred from the DSC and optical microscopy results that D6T24 was enantiotropic. Subsequent experiments, detailed below, lead to the conclusion that D6T24 is in fact monotropic.

One of the objectives of this project is to relate the properties of D6T24 to its structure. The key structural features that give rise to its unusual properties are: 1) the semiflexibility brought about by the biphenyl group and the adjacent hexamethylene spacers; 2) the urethane linkages, capable of hydrogen bonding; and 3) the asymmetric placement of the methyl group on the 2,4-TDI linkage. Semiflexibility is a near-universal feature of thermotropic liquid-crystalline polymers, but the hydrogen-bonding capability and asymmetry of D6T24 are worthy of further discussion.

Strong intermolecular attractions usually hinder the formation of a liquid-crystalline phase by providing a driving force for crystallinity. In the absence of intermolecular attractions, mesogenic molecules or polymer chains are able to maintain disorder within a closely packed, near-parallel arrangement. In the presence of these attractions, however, attainment of close packing leads directly to the formation of a three-dimensional crystal. Hydrogen bonding between the C=O and N-H groups should be expected to have just such an effect on D6T24. It is likely that hydrogen bonding contributes to the high crystalline melting temperatures reported in some of the known liquid-crystalline polyurethanes.

Two examples of liquid-crystalline polyurethanes that are incapable of hydrogen bonding have been reported.

Papadimitrakopoulos et al.² studied a polyurethane whose structure was identical to D6T24 except that the hydrogen atoms on the urethane nitrogens were replaced by methyl groups. This modification was found to lower the transition temperatures by approximately 100 °C.

Kricheldorf³ reported a series of piperazine- and bipiperidine-based liquid-crystalline polyurethanes, which had quite low crystalline melting temperatures (as low as 125 °C) despite highly regular structures.

The driving force for crystallinity in D6T24 brought about by hydrogen bonding (and by the biphenyl units) is somewhat offset by the asymmetric placement of the methyl group. A 2,4-TDI molecule has two non-equivalent isocyanate groups, either of which can add to a growing polymer chain. The methyl group in each 2,4-TDI linkage along the chain can be in one of two positions, and the result is that the structure of the polymer is akin to that of a random copolymer. The resulting asymmetry is generally sufficient to prevent crystallization in polyurethanes based on 2,4-TDI. D6T24 does in fact crystallize, probably because the 2,4-TDI linkage makes up only a small part of the polymer repeat unit, rendering its influence relatively small. The structural asymmetry does, however, have the effect of lowering the crystalline melting temperature of D6T24 relative to a similar symmetrical polyurethane, as will be shown later.

The methyl group has a large effect on the conformations of the nearby bonds. In the absence of steric factors, the urethane group would be expected to lie in the plane of the aromatic ring. This provides resonance stabilization. However, when a methyl group is attached to the ring ortho to the urethane group, the urethane group is sterically forced to rotate out of the plane of the ring. The consequences of this can be seen in the ¹H NMR spectra of 2,4-TDI-based polyurethanes. The chemical shifts of the two N-H protons are separated by approximately

0.8 ppm, suggesting a difference in the chemical environment of the two protons resulting from differences in conformation.

The results of a detailed investigation of D6T24 are presented below. Two samples of D6T24 were studied, with intrinsic viscosities of 0.322 dl/g and 0.573 dl/g. These will be referred to as "low molecular weight" and "high molecular weight," respectively. Later in the chapter, the properties of D6T24 will be compared to those of D6T26, a polyurethane similar to D6T24 but with a symmetrical structure.

3.2 D6T24: An Asymmetric Mesogenic Polyurethane

3.2.1 Synthesis of D6T24

D6T24 was synthesized by two methods: solid-state polymerization and solution polymerization. In the solid-state procedure, developed by Jadhav¹, BHHBP and 2,4-TDI were melted together under nitrogen in a closed vessel at 155-160 °C, and held at that temperature for 5 minutes to allow for mixing. The system was then cooled to 90 °C, and the mixture was allowed to react in the solid state for 24 hours. The solid chunk of crude polymer was ground into a powder with a mortar and pestle, dissolved in DMSO, and precipitated in methanol. The precipitate was collected by vacuum filtration, and dried under vacuum for 24 hours at 60 °C.

In the solution procedure, BHHBP was dissolved in DMF at 80-90 °C in a 5-necked round-bottom flask fitted with a condenser, a mechanical stirrer, a thermometer, and two addition funnels, one containing DMF and one containing 2,4-TDI. Dry nitrogen was bubbled through the BHHBP/DMF solution for 5 minutes; thereafter, nitrogen

was kept flowing continuously over the solution. 2,4-TDI was added dropwise to the solution, and the reaction was allowed to proceed at 80-90 °C for 20-24 hours. A stoichiometric excess of 2,4-TDI (between 0.5% and 1.0%) was used to compensate for side reactions involving isocyanate groups. As the reaction proceeded, DMF was added as needed to keep the solution viscosity low enough to allow fast stirring. The solution was poured into cold methanol to precipitate the polymer in the form of a white, fibrous material. The polymer was filtered, washed with fresh methanol, and dried under vacuum at 90 °C for 36 - 72 h.

Solid-state polymerization of D6T24 was carried out twice. The first attempt produced polymer with an intrinsic viscosity of 0.24 dl/g; the second attempt produced polymer which was insoluble in DMSO, indicating that crosslinking had occurred. Solution polymerization was more successful in producing high molecular weights. Eight batches of D6T24 were synthesized in solution; with intrinsic viscosities ranging from 0.300 dL/g to 0.573 dL/g. The highest-scale polymerizations produced the highest molecular weights, probably because the large scale minimized the influence of impurities and side reactions. Dibutyltin dilaurate was used as a catalyst in four of the runs; higher molecular weights were attained without the catalyst.

The samples of D6T24 with $[\eta] = 0.573$ dl/g and $[\eta] = 0.322$ dl/g are referred to in this dissertation as "high molecular weight" and "low molecular weight" respectively.

3.2.2 Crystalline and Liquid-Crystalline Phases

The DSC heating and cooling scans of low molecular weight D6T24 (Figure 3.2) show two endothermic peaks on heating and two exothermic peaks on cooling. This behavior is typical of thermotropic liquid-crystalline polymers, in which the lower-temperature peaks correspond to the crystal/mesophase transition (T_m) and the higher-temperature peaks correspond to the mesophase/isotropic transition (T_i).

To determine whether the DSC peaks of D6T24 arise from such transitions, POM and WAXS measurements were made in the temperature region between the two cooling peaks. POM measurements were made by observing D6T24 under the optical microscope while cooling the sample from temperatures above 180 °C at 5 °C/min. At high temperatures, no birefringence was seen, indicating that the sample was isotropic. A threaded texture indicating a mesophase (Figure 3.3) appeared at 132 °C; no other changes in texture were observed on continued cooling to 25 °C. Samples for WAXS were prepared by placing powdered D6T24 into a sealed capillary, heating to above the isotropization temperature, and then cooling slowly to the measurement temperature. The samples were exposed to the X-ray beam at constant temperature for 4 to 6 hours. Diffraction patterns indicating crystallinity (Figure 3.4) were observed at all temperatures between 100 °C and 160 °C.

The apparent contradiction between the POM and WAXS results is due to the different time scales of the experimental techniques. POM can monitor changes in texture almost instantaneously, while WAXS

measurements require several hours. A monotropic mesophase which forms quickly from the isotropic melt and then crystallizes when held at constant temperature would produce exactly the POM and WAXS results described above: POM would observe the rapidly formed mesophase, while WAXS would observe the slowly formed crystalline phase.

In order to observe the mesophase by WAXS, it is necessary to quench the sample to below its glass transition temperature shortly after the mesophase is formed. A simple way to accomplish this is to draw fibers from the isotropic melt at approximately 175 °C. The polyurethane cools to room temperature slowly enough to allow the mesophase to form, but quickly enough to prevent crystallization. This method has the added advantage of inducing orientation in the sample.

WAXS diffraction patterns of melt-drawn fibers at room temperature (Figure 3.5) indicate a smectic phase. When the fibers are heated to temperatures in the range 150 - 170 °C, the polyurethane crystallizes (Figure 3.6). Therefore it is concluded that D6T24 exhibits a monotropic smectic mesophase, with $T_i = 132$ °C and $T_m > 150$ °C. As will be shown later, T_m is highly dependent on molecular weight and thermal history.

Returning to the DSC scans (Figure 3.2), the cooling ramp is now understood. The higher-temperature exotherm is assigned to formation of the mesophase and the lower-temperature exotherm to crystallization. It is difficult at this stage to assign the two endotherms observed on heating. It is possible to assign the endotherms to the melting of two different crystalline forms, or to a two-stage crystal melting process.

Experiments to be discussed later give evidence for the former interpretation.

DSC heating and cooling scans of high molecular weight D6T24 (Figure 3.7) differ from those of the low molecular weight sample in two significant ways. First, the cooling exotherm assigned to crystallization occurs at a higher temperature (123 °C compared to 105 °C). This suggests that crystallization from the mesophase occurs more rapidly in the high molecular weight sample. Subsequent experiments⁴ provide more evidence for this interpretation. Second, the heating scan of the high molecular weight sample shows only one endotherm, at 169 °C. This phenomenon will be discussed later, in the section regarding the kinetics of crystallization and mesophase formation.

WAXS and optical microscopy results are virtually independent of molecular weight. WAXS shows the same crystal and mesophase ordering for both high and low molecular weight D6T24. The optical textures of the two samples are similar, except that the threaded texture is less distinct in the high molecular weight sample.

3.2.3 Kinetics of Crystallization and Mesophase Formation

Because D6T24 is monotropic, there are two available paths to crystallization: from the mesophase and from the isotropic melt. Studies of the crystalline phase mentioned above have dealt only with crystals formed from the mesophase. Crystallization from the isotropic melt can be accomplished by cooling to a temperature which is below T_m but above T_i , and annealing at that temperature. Such thermal treatment results in the appearance of spherulites in the optical

microscope (Figure 3.8). The photograph shown is of a sample annealed at 150 °C for approximately 1 day. Annealing at 140 °C produces smaller spherulites which form more quickly, indicating a higher rate of nucleation at the lower temperature. This phenomenon is observed in both high and low molecular weight samples of D6T24. On reheating the sample, the spherulites disappear at 165 - 170 °C.

Cooling the isotropic melt to 130 °C produces a threaded texture similar to that of Figure 3.3. In the first two minutes or so after this texture forms, it is possible to shear the sample between the two microscope slides. However, after two minutes this becomes impossible without fracturing the sample.⁴ This indicates that the appearance of the threaded texture corresponds to the formation of a fluid liquid-crystalline phase, and that isothermal annealing causes crystallization from this phase. Crystallization is not accompanied by any significant changes in the threaded texture. This is true whether crystallization from the mesophase occurs isothermally or during cooling.

It is possible to thermally treat the sample so that both melt-formed crystals and mesophase-formed crystals can be observed at once in the optical microscope. The sample is cooled from the isotropic melt to between 140 °C and 150 °C and held at constant temperature. Spherulites appear gradually against a black (isotropic) background. The sample is then cooled to below 132 °C; on reaching that temperature, the threaded (mesophase) texture appears in the areas that had been isotropic. An interesting effect is observed when the sample is reheated. The threaded texture disappears at a slightly lower temperature than the spherulites, indicating that the spherulitic crystalline form has a

higher melting temperature than the crystals formed from the mesophase. This is probably because the polymer chains have a greater degree of mobility in the isotropic phase than in the mesophase, which allows for the formation of larger crystals with fewer imperfections. The two crystalline forms are shown by WAXS to have the same unit cell; they differ solely in their long-range ordering.

Several experiments were conducted to measure the kinetics of crystallization from the isotropic melt. In one experiment, samples were cooled from the isotropic melt to 150 °C, annealed for various times, and then reheated.⁴ The enthalpy of the crystalline melting transition was measured. The results show that the crystalline phase forms more rapidly from the melt in the low molecular weight sample than in the high molecular weight sample. This is probably because the shorter chains have a greater degree of mobility. Crystallization from the mesophase, however, occurs more rapidly in the high molecular weight sample, as will be discussed below.

The data were fitted to an Avrami equation⁵⁻⁷, defined as

$$[\Delta H_{\infty} - \Delta H(t)]/\Delta H_{\infty} = -\exp(-kt^n) \quad (2.1)$$

where $\Delta H(t)$ is the crystal melting enthalpy for a sample annealed for a given time t , and ΔH_{∞} is the limiting value of $\Delta H(t)$ at long annealing times. The data give an Avrami exponent of $n = 2.6 \pm 0.2$.⁴ Three-dimensional crystal growth is theoretically associated with an Avrami exponent of 3.

The kinetics of crystallization from the mesophase were followed by means of an isothermal DSC scan, in which the sample was annealed at 128 °C and the heat evolved was measured as a function of time. It was found that the low molecular weight sample crystallizes more slowly, which is consistent with the DSC cooling scans of Figures 3.2 and 3.7. The Avrami exponents estimated were $n = 1.8 \pm 0.2$ for the low molecular weight sample and 1.4 ± 0.2 for the high molecular weight sample.⁴

The effect of heating rate on the thermal behavior of D6T24 was studied by cooling the samples from the isotropic melt to 40 °C at 10 °C/min and then reheating at 10, 1.0, 0.5 and 0.2 °C. The results are shown in Figure 3.9 (low molecular weight) and Figure 3.10 (high molecular weight). Slow heating allows for the melting and reformation of imperfectly formed crystals, allowing for the formation of more-perfect crystals which melt at higher temperatures. In both the high and low molecular weight samples, slow heating gives rise to a new endothermic peak at high temperatures.

Heating the low molecular weight sample at 1.0 °C/min and 0.5 °C/min results in broadening and weakening of the low-temperature endotherm and the appearance of a shoulder on the high-temperature end of the high-temperature endotherm (Figure 3.9b-c). The shoulder develops into a significant peak only at a heating rate of 0.2 °C/min (Figure 3.9d). The effect of slow heating is much more pronounced in the high molecular weight sample (Figure 3.10). The melting endotherm shows a large high-temperature shoulder when the heating rate is 1.0 °C/min (Figure 3.10b). At a heating rate of 0.5 °C/min, the

shoulder changes to a broad peak with roughly the same enthalpy as the original peak (Figure 3.10c). Finally, at a heating rate of 0.2 °C/min, the new, higher-temperature peak is larger than the original peak (Figure 3.10d). The difference in behavior of the low and high molecular weight samples indicates that cooling low molecular weight D6T24 at 10 °C/min produces crystals that are less amenable to perfection than those formed in the high molecular weight sample.

Slow heating was also performed on samples that were annealed for 8 hours at one of three temperatures: 130, 140, and 150 °C. The annealed samples were cooled to room temperature and reheated at 0.5 °C/min.⁴ In both low and high molecular weight D6T24, the sample annealed at 130 °C shows a new melting peak above 170 °C. This effect does not occur in the samples that were annealed at 140 °C or 150 °C, which indicates that the crystals grown from the isotropic melt are less amenable to perfection than those grown from the mesophase.

To better understand the origin of the high-melting crystal phase, a series of high-temperature annealing experiments was carried out.⁴ Samples which had been cooled from the isotropic melt at 10 °C/min were heated to temperatures between 160 °C and 190 °C and annealed for various times before quenching to room temperature and reheating at 10 °C/min. Annealing at temperatures up to 184 °C produces a small high-temperature endotherm, called the annealing peak, whose peak temperature is always higher than the annealing temperature. Peak enthalpy and peak temperature both increase with annealing time.

The aforementioned annealing peak is not observed in samples that are cooled to the annealing temperature from the isotropic melt.

The high-temperature melting phase observed on slow heating must therefore be due to the perfection of an existing lower-melting phase and not from a phase that forms directly from the isotropic melt.

The differences between crystals formed from the melt and those formed from the mesophase can be summarized as follows: Crystallization from the melt is faster for the low molecular weight sample, while crystallization from the mesophase is faster for the high molecular weight sample; the Avrami exponents are higher for crystallization from the isotropic melt than from the mesophase; the optical textures of the two crystal forms are different (spherulitic for melt-grown crystals, threaded for mesophase-grown crystals); and crystals formed from the mesophase are more readily perfected by slow heating and by annealing than those formed from the melt.

A possible physical interpretation for these results is that melt-grown crystals are chain-folded (hence the spherulitic texture)⁸, while the mesophase-grown crystals are chain-extended. This would explain why the mesophase-grown crystals are more amenable to perfection. This would also be consistent with the Avrami exponents, given that values of the Avrami exponent near 3 are physically interpreted to correspond to three-dimensional crystal growth, while lower values correspond to one- or two-dimensional growth.

The difference in the heating scans of the low and high molecular weight D6T24 may be explained as follows. On cooling the low molecular weight sample at 10 °C/min to below the isotropic-to-mesophase transition, formation of the mesophase may be accompanied by the formation of a number of chain-folded crystals directly from the isotropic

melt. These two processes occur at the same temperature, so only one DSC exotherm is observed. On further cooling, the mesophase crystallizes, resulting in the coexistence of melt-grown crystals and mesophase-grown crystals. Reheating leads to the melting of each crystal form, giving rise to two DSC endotherms. That this effect is not observed in the high molecular weight sample may be due to its slower rate of crystallization from the isotropic melt. On cooling at 10 °C/min, virtually all of the crystallization in the high molecular weight sample occurs from the mesophase.

Another experiment was performed to test the supposition that the lower- and higher-temperature endotherms in the heating scan of low molecular weight D6T24 arise from mesophase-grown and melt-grown crystals respectively. A series of DSC scans was done in which low molecular weight D6T24 was cooled from the isotropic melt to a given temperature (T_r) and then immediately reheated. The cooling and heating rates were 10 °C/min in all runs. The results are shown in Figure 3.11.

The DSC scans resulting from cooling to 40 °C and reheating (previously presented in Figure 3.2) are included in Figure 3.11 for the purpose of comparison. The two endotherms in this heating scan appear at 154 °C and 166 °C.

Three of the values of T_r (122 °C, 124 °C and 125 °C) are well below T_i but above the onset of the crystallization exotherm. Reheating from these temperatures produces first an exothermic region (indicating cold crystallization) and then two endotherms at 153 ± 1 °C and 167 ± 1 °C.

The lower-temperature endotherm decreases in enthalpy as T_r increases.

Reheating from 128 °C, a temperature just slightly below T_i , produces first an endotherm, which indicates disordering of the mesophase. Next an exotherm appears, indicating crystallization from this disordered state. Finally, two endotherms appear, corresponding to crystal melting. This time, the endotherm at 167 °C is many times larger than the one at 153 °C. This is consistent with the supposition that the lower-temperature endotherm corresponds to crystals formed from the mesophase, while the higher-temperature endotherm corresponds to crystals formed from the isotropic melt. Further evidence for this interpretation is given by reheating from 136 °C. Cooling only to this temperature, which is above T_i , does not allow the mesophase to form. Reheating results in a broad exotherm indicating crystallization from the melt, followed by a single endotherm at 167 °C. The lower-temperature endotherm does not appear, suggesting that it corresponds to melting of mesophase-grown crystals.

3.3 D6T26: A Symmetrical Variant of D6T24

3.3.1 Motivation for Studying D6T26

One of the notable features of the structure of D6T24 is the asymmetry brought about by the 2,4-TDI linkage. To investigate the effect of removing this asymmetry, a polyurethane was studied which differs from D6T24 only in that the methyl group near the urethane linkages is in a symmetrical location. This symmetrical polyurethane is

called D6T26 and its structure is shown, alongside the structure of D6T24, in Figure 3.12.

As mentioned earlier, polyurethanes based on 2,4-TDI are structurally akin to random copolymers. As the polymerization reaction proceeds, either of the two non-equivalent isocyanate groups in 2,4-TDI may add to the growing polymer chain, leading to a randomly distributed sequence of non-equivalent repeat units. The isocyanate groups in 2,6-TDI, however, are equivalent, and polyurethanes based on 2,6-TDI and a symmetrical diol therefore have a regular, symmetrical structure. It was anticipated that this difference in structure would render D6T26 more readily crystallizable than D6T24. It was not, however, assumed that this would prevent D6T26 from forming a liquid-crystalline phase, as changes in crystallization kinetics or mesophase stability could also result from the modification in structure. D6T26 was characterized by techniques already used on D6T24, in order to ascertain whether asymmetry was a necessary condition for liquid crystallinity in this system.

3.3.2 Synthesis and Solution Properties

D6T26 was synthesized in solution by a procedure similar to that used for D6T24. 2,6-TDI was substituted for 2,4-TDI; no catalyst was used.

One of the first noticeable differences between D6T24 and D6T26 is the much lower solubility of D6T26 in DMF and DMSO at low temperatures. At temperatures above 80 °C, both polyurethanes are soluble in DMF and DMSO at weight fractions of up to 40%. At room

temperature, D6T24 remains soluble up to about 20%; above this concentration, a solution cooled to room temperature forms a gel over a period of 12 - 24 hours. This is a result of crystallization, as confirmed by WAXS. The same phenomenon is observed in solutions of D6T26, except that it occurs in solutions with concentrations as low as 2%. In both cases the effect is reversible; heating the solution causes the polymer to redissolve.

Because of the poor solubility of D6T26 at low temperatures, viscosity measurements were made in DMF at 60 °C. At that temperature, the intrinsic viscosity of D6T26 is 0.535 dL/g.

3.3.3 Crystalline and Liquid-Crystalline Phases

DSC heating and cooling traces of D6T26 are shown in Figure 3.13. The scan rate is 10 °C per minute. The heating trace shows one large endothermic peak at 190 °C and a very small endothermic peak at 198 °C. Only one exotherm is observed on cooling, at 154 °C.

WAXS results are qualitatively similar to those of D6T24. WAXS patterns at temperatures ranging from 23 °C to 160 °C show D6T26 to be crystalline. The diffraction pattern of crystalline D6T26, shown in Figure 3.14, indicates that the crystalline unit cell of D6T26 is different from that of D6T24 (Figure 3.4). This is not surprising, given the steric effect that the methyl group asserts on the carbonyl group on the urethane linkage. In D6T24, only one urethane group is ortho to the methyl group, while in D6T26, both urethane groups are ortho to the methyl group. The bond angles in and near the urethane linkages are hence different in the two polyurethanes, which causes their crystal

structures to be different. A detailed analysis of the crystal structure of D6T26 was conducted by Papadimitrakopoulos et al.⁹

Under the optical microscope, a threaded texture appears on cooling D6T26 to below 154 °C. In contrast to what was observed for D6T24, it is not possible to shear the D6T26 sample between the microscope slides upon the appearance of this texture. This suggests that the sample has crystallized.

Smectic ordering can be seen in D6T26 by drawing a fiber from the isotropic melt at 220 °C. The WAXS diffraction pattern of such a fiber is shown in Figure 3.15. Annealing the sample at 150 °C causes the sample to crystallize, leading to a diffraction pattern similar to Figure 3.14.

A possible interpretation of these results is that D6T26, like D6T24, is also a monotropic liquid-crystalline polymer. D6T26, however, has a much greater driving force for crystallization due to its regular structure. A mesophase which forms at 154 °C, but crystallizes much faster than the mesophase of D6T24, could plausibly give rise to only one peak in the DSC cooling scan.

To investigate whether thermal events too weak to be seen in the DSC cooling scan occur in D6T26 at temperatures below the single exothermic peak, a series of reheating experiments was performed (Figure 3.16) similar to those done on D6T24 (Figure 3.11). On reheating from 145 °C and 150 °C, the high-temperature DSC peaks are identical to those obtained on reheating from 40 °C. This indicates that no significant thermal events occur below 150 °C.

If D6T26, like D6T24, is monotropic, it should be expected to also display two different crystalline forms - one grown from the mesophase, and one grown from the isotropic melt. A slow heating study was done on D6T26 (Figure 3.17) that parallels those done on D6T24 (Figures 3.9 and 3.10). Slow heating results in a dramatic increase in the enthalpy of the higher-temperature endotherm in the heating scan, which suggests that the higher-temperature peak corresponds to imperfectly formed crystals which are perfected by slow heating.

The observations described above indicate that both D6T24 and D6T26 form monotropic smectic phases. The behavior of the two polyurethanes is qualitatively similar; the primary effect of the asymmetry of D6T24 is that it lowers both T_m and T_i . Both polyurethanes fulfill the primary requirements set forth at the outset of this research project: They are polyurethanes which exhibit liquid crystallinity at low temperatures. However, the tendency of both polyurethanes to crystallize renders their liquid-crystalline phases monotropic, making characterization of these phases difficult. Therefore, it was deemed worthwhile to find a way to suppress crystallization. Blending and copolymerizing D6T24 and D6T26 proved to be an effective way to do this; the results are discussed in the next chapter.

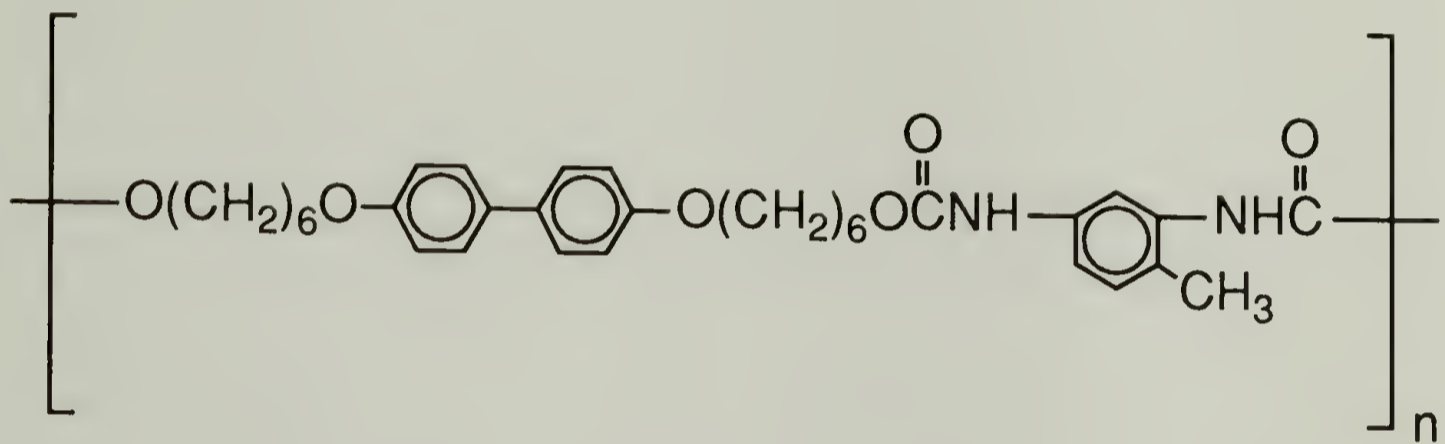


Figure 3.1. Structure of D6T24.

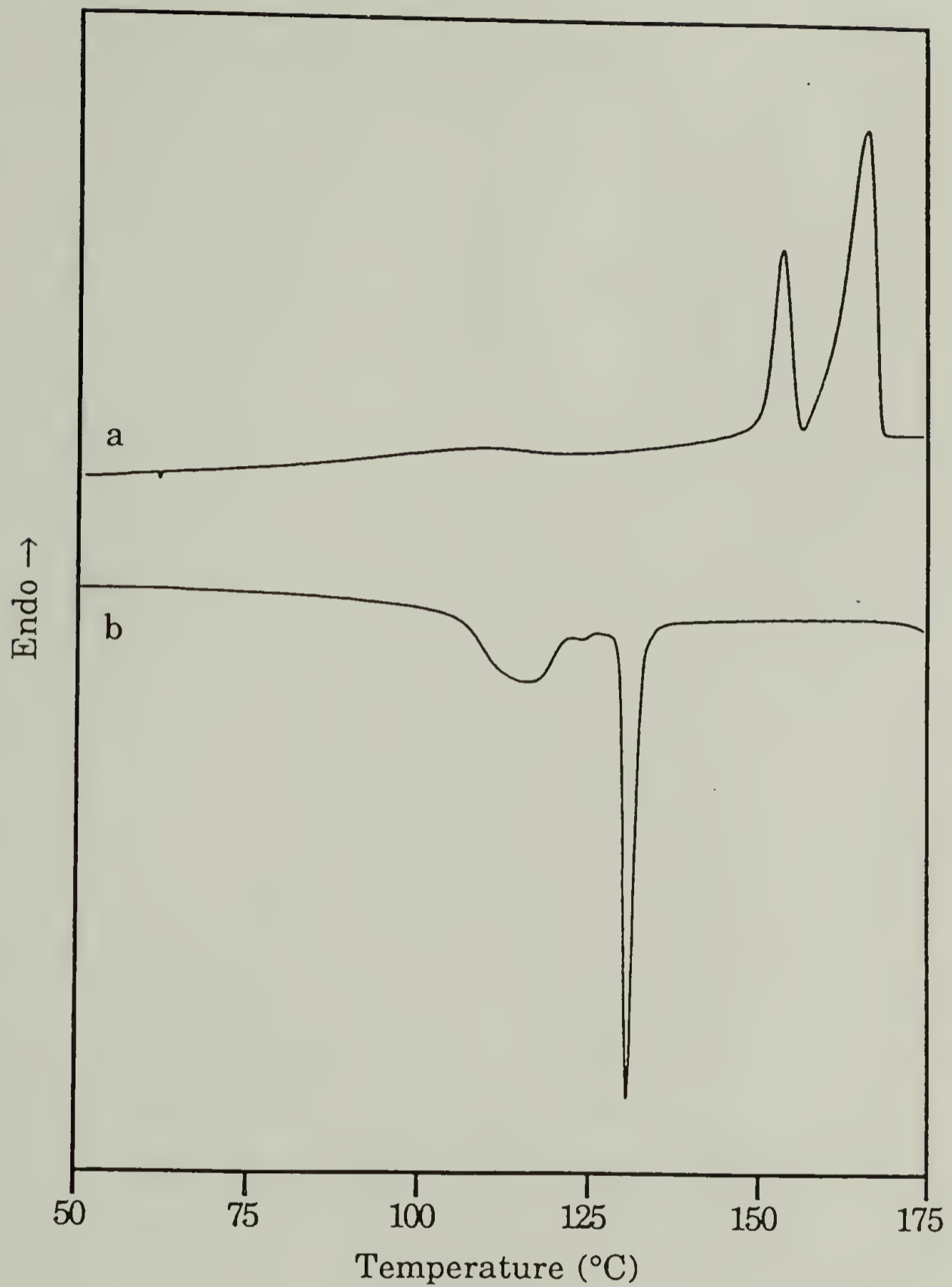


Figure 3.2. DSC scans (10 °C/min) of low molecular weight D6T24 after cooling from the isotropic melt at 10 °C/min: a) heating; b) cooling.

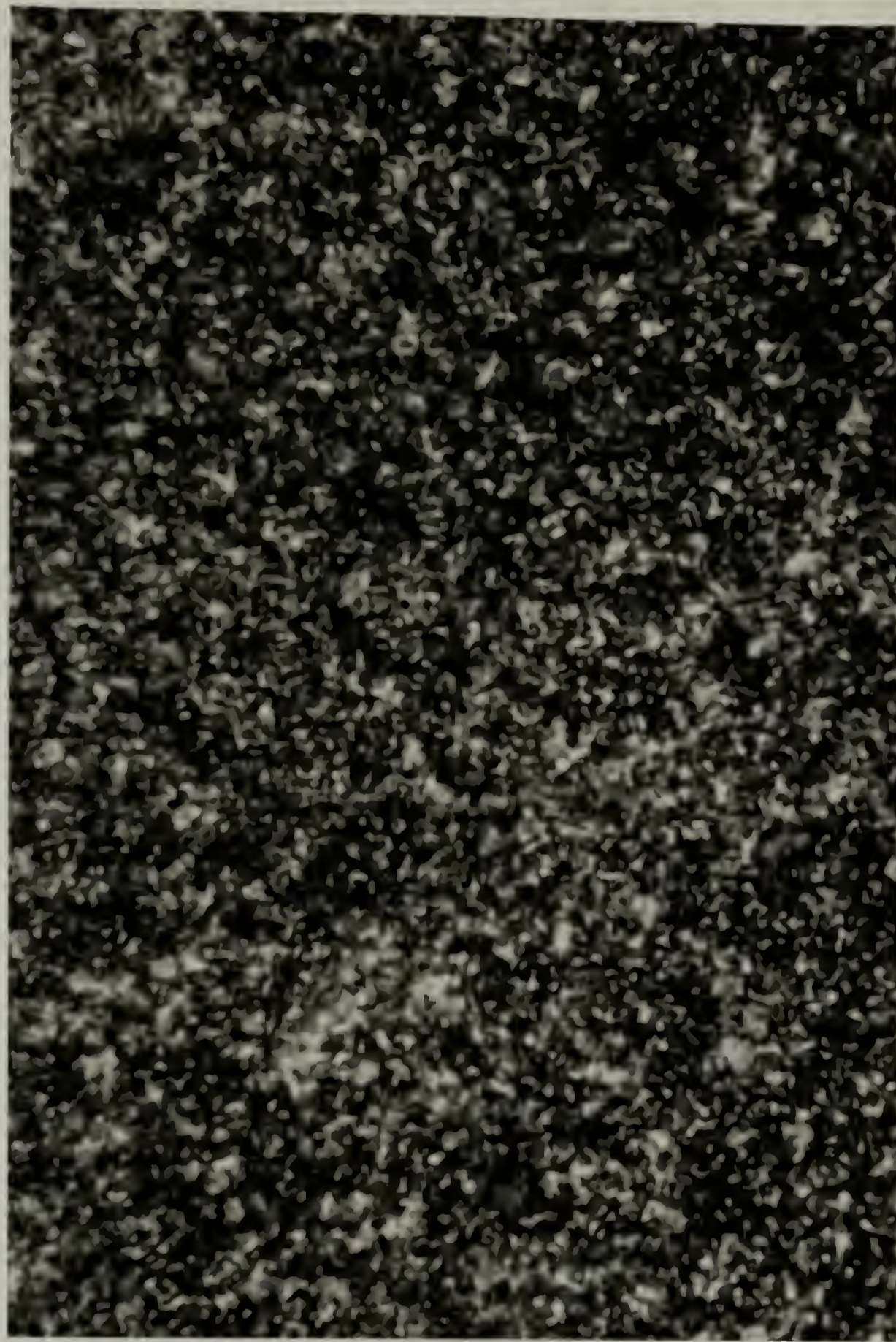


Figure 3.3. Texture of low molecular weight D6T24 seen in the polarizing optical microscope after cooling to below 132 °C.

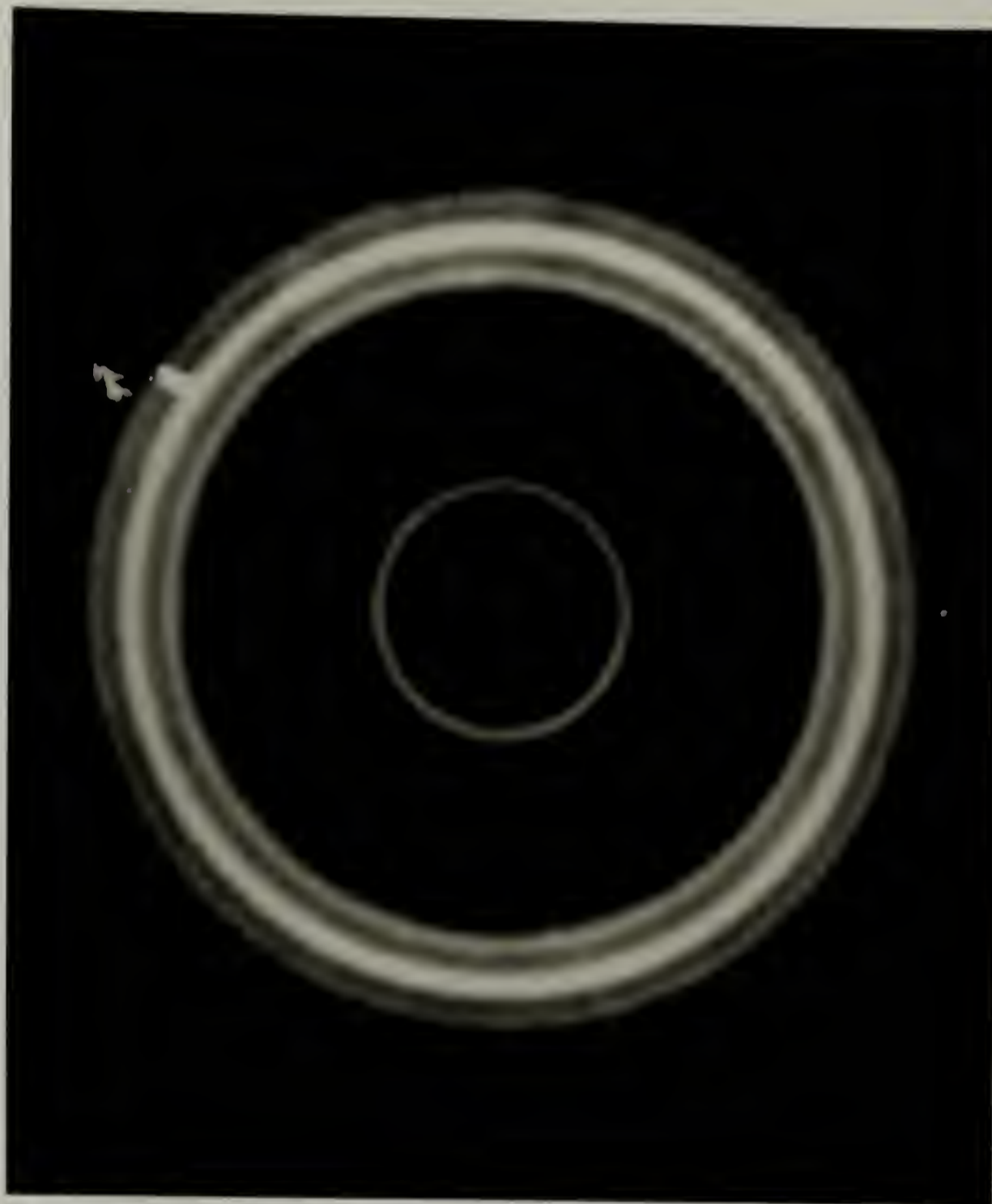


Figure 3.4. WAXS diffraction pattern of high molecular weight D6T24 in the crystalline state.



Figure 3.5. WAXS diffraction pattern of D6T24 fibers drawn from the isotropic melt at 178 °C, before thermal treatment.



Figure 3.6. WAXS diffraction pattern of D6T24 melt-drawn fibers after annealing 16.5 h at 174 °C.

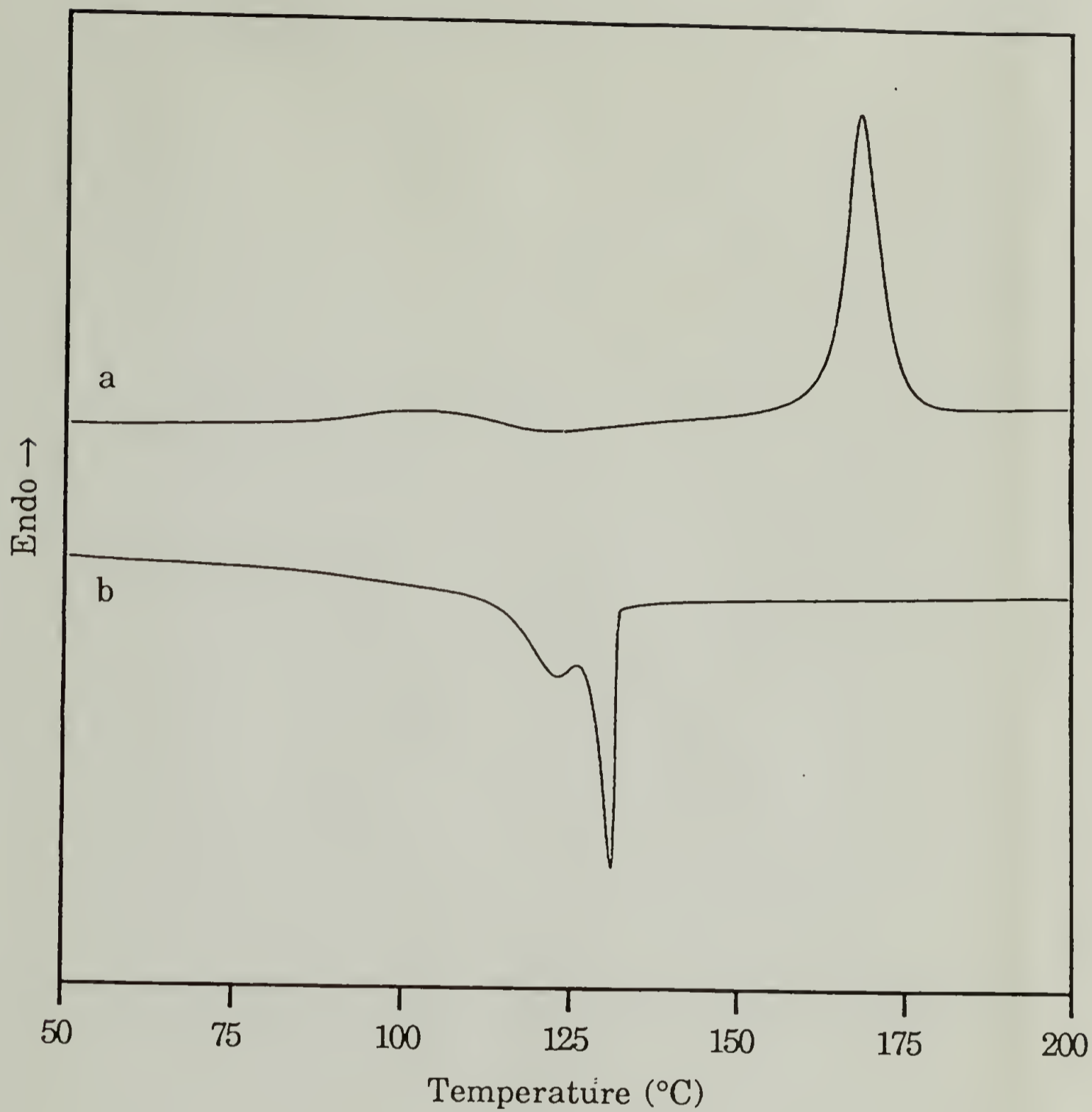


Figure 3.7. DSC scans (10 °C/min) of high molecular weight D6T24 after cooling from isotropic melt at 10 °C/min: a) heating; b) cooling.

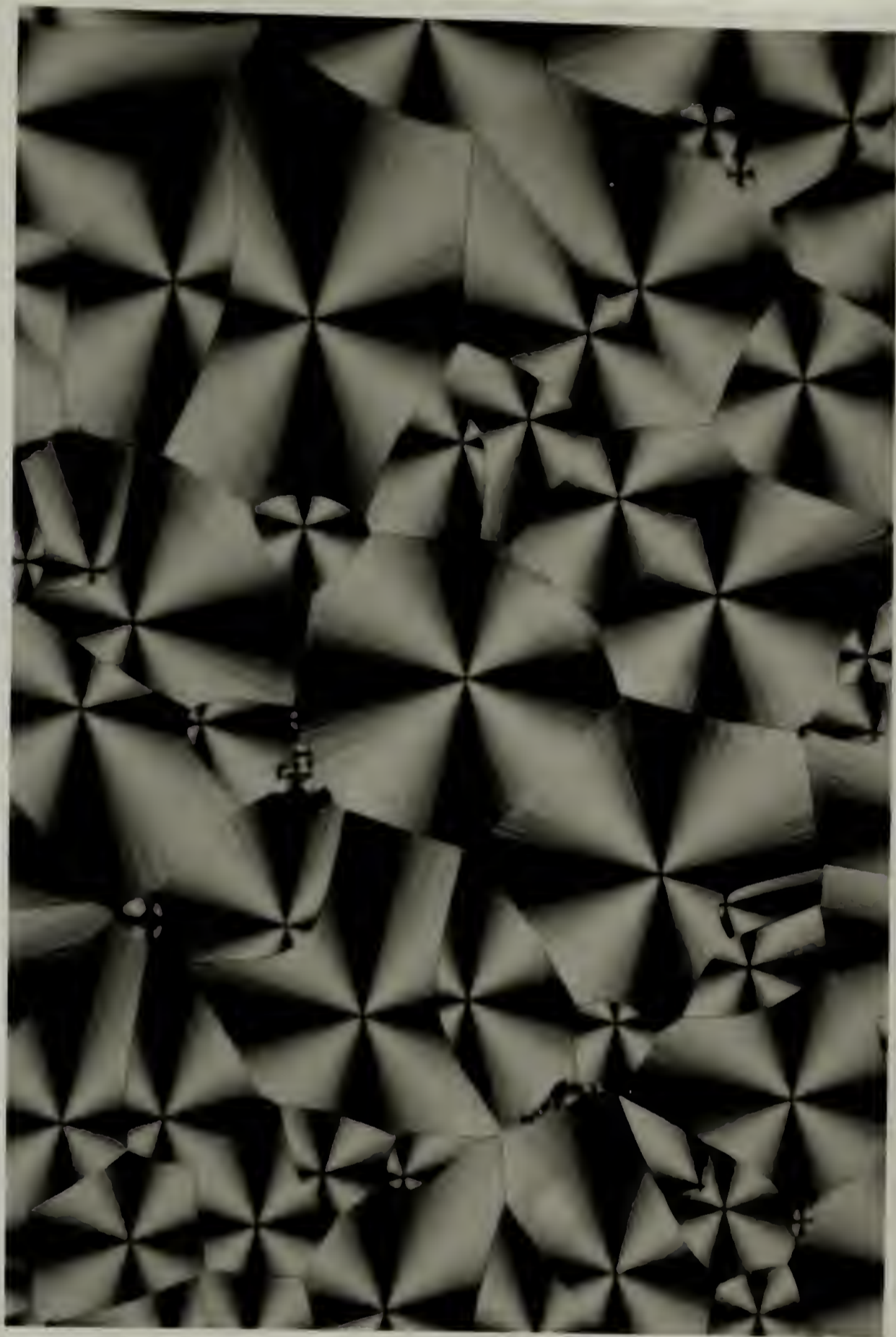


Figure 3.8. Texture of D6T24 seen in the polarizing optical microscope after annealing at 150 °C.

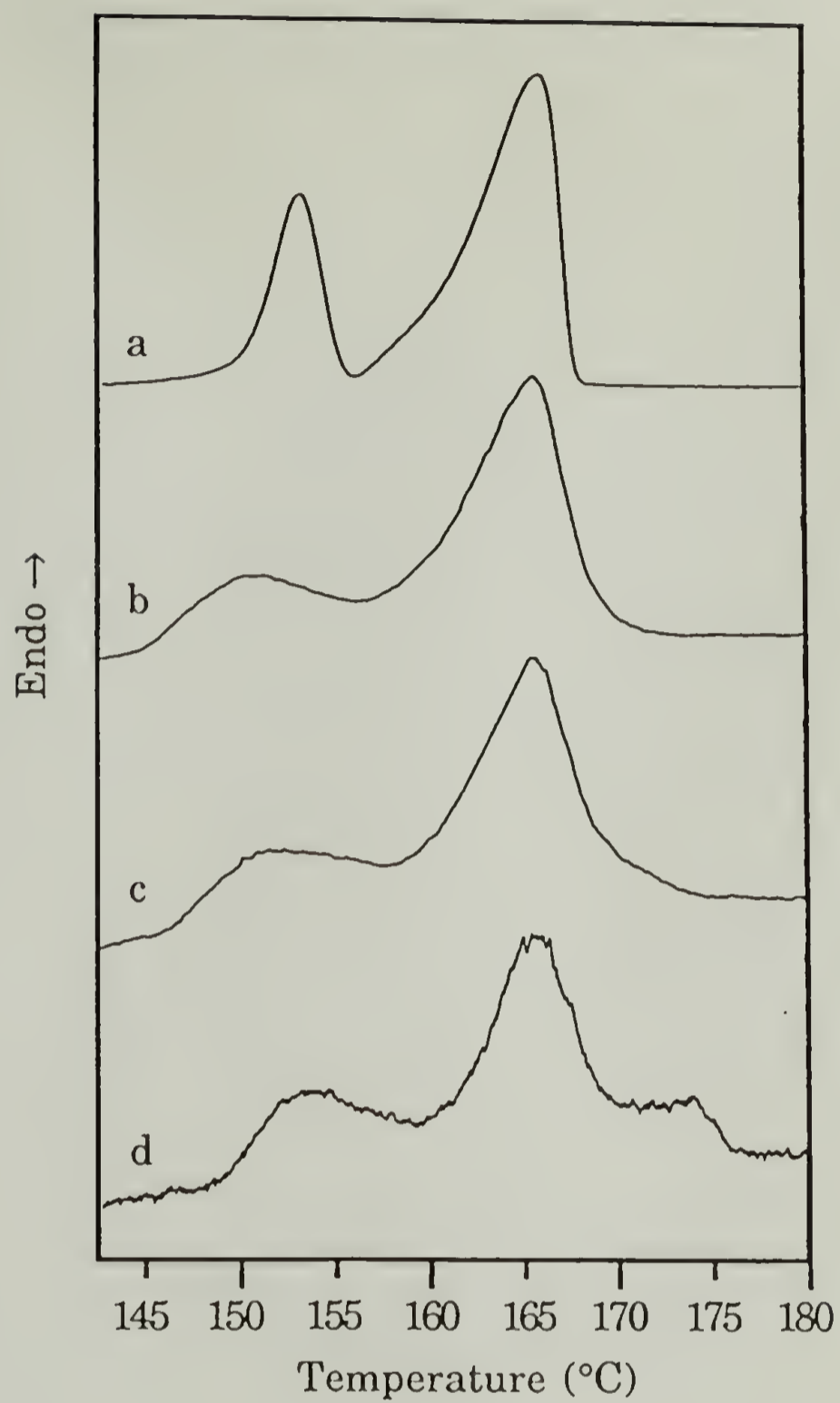


Figure 3.9. DSC heating scans of low molecular weight D6T24 at various rates: a) 10 °C/min; b) 1.0 °C/min; c) 0.5 °C/min; d) 0.2 °C/min.

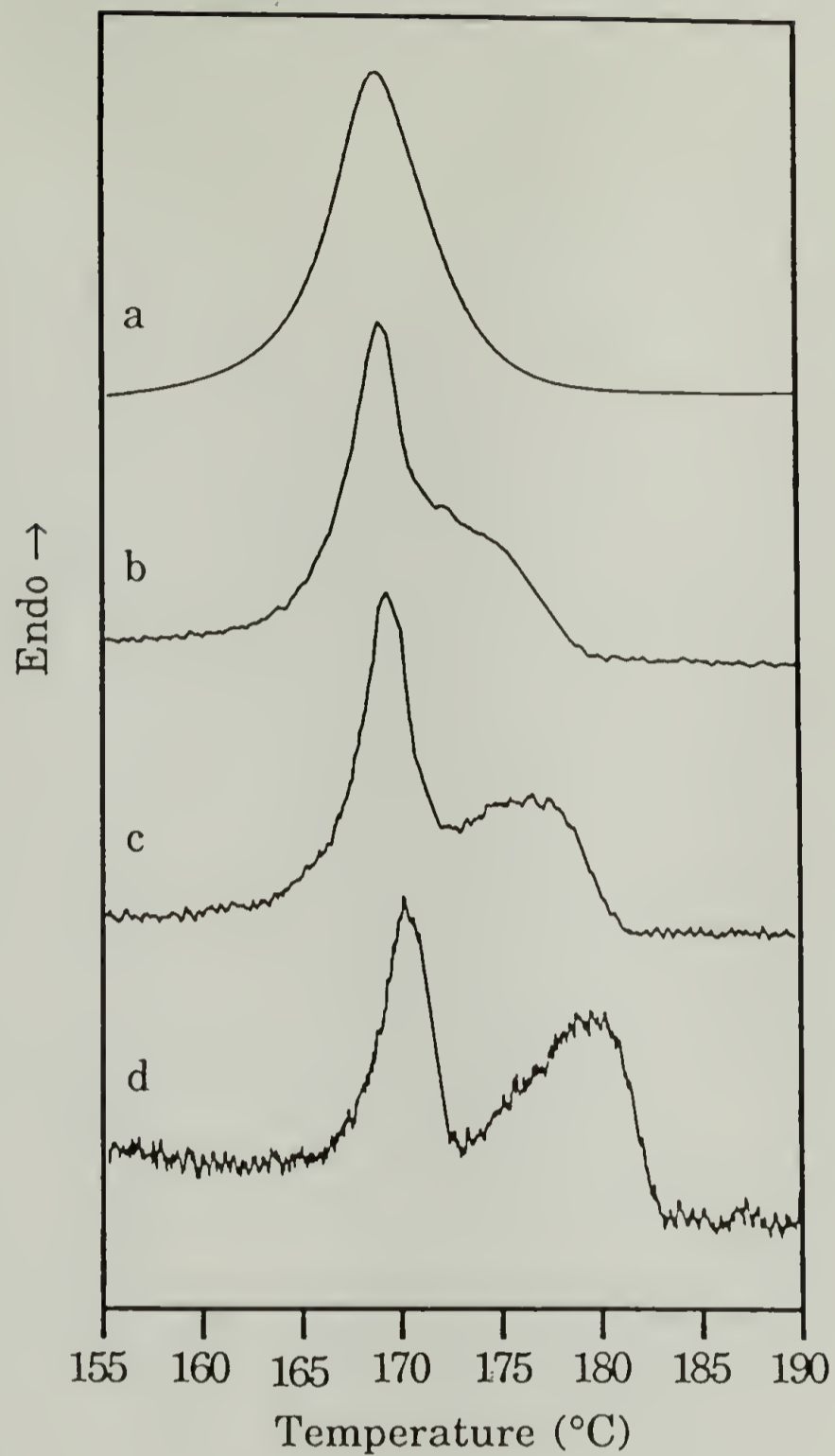


Figure 3.10. DSC heating scans of high molecular weight D6T24 at various rates: a) 10 °C/min; b) 1.0 °C/min; c) 0.5 °C/min; d) 0.2 °C/min.

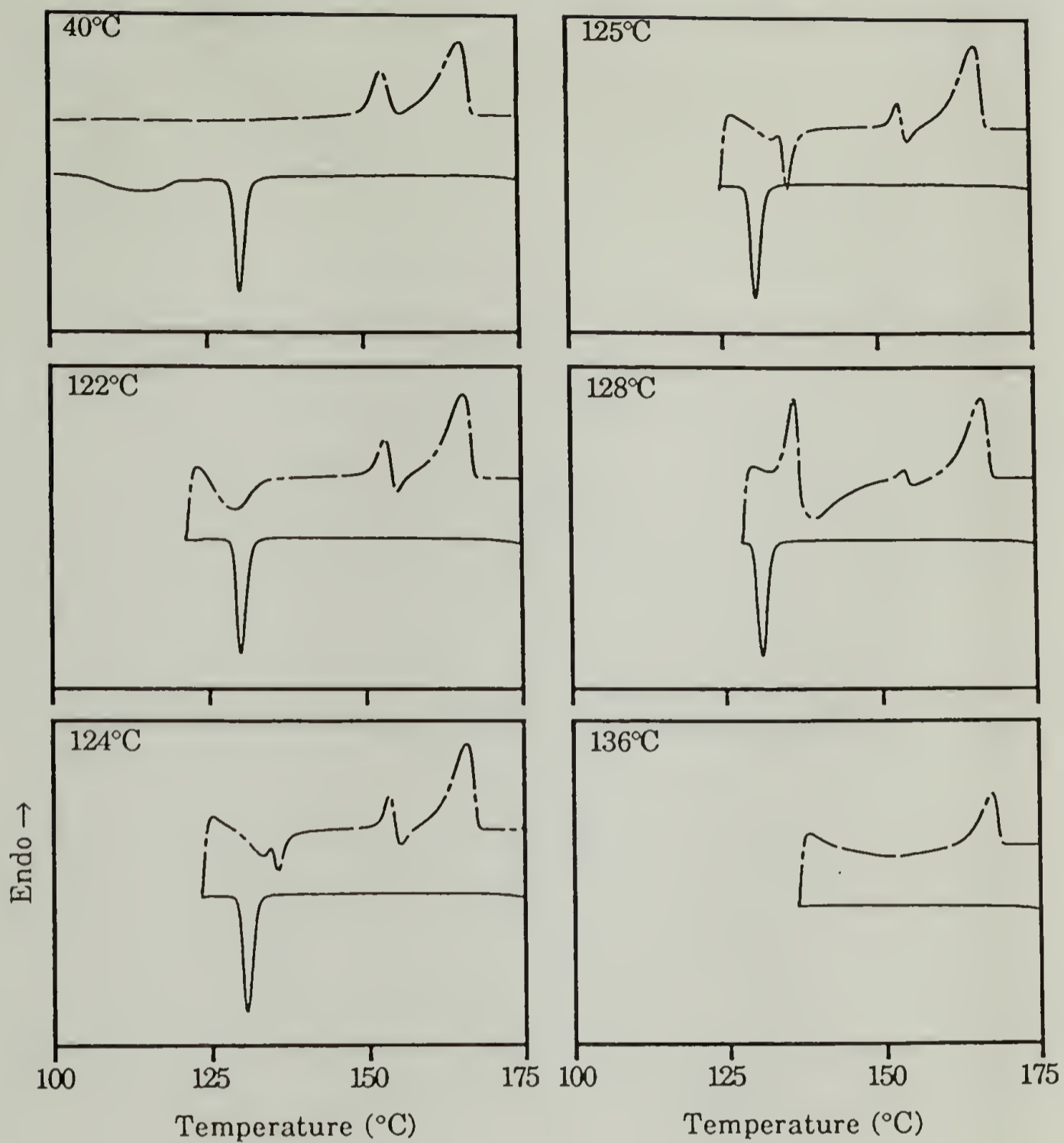
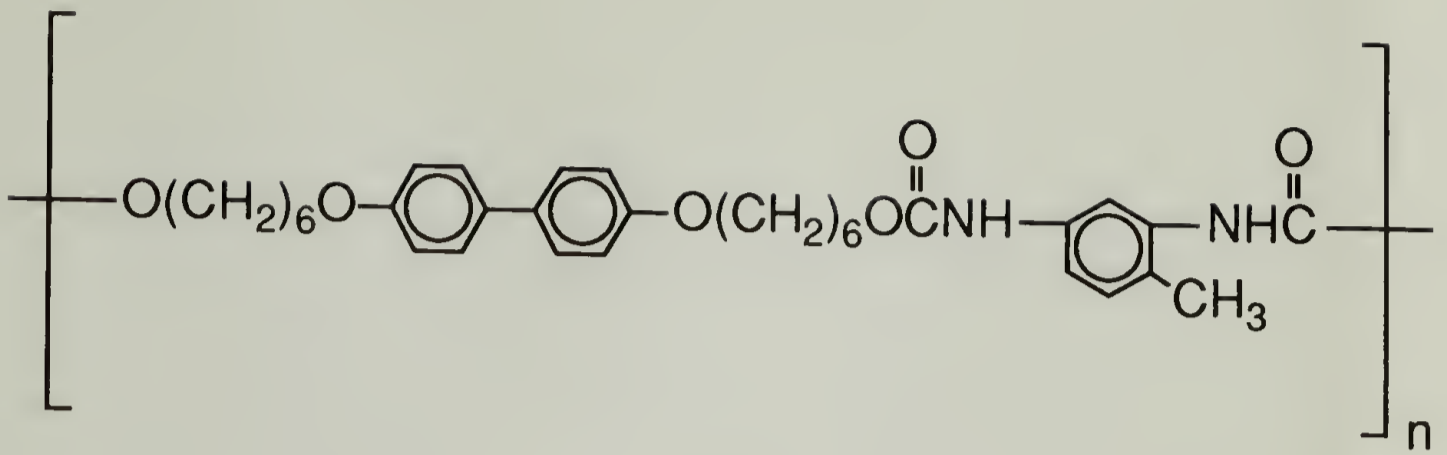
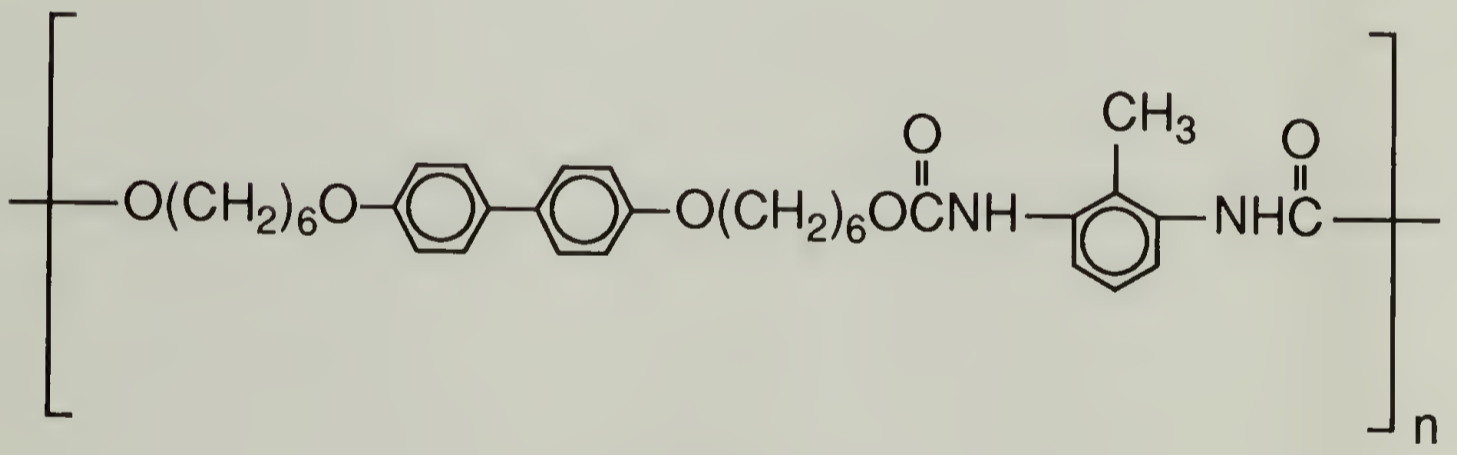


Figure 3.11. DSC scans (10 °C/min) of low molecular weight D6T24, cooled from the isotropic melt to various temperatures and then immediately reheated. Solid lines represent cooling; broken lines represent heating.



D6T24



D6T26

Figure 3.12. Structures of D6T24 and D6T26.

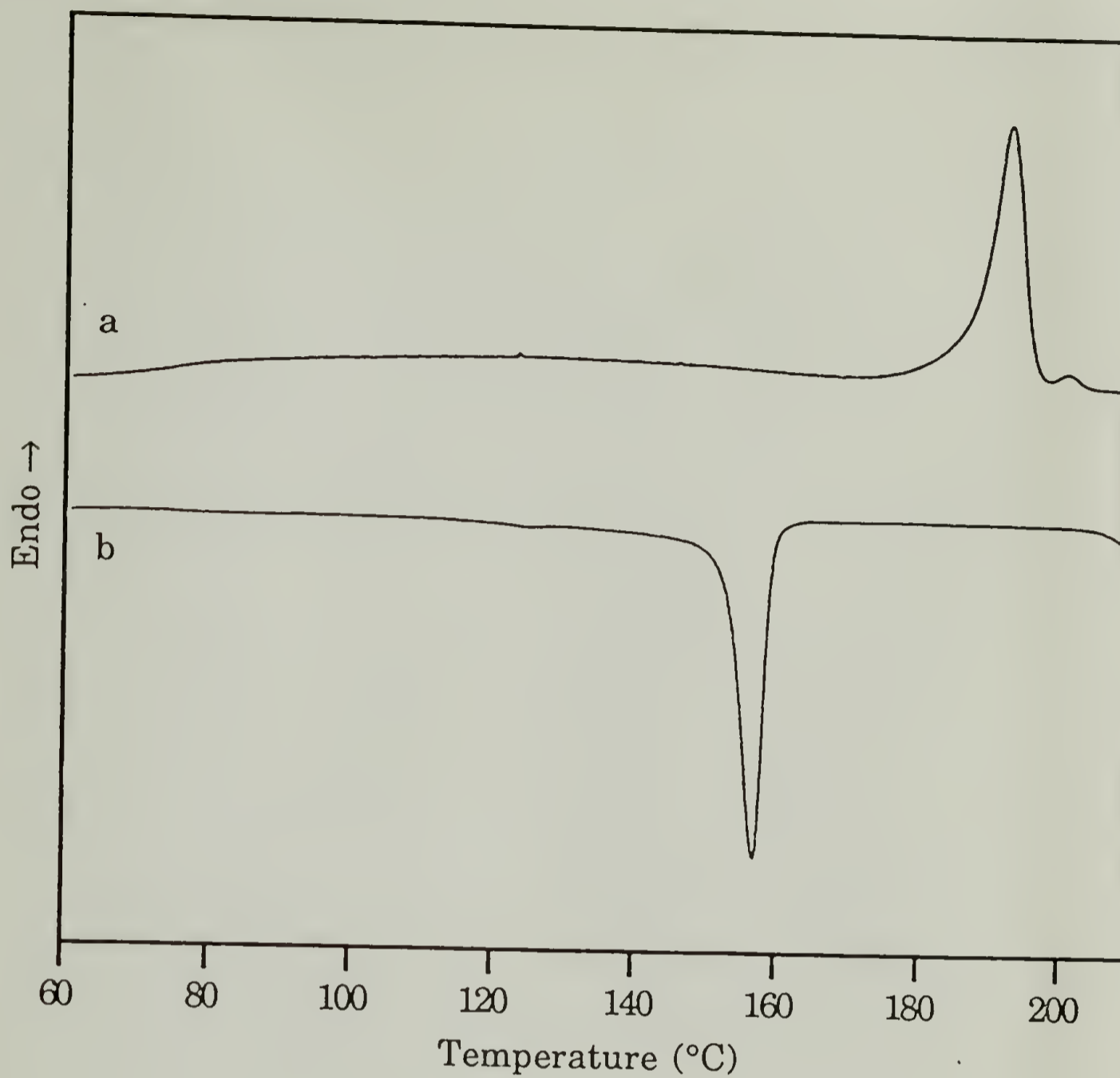


Figure 3.13. DSC scans (10 °C/min) of D6T26 after cooling at 10 °C/min from isotropic melt: a) heating; b) cooling.

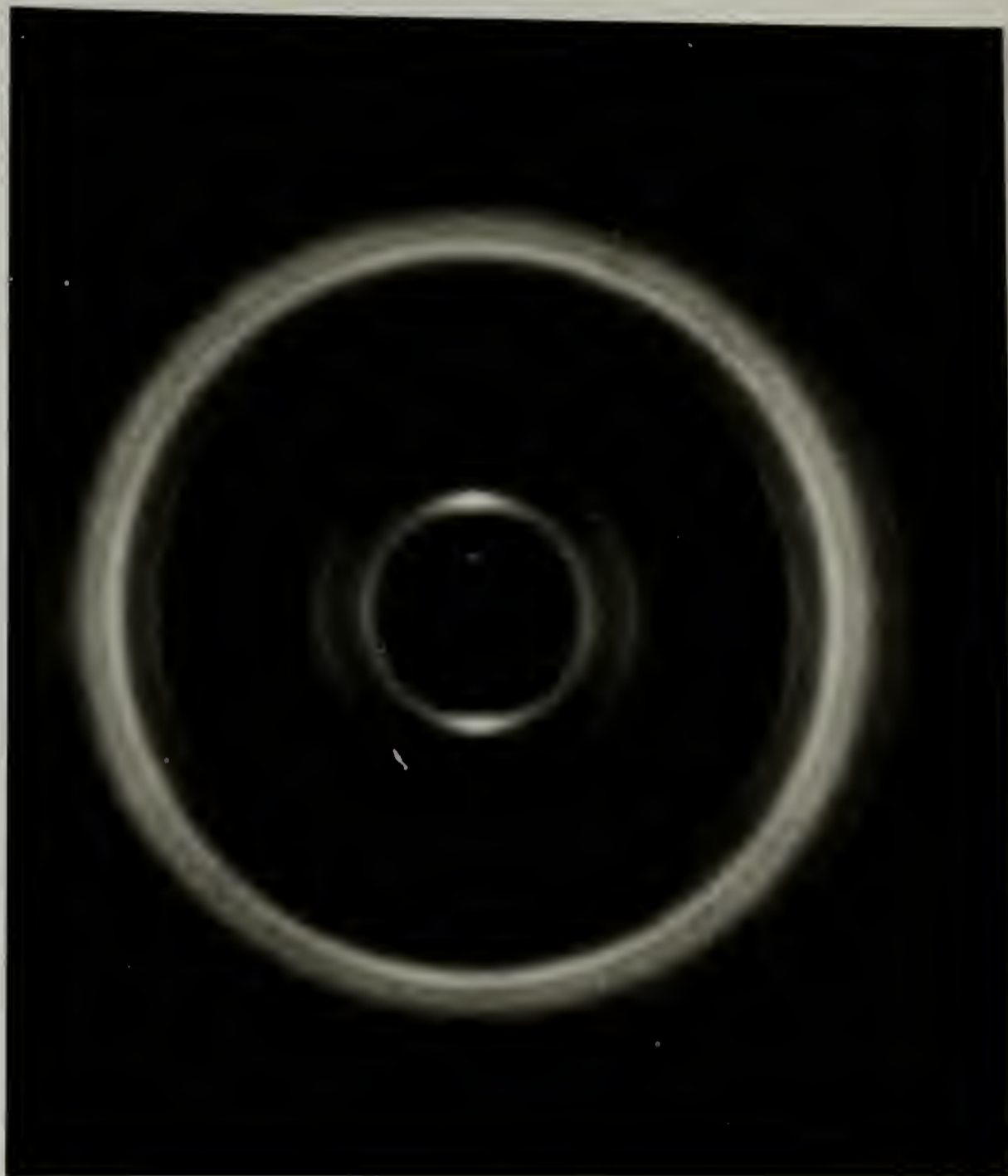


Figure 3.14. WAXS diffraction pattern of a melt-drawn fiber of D6T26 (150 °C).



Figure 3.15. WAXS diffraction pattern of a melt-drawn fiber of D6T26 (23 °C).

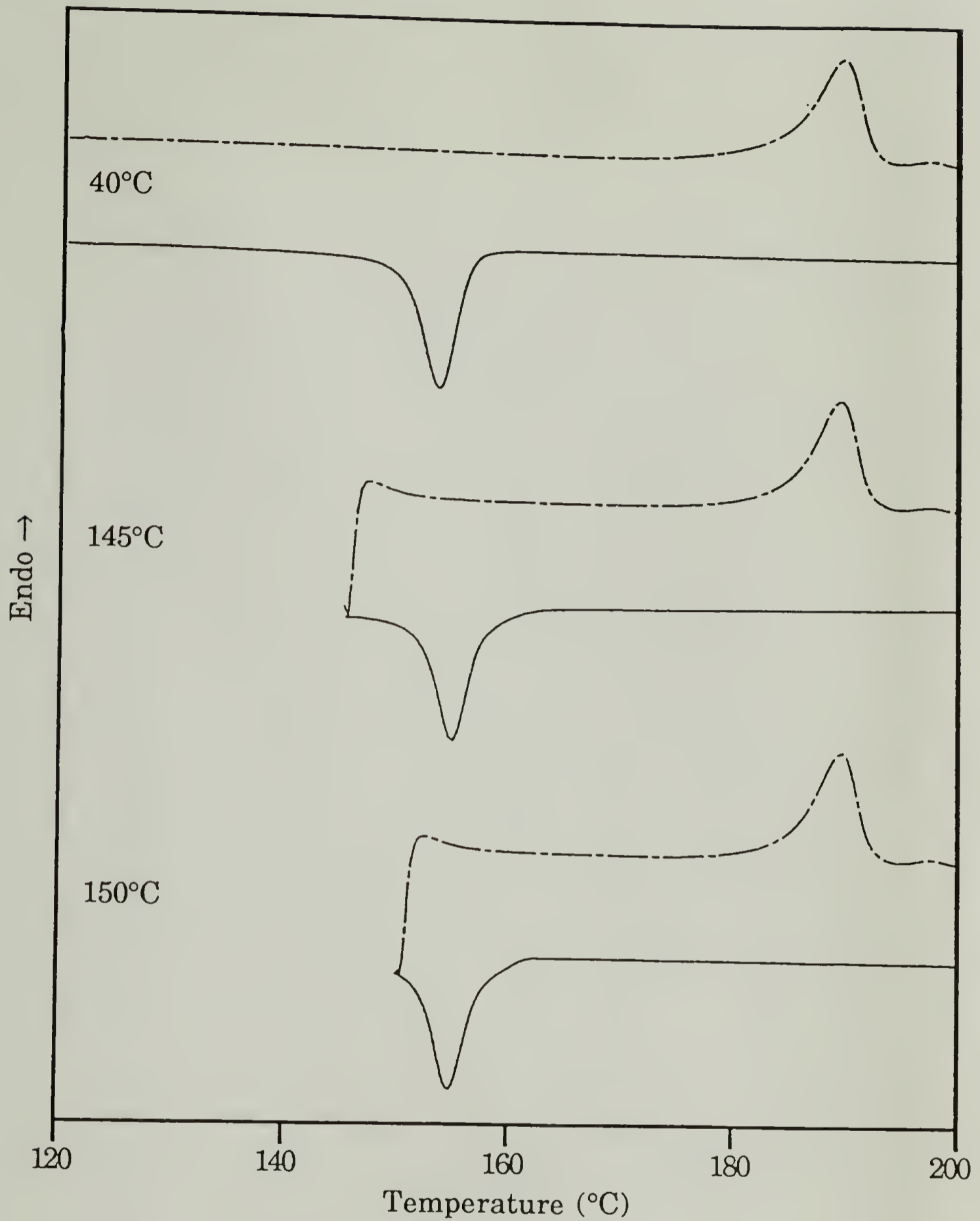


Figure 3.16. DSC scans (10 °C/min) of D6T26, cooled from the isotropic melt to various temperatures and then immediately reheated. Solid lines represent cooling; broken lines represent heating.

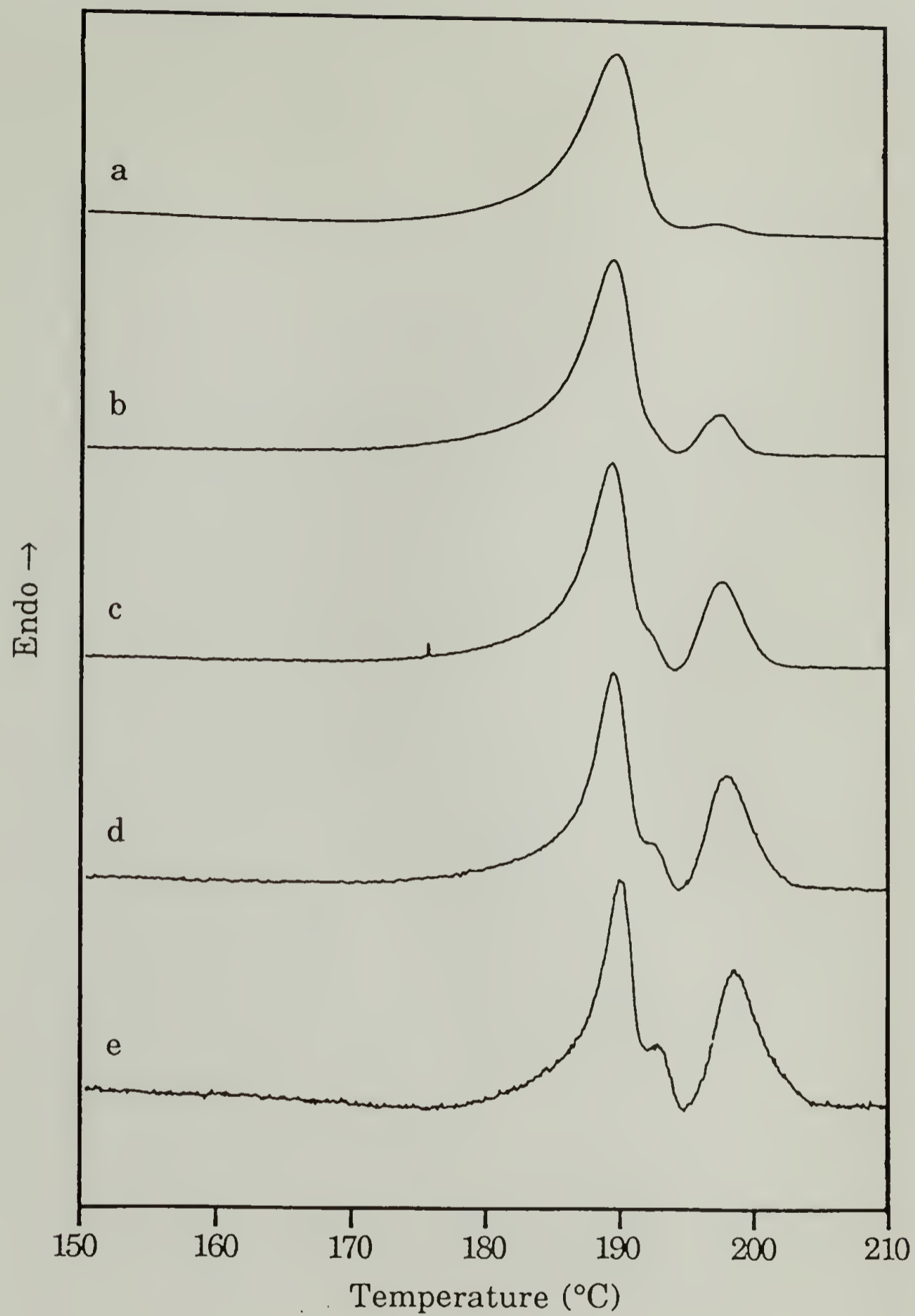


Figure 3.17. DSC heating scans of D6T26 at various rates: a) 10 °C/min; b) 5 °C/min; c) 2 °C/min; d) 1 °C/min; e) 0.5 °C/min.

References

- (1) Jadhav, J. Y., Kantor, S. W. Submitted for publication.
- (2) Papadimitrakopoulos, F., Stenhouse, P. J., MacKnight, W. J. To be submitted.
- (3) Kricheldorf, H. R., Awe, J. *Makromol. Chem.* **1989**, *190*, 2579.
- (4) Smyth, G., Vallés, E. M., Pollack, S. K., Grebowicz, J., Stenhouse, P. J., Hsu, S. L., MacKnight, W. J. *Macromolecules* **1990**, *23*, 3389.
- (5) Avrami, M. J. *J. Chem. Phys.* **1939**, *7*, 1103.
- (6) Avrami, M. J. *J. Chem. Phys.* **1941**, *8*, 212.
- (7) Avrami, M. J. *J. Chem. Phys.* **1941**, *9*, 177.
- (8) Bassett, D. C. *Principles of Polymer Morphology*; Cambridge University Press: Cambridge, 1981.
- (9) Papadimitrakopoulos, F., Hsu, S. L., MacKnight, W. J. Submitted for publication.

CHAPTER 4

BLEND AND COPOLYMERS OF D6T24 AND D6T26

4.1 Motivation for Preparing Blends and Copolymers

As was noted earlier, there are several methods of altering the structure of a monotropic liquid-crystalline polymer so as to bring about enantiotropic behavior.¹⁻⁷ One such method is copolymerization.^{1,2} Because the crystalline phases of D6T24 and D6T26 are dissimilar, copolymers of D6T24 and D6T26 should be expected to have a much lower tendency to crystallize than either homopolymer. If the copolymers crystallize at all, the melting temperature should be lowered. If a copolymer forms a mesophase, and the crystalline melting temperature is lowered enough that it is below T_i , enantiotropic behavior will result.

Blending of D6T24 and D6T26 may have the same effect as copolymerization, if the blends are miscible under the relevant conditions. To study the effects of combining D6T24 and D6T26 in one system, a series of blends was prepared. There are several advantages to using blends rather than copolymers in a study such as this one. One advantage is that preparing blends of available polymers is much less time-consuming than synthesizing new polymers. Another advantage is that a series of blends with a range of compositions can be made from one sample of each homopolymer, thereby assuring that the molecular weights are uniform throughout the series. The primary disadvantage of using blends is that the crystallization and mesophase-forming

behavior of the mixed system, which is the focus of the study, may be complicated by mixing and unmixing effects. To determine whether such effects cause the blends to behave much unlike the analogous copolymers, one copolymer of D6T24 and D6T26 was synthesized and characterized.

4.2 Blends of D6T24 and D6T26

4.2.1 Preparation of Blends

Blends of D6T24 and D6T26 were obtained by first dissolving the two components in DMF (approximately 50 mg polymer/3 mL DMF) at 70-75 °C, and then pouring the solution into 40 mL methanol to precipitate the polymer blend. The blends were dried in a vacuum oven overnight at 50 60 °C. Low molecular weight D6T24 was used.

Nine blends were prepared, with D6T24 weight fractions of 10%, 20%, 30%, 40%, 50%, 60%, 70%, 80% and 90%. The blends are identified henceforth as B_x, where x is the percent by weight of D6T24.

4.2.2 Properties of Blends

The WAXS pattern given by a typical blend (B60) after precipitation from solution is shown in Figure 4.1. The diffraction pattern appears to consist of the crystalline diffraction patterns of D6T24 and D6T26 superimposed on one another. The DSC scans of B60 are shown in Figure 4.2. The first heating scan (Figure 4.2a) shows endothermic peaks at 173 °C and 185 °C which, in conjunction with the WAXS results, appear to correspond to melting of crystalline D6T24 and

D6T26 respectively. It appears that as the blend precipitates from solution, the two components phase separate and crystallize.

Optical microscopy indicates that the sample is isotropic above the two melting peaks described above. In the DSC cooling scan, a sharp exothermic peak appears at 128 °C (Figure 4.2b) accompanied by a small low-temperature shoulder. In the optical microscope, this transition is accompanied by the appearance of a threaded texture similar to that of Figure 3.3. No further changes are seen in the optical microscope on cooling to room temperature.

WAXS measurements of the once-heated and once-cooled B60 give the scattering pattern shown in Figure 4.3. The sharp inner ring and diffuse outer ring are indicative of a smectic phase. Reheating the sample gives the DSC scan of Figure 4.2c. One sharp endotherm appears, which has a peak temperature of 136 °C and is accompanied by a long, weak low-temperature shoulder. No other transitions are seen on further heating. Subsequent cooling and heating scans reproduce Figure 4.2b and Figure 4.2c exactly.

The most likely interpretation of these results is that the blend, once it is allowed to phase-mix in the isotropic melt, forms a smectic phase on cooling to below 128 °C. The smectic phase does not crystallize on further cooling. Therefore, blending D6T24 and D6T26 produces an enantiotropic mesophase.

In some of the blends, producing a homogeneous system requires more extensive thermal treatment than the single heating and cooling cycle described above for B60. The results of repeatedly heating and cooling B40 at 10°C/min are shown in the DSC heating scans of Figure

4.4. The first heating scan (Figure 4.4a) once again shows the melting of the crystalline phases of pure D6T24 and D6T26. Note that the relative sizes of the lower-temperature peak (melting of D6T24) and the higher-temperature peak (melting of D6T26) reflect the different compositions of blends B60 and B40. The second heating scan (Figure 4.4b) gives a sharp endothermic transition similar to the one in the second heating scan of B60 (Figure 4.2). The peak temperature is 5 °C higher (141 °C) and the low-temperature shoulder is more significant in B40 than in B60. After the sharp endotherm, a weak exothermic peak appears at 156 °C followed by an endothermic peak at 181 °C. These two peaks appear to correspond to cold crystallization and subsequent melting of D6T26. These higher-temperature transitions become less intense on repeated heating and cooling. By the fourth heating (Figure 4.4c) only a very small endotherm is noticeable at 180 °C, and by the eighth heating (Figure 4.4d) the higher-temperature peaks are gone completely.

The same result can also be accomplished by annealing the sample for a long time in the isotropic melt. An as-precipitated sample of B40 was heated to 200 °C, cooled to 170 °C, and annealed for 6 hours before cooling at 10 °C/min to room temperature. Reheating gave a DSC scan similar to Figure 4.4d, with no high-temperature transitions.

It is apparent that thermal treatment of the D6T24/D6T26 blends in the isotropic melt produces a homogeneous system. However, the experiments discussed up to this point do not address whether the changes in the system are the result of improved phase mixing, chemical reactions, or both. In polyurethanes, exposure to high temperatures leads to breaking and reforming of the urethane linkage.

Breaking of the urethane linkage results in one polymer chain with an isocyanate end group and another polymer chain with a hydroxyl end group. Each of these end groups may connect with an end group from a different polymer chain, leading to a new urethane linkage; the reaction is known as transurethanification. In segmented polyurethanes, transurethanification can lead to a change in the distribution of hard segment lengths, commonly referred to as "scrambling." In the blends of D6T24 and D6T26, such a process would cause the system to change first from a blend to a block copolymer, as fragments of D6T24 chains connect with fragments of D6T26 chains, and then to a random copolymer. Experiments to be discussed later in this chapter suggest that the blends do indeed become copolymers as a result of annealing at high temperatures.

Several attempts were made to prepare blends of D6T24 and D6T26 without the initial step of dissolving and reprecipitating the homopolymers in a common solvent. Powdered samples of D6T24 and D6T26 were ground together with a mortar and pestle, placed in a DSC pan, and annealed at 180 °C after first heating to 220 °C. DSC heating scans were taken after cooling the annealed samples to room temperature, and the results showed only a small endotherm corresponding to the mesophase, followed by fairly large endotherms corresponding to the crystalline phases of the pure homopolymers. This holds true for annealing times of up to 36 hours. It appears that dissolving and reprecipitating is a crucial step in the efficient mixing of the two polymers, even though precipitation causes phase separation and crystallization of each homopolymer. Most likely, precipitation

causes the polymers to separate into small domains, which have a large interfacial area and are therefore able to rapidly mix or react with one another, while simply grinding the two components together in the solid state and then melting results in large domains which have less interfacial area and do not mix or react as rapidly.

DSC heating scans of blends B80, B60, B40, B20 are shown in Figure 4.5 along with the heating scans of pure D6T24 and D6T26. In all cases, the blends were annealed in the isotropic melt until subsequent DSC heating and cooling scans at 10 °C/min were reproducible. B80, B60 and B40 appear to form enantiotropic smectic phases. B90, B70, and B50, not shown in the figure, behave similarly. At higher weight fractions of D6T26, however, behavior is different. B20 does not form a smectic phase, but rather forms a crystalline phase with the same unit cell as pure D6T26. The melting temperature is depressed slightly, as is the enthalpy of the melting transition, indicating a greater degree of imperfection in the crystalline phase than in pure D6T26. At this composition, the relatively small amount of D6T24 acts as an impurity. B10, not shown in the figure, is similar to B20.

The critical composition for the formation of an enantiotropic smectic phase appears to be near 30% D6T24. B30, not shown in the figure, is capable of forming a mesophase, but the annealing time required to bring about reproducible DSC scans is very long. Even after more than 24 hours at 170 °C, a DSC heating scan similar to Figure 4.4b is obtained, indicating the coexistence of a mixed phase (forming a mesophase on cooling) and pure D6T26 (crystallizing on cooling). It is possible that the inability to produce a mesophase in blends with a high

weight fraction of D6T26 is caused by the fact that the molecular weight of D6T26 in these samples is higher than that of D6T24. This would result in a lower degree of chain mobility in the D6T26-rich blends, requiring a longer time for the system to reach an equilibrium degree of mixing (or reaction). However, the reproducibility of the DSC scans of B20 and B10 after very long annealing times indicates that those systems are at equilibrium, and that their tendency to crystallize rather than form a mesophase is not a result of phase separation.

4.3 C47: A Random Copolymer of D6T24 and D6T26

A random copolymer of D6T24 and D6T26 was synthesized by the condensation of BHHBP with a mixture of 2,4-TDI (47%) and 2,6-TDI (53%). This copolymer, which will be referred to as C47, was found to exhibit behavior similar to that of the annealed blends.

4.3.1 Synthesis of C47

The synthesis of C47 was carried out in solution. BHHBP (9.165 g) was dissolved in 95 ml DMF at 81 °C with constant stirring. Argon was bubbled through the solution for 30 minutes; subsequently, argon was kept continuously flowing into and out of the reaction flask. 2,4-TDI (1.96 g), 2,6-TDI (2.19 g) and DMF (5 mL) were injected into an addition funnel by means of a syringe. These quantities of reactants correspond to a 1.005-to-1 mole ratio of diisocyanate to diol. The diisocyanate mixture was added dropwise over a period of approximately 2 hours, and the reaction was continued at 81 ± 1 °C for an additional 22 hours. The polymer was precipitated in methanol, Soxhlet extracted with methanol,

and dried under vacuum at 55 °C for 15 hours. The yield was 11.25 g (84%).

4.3.2 Properties of C47

DSC scans of C47 (second heating and second cooling) are shown in Figure 4.6. These results are very similar to those found for the annealed blends. The peak temperatures are 144 °C on heating and 132 °C on cooling. Repeated heating and cooling gives identical results.

Optical microscopy and WAXS results confirm that the peaks correspond to a smectic/isotropic phase transition. Cooling C47 to below 132 °C in the optical microscope gives threaded textures similar to Figure 3.3, indicating a mesophase. The WAXS pattern of a melt-drawn fiber of C47 (Figure 4.7) consists of the sharp, low-angle meridional reflection and diffuse, high-angle equatorial reflection indicative of smectic ordering. Powder samples of C47, at temperatures below 132 °C, give similar results, except that due to lack of orientation the reflections are rings rather than arcs.

4.4 Annealing Studies of Copolymers and Blends

It has been established that annealing D6T24/D6T26 blends at high temperatures is an effective way to combine the two polyurethanes into a homogeneous system. Lower-temperature annealing studies were also carried out, for two objectives: to determine whether a homogeneous system could be converted back to a heterogeneous system by thermal treatment, and to determine whether a crystalline phase

could be obtained which incorporated both D6T24 and D6T26 into one unit cell.

First, parallel annealing studies were done on C47 and a sample of B60 that had been heated to the isotropic melt only briefly and then cooled to room temperature. Melt-drawn fibers of both samples were annealed at 120 °C for 6.5 hours. The DSC heating scans for the annealed samples are shown, along with those for samples that were not annealed, in Figure 4.8. In both the copolymer and the blend, annealing causes the small, broad low-temperature endotherm to increase in enthalpy and move to higher temperature. In B60, but not in C47, an additional endotherm appears at 158 °C. These phenomena are explained by the WAXS results.

The WAXS pattern for the annealed copolymer is shown in Figure 4.9. Annealing has caused the reflection corresponding to interchain spacing to sharpen into two distinct components (compare Figure 4.7), indicating increased ordering within the smectic layers. This is reflected in the DSC scan (Figure 4.8a-b) by a two-stage clearing transition, with the first peak corresponding to loss of order within the smectic layers and the second peak corresponding to isotropization. There are no further thermal events on continued heating.

The WAXS diffraction patterns of the B60 fibers are shown in Figure 4.10 (before annealing) and Figure 4.11 (after annealing). The most striking change upon annealing is the appearance of reflections corresponding to crystalline D6T24 (compare Figure 3.6). Annealing has allowed some of the D6T24 in the blend to phase-separate and crystallize. Melting of this crystalline phase is shown by the small

endotherm at 158 °C in Figure 4.8d. The crystalline D6T24 reflections dominate the WAXS pattern so it is difficult to see the reflections arising from the smectic phase, but the DSC scan (Figure 4.8d) shows a change in the clearing transition similar to that seen for C47, indicating that an increase in the ordering within the smectic layers occurs in B60 as well. No crystalline phase incorporating both D6T24 and D6T26 is observed in either case.

The only major difference between the blend and the copolymer in these experiments is that in the untreated blend, annealing under the conditions described can induce phase separation and crystallization of one of the homopolymers. This is not possible in the copolymer because it would require breaking of the covalent bonds that keep the D6T24 and D6T26 repeat units in one phase. It was mentioned earlier that annealing at high temperatures may cause the blends to be transformed into copolymers by means of transurethanification reactions. To test this theory, a sample of B60 was held at 180 °C for 8 hours and then subjected to the same annealing conditions as described in the preceding paragraphs. If high-temperature annealing does in fact cause the blends to be transformed into copolymers, then subsequent annealing at 120 °C should not be sufficient to bring about phase separation and crystallization of pure D6T24.

The DSC heating scan of B60 following this two-stage annealing process is shown in Figure 4.12. The isotropization transition is resolved into two sharp peaks, just as in the other B60 sample, but in this sample there is no endotherm at 158 °C. No phase separation and crystallization of D6T24 has occurred. The results are consistent with

the interpretation that high-temperature annealing induces transurethanification reactions that transform the blends into copolymers.



Figure 4.1. WAXS diffraction pattern (23 °C) of B60, as precipitated from solution.

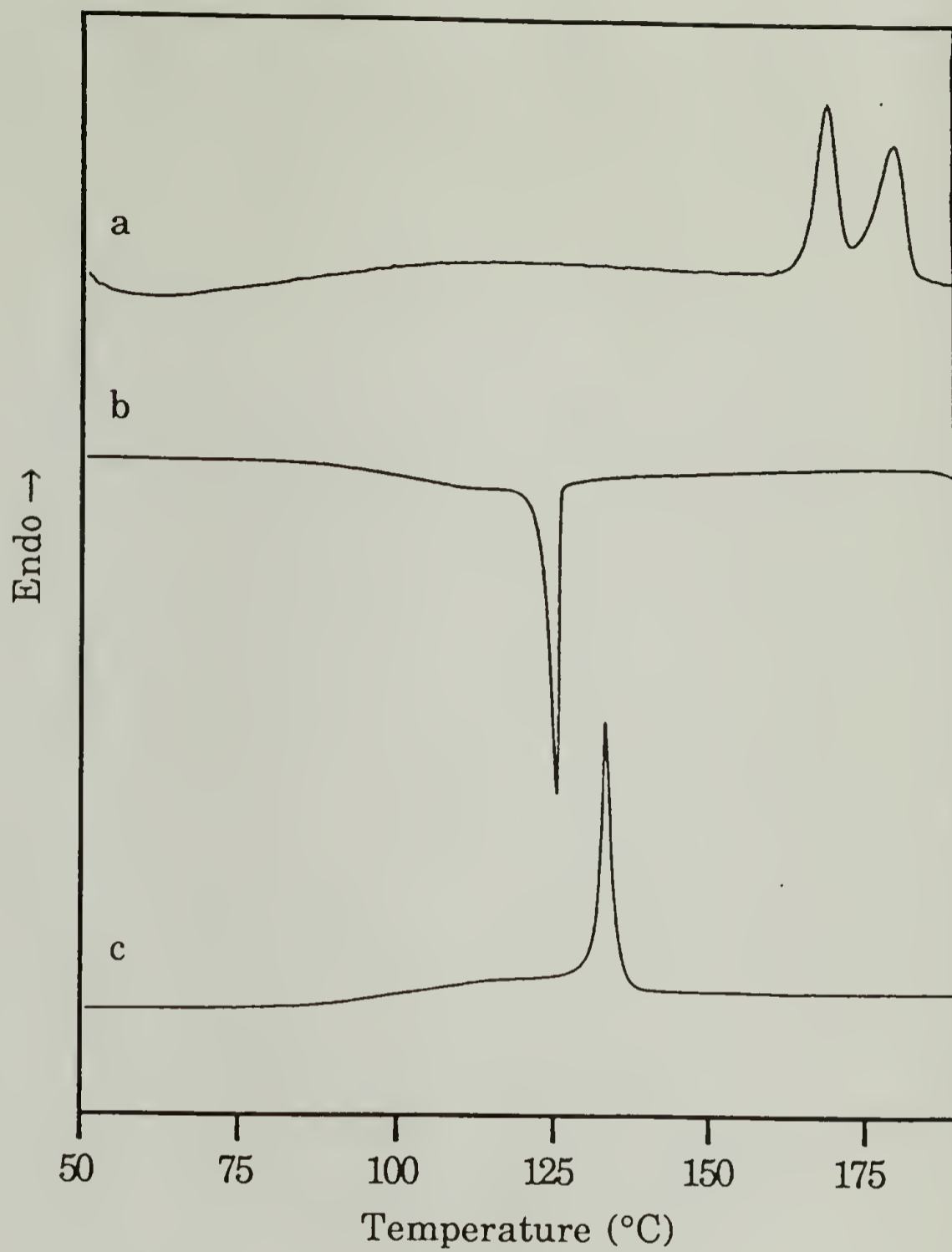


Figure 4.2. DSC scans (10 °C/min) of B60 after precipitation from solution: a) first heating; b) first cooling; c) second heating.

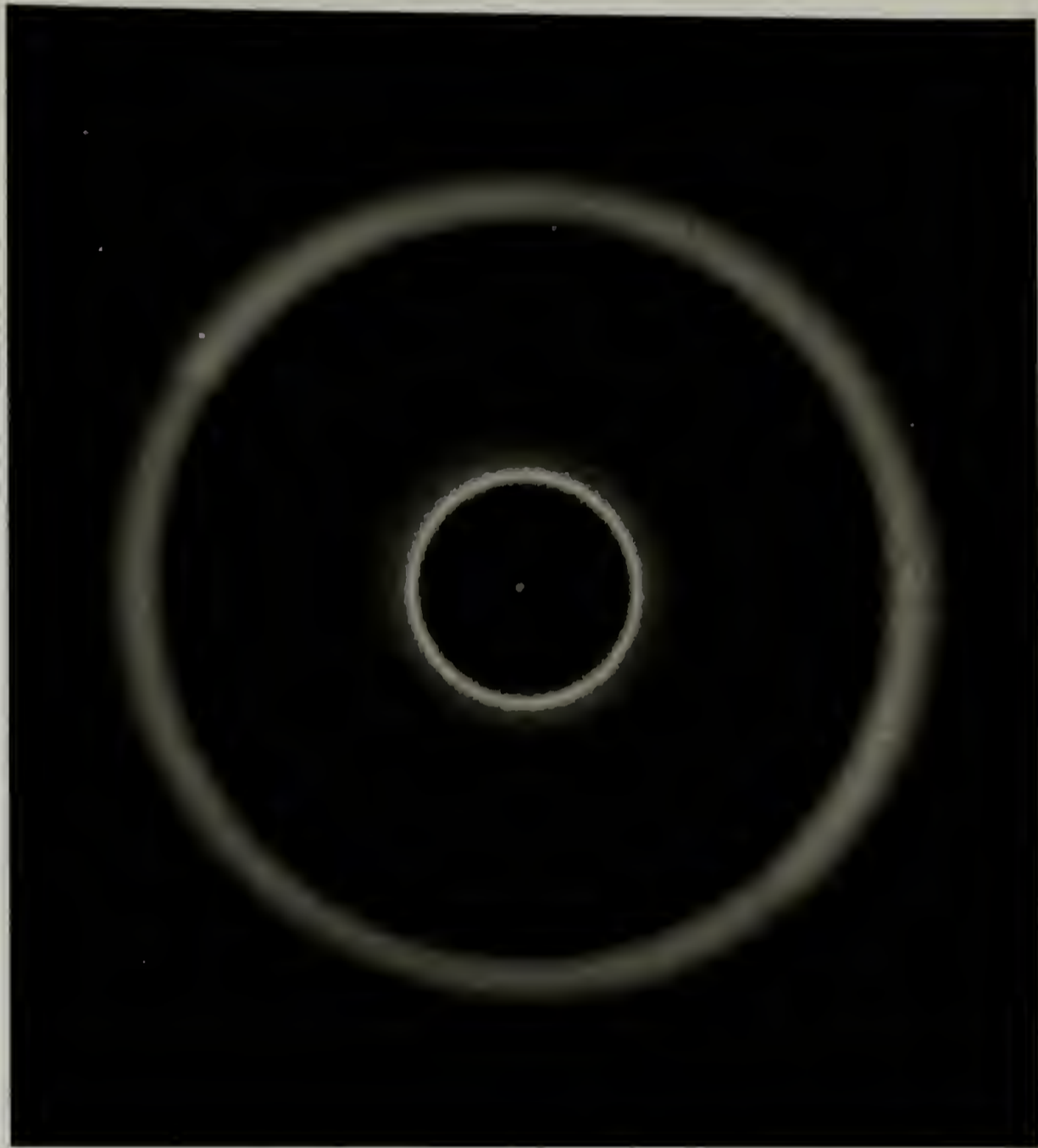


Figure 4.3. WAXS diffraction pattern of B60, heated to 220 °C and cooled at 10 °C/min to 23 °C.

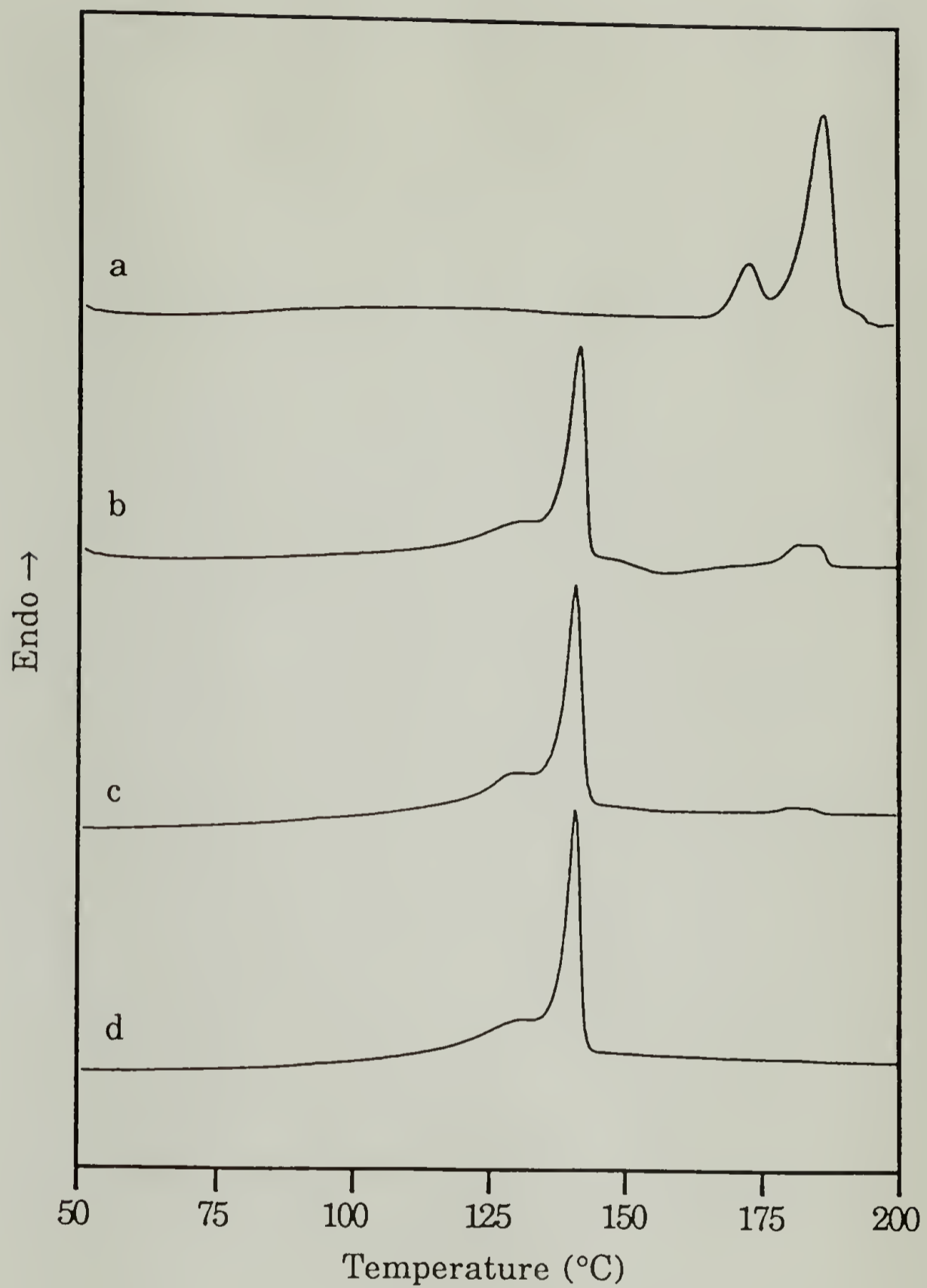
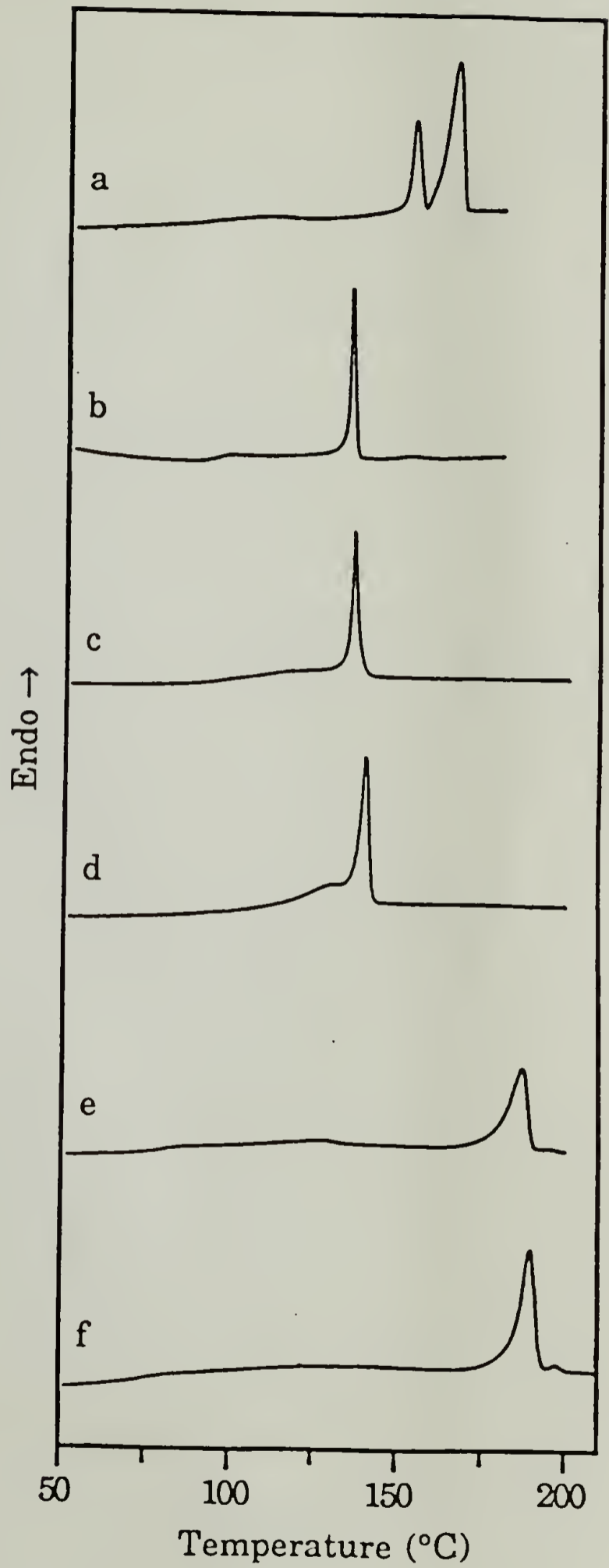


Figure 4.4. DSC scans of B40, heated and cooled repeatedly between 40 °C and 200 °C at 10 °C/min: a) first heating after precipitation from solution; b) second heating; c) fourth heating; d) eighth heating.

Figure 4.5. DSC heating scans (10 °C/min) of blends of D6T24 and D6T26: a) pure D6T24; b) B80; c) B60; d) B40; e) B20; f) pure D6T26.



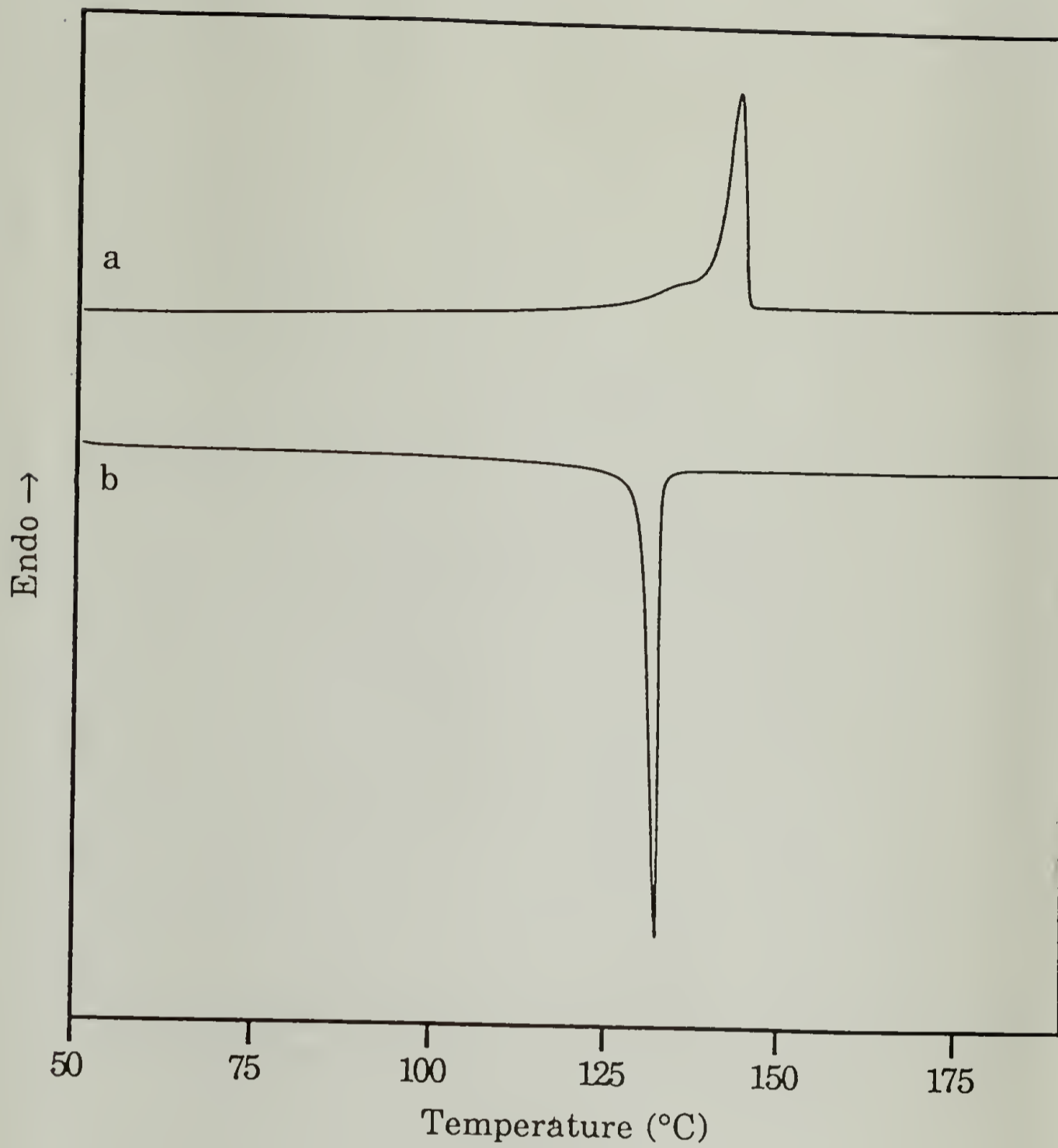


Figure 4.6. DSC scans (10 °C/min) of C47 after cooling at 10 °C/min from the isotropic melt: a) heating; b) cooling.

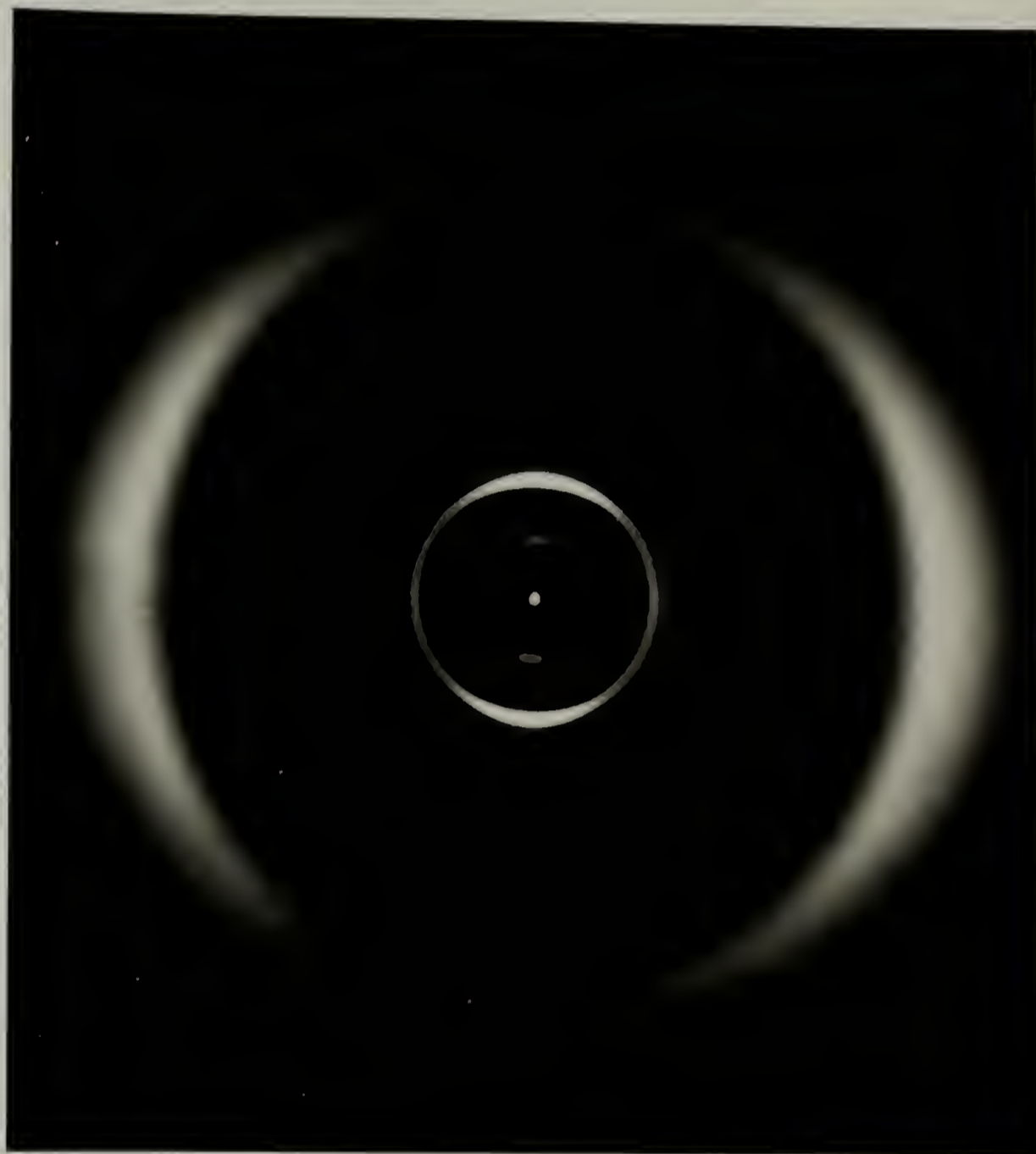


Figure 4.7. WAXS diffraction pattern (23 °C) of a melt-drawn fiber of C47, before thermal treatment.

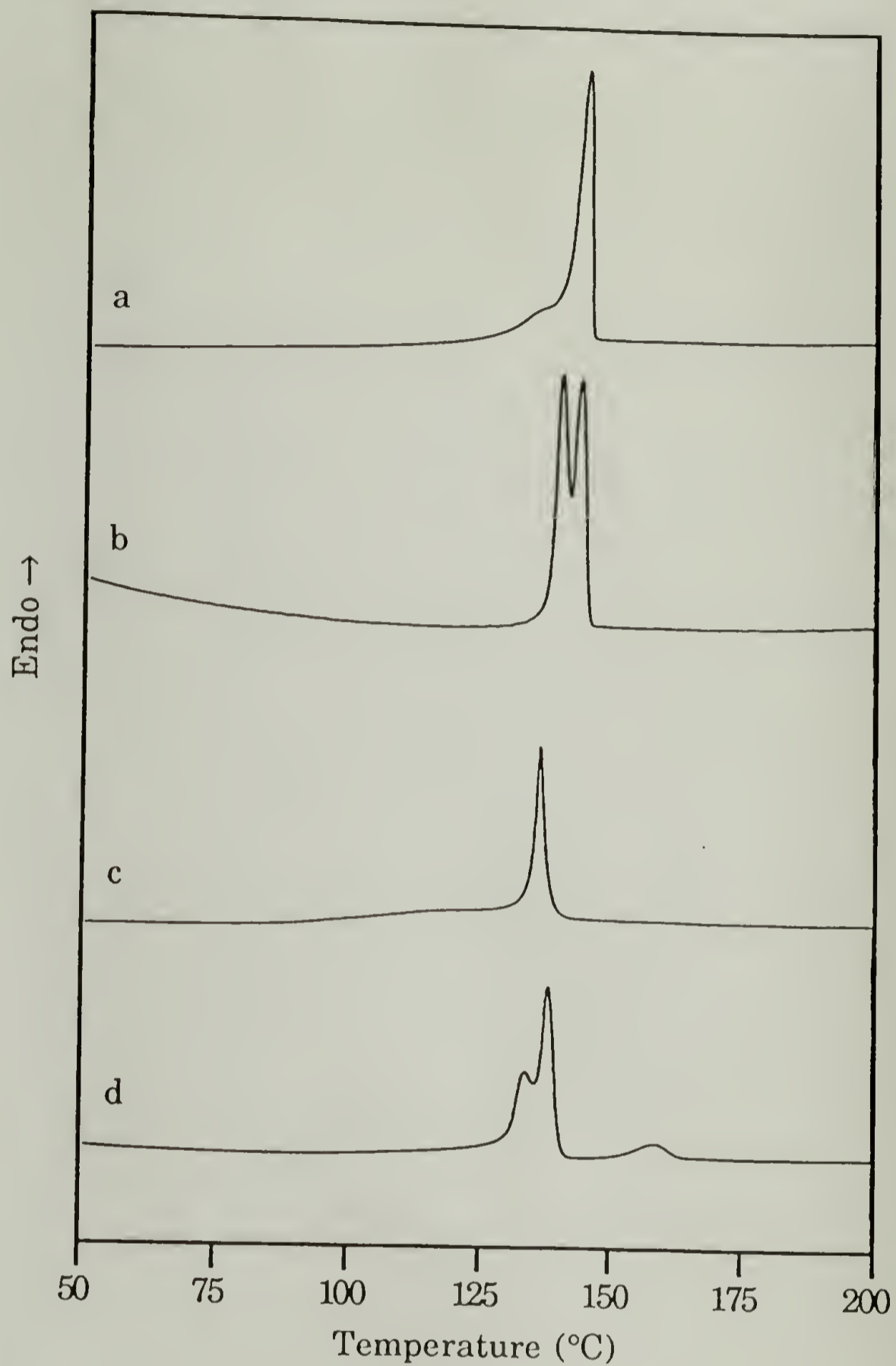


Figure 4.8. DSC heating scans (10 °C/min) of: a) C47, cooled from the isotropic melt at 10 °C/min; b) C47, annealed 6.5 hours at 120 °C; c) B60, cooled from the isotropic melt at 10 °C/min; d) B60, annealed 6.5 hours at 120 °C.



Figure 4.9. WAXS diffraction pattern (23 °C) of a melt-drawn fiber of C47 after annealing for 6.5 hours at 120 °C.

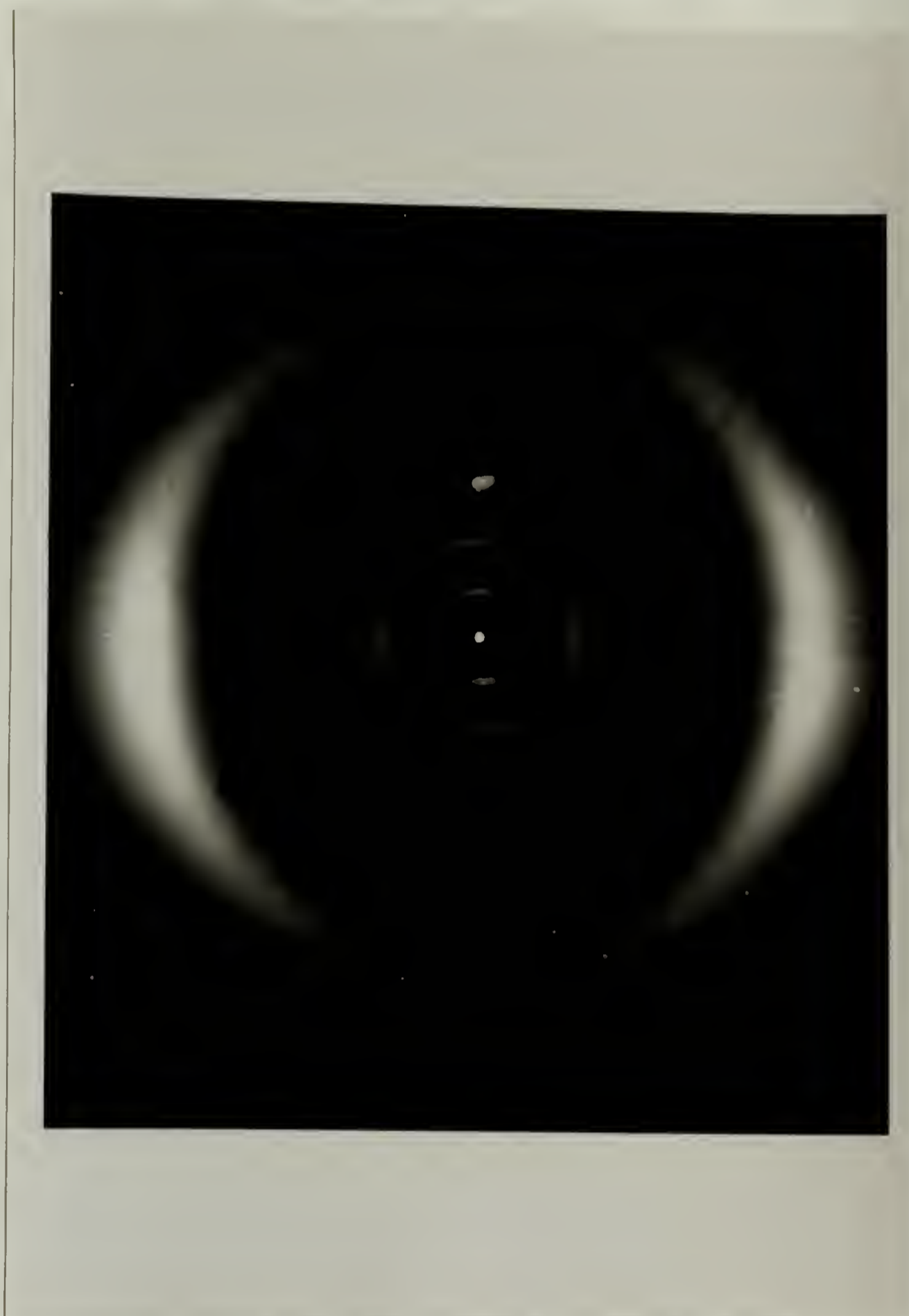


Figure 4.10. WAXS diffraction pattern (23 °C) of a melt-drawn fiber of B60, before thermal treatment.

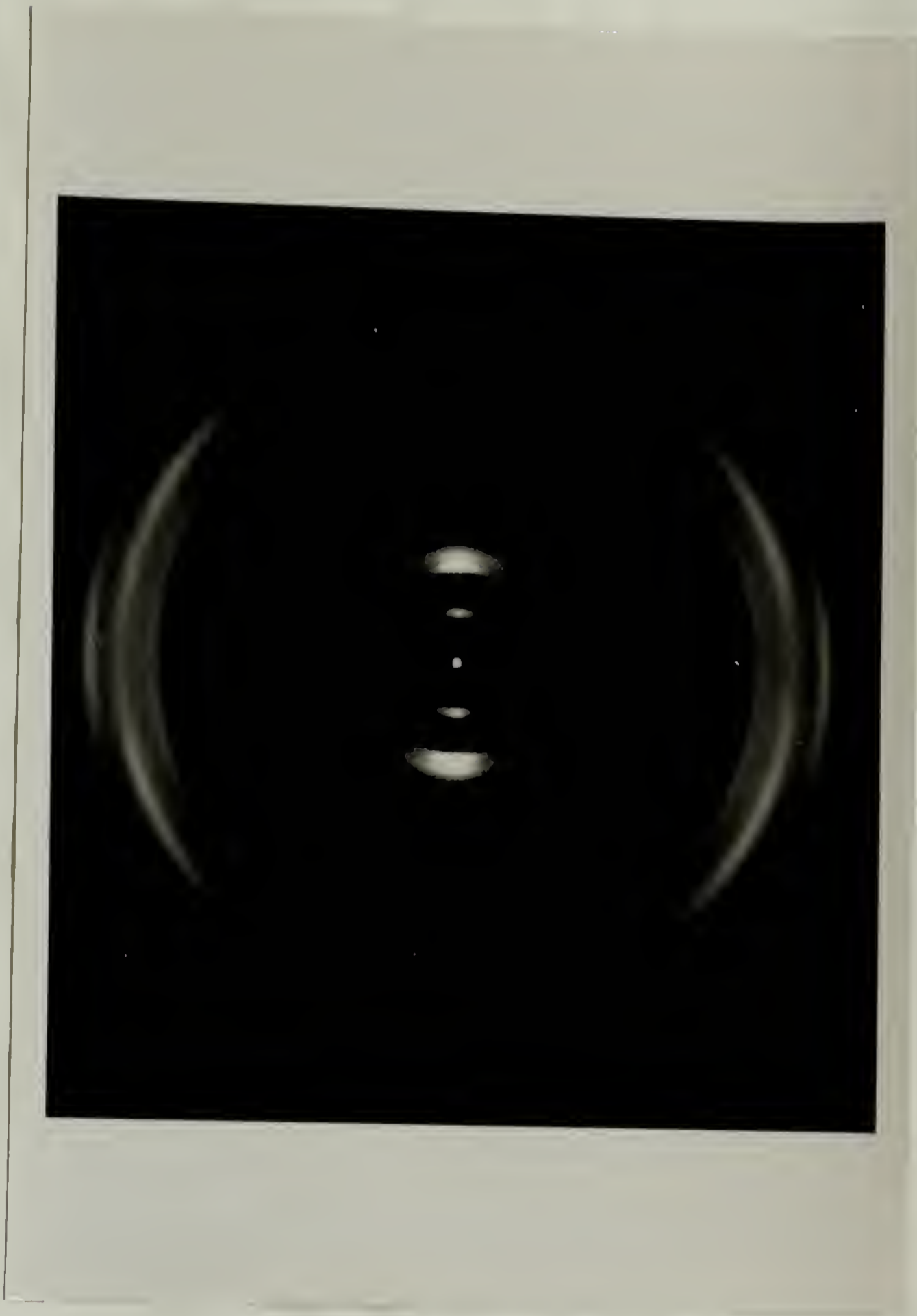


Figure 4.11. WAXS diffraction pattern (23 °C) of a melt-drawn fiber of B60 after annealing for 6.5 hours at 120 °C.

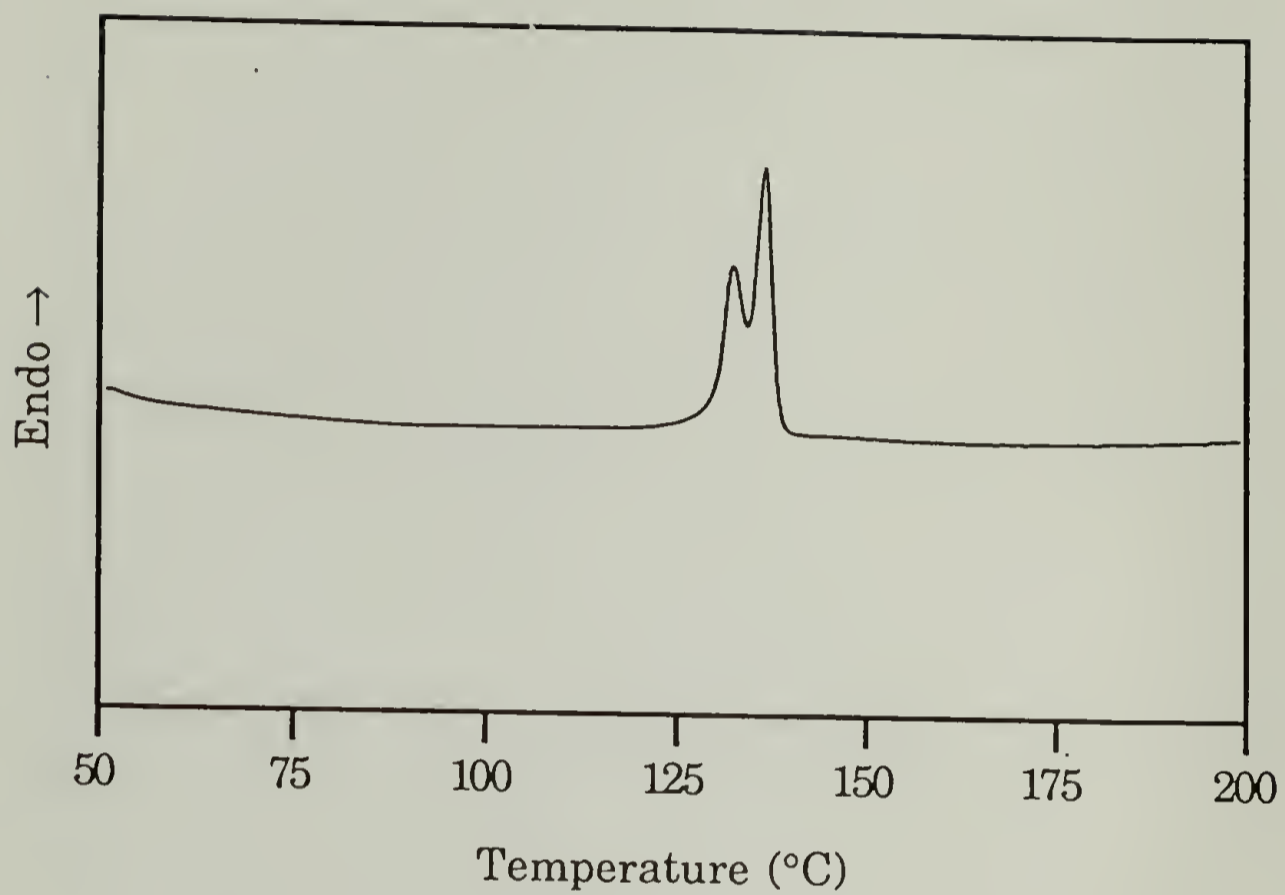


Figure 4.12. DSC heating scan (10 °C/min) of B60 after annealing for 8 h at 180 °C followed by 6.5 h at 120 °C.

References

- (1) Percec, V., Tomazos, D., Pugh, C. *Macromolecules* **1989**, 22, 3259.
- (2) Zhou, Q.-F., Jin, J.-I., Lenz, R. W. *Can. J. Chem.* **1985**, 63, 181.
- (3) Blumstein, R. B., Stickles, E. M. *Mol. Cryst. Liq. Cryst.* **1982**, 82, 151.
- (4) Blumstein, R. B., Stickles, E. M., Blumstein, A. *Mol. Cryst. Liq. Cryst.* **1982**, 82, 205.
- (5) Blumstein, R. B., Stickles, E. M., Gauthier, M. M., Blumstein, A., Volino, F. *Macromolecules* **1984**, 17, 177.
- (6) Zhou, Q. F., Duan, X. L., Liu, Y. L. *Macromolecules* **1986**, 19, 247.
- (7) Roviello, A., Sirigu, A. *Makromol. Chem.* **1982**, 183, 409.

CHAPTER 5

CONCLUSIONS AND FUTURE WORK

The crystalline and liquid-crystalline phases of two mesogen-containing polyurethanes have been studied. The asymmetric polyurethane D6T24 displays a monotropic smectic mesophase. D6T24 may crystallize either from the mesophase or from the isotropic melt; the two crystal forms have the same unit cell but differ in their long-range ordering and in their response to thermal treatment. Molecular weight plays an important role in the kinetics of crystallization and mesophase separation. Crystallization from the melt occurs faster in low molecular weight D6T24, but crystallization from the mesophase occurs faster in high molecular weight D6T24. Crystals formed from the mesophase are more amenable to perfection by annealing and slow heating. The symmetrical polyurethane D6T26 also displays a monotropic smectic mesophase. The crystalline melting temperature of D6T26 is approximately 40 °C higher than that of D6T24, owing to the more-regular structure of the former. The crystalline unit cells of D6T24 and D6T26 are significantly different.

Blending and copolymerizing D6T24 and D6T26 can prevent crystallization, resulting in enantiotropic systems. Blends of D6T24 and D6T26 with D6T24 weight fractions between 30% and 90% display enantiotropic smectic phases which do not crystallize. The same is true of a random copolymer containing 47% D6T24 units and 53% D6T26 units. Annealing the copolymer in the smectic phase at 120 °C leads to an increase in the ordering within the smectic layers. Annealing a

blend of 60% D6T24 and 40% D6T26 produces a similar result, but is accompanied by the crystallization of a small amount of pure D6T24. This indicates that thermal treatment may induce phase separation in the blends. However, when the same blend is annealed for 8 hours at 180 °C before it is annealed at 120 °C, the increase in the smectic ordering is not accompanied by phase separation. This suggests that the high-temperature annealing induces transurethanification reactions which transform the blends into copolymers.

All of the liquid-crystalline phases that have been reported in this work are smectic. One of the most useful properties of liquid-crystalline polymers is low viscosity in the mesophase, which occurs in nematic phases but not in smectic phases. Therefore, it may be advantageous to modify the D6T24/D6T26 system to change the mesophase from smectic to nematic. The key to such a modification is to prevent the arrangement of the mesogenic units into layers. This may be achieved by using two different flexible spacer lengths, or two different mesogens.

Segmented polyurethanes may be obtained by combining D6T24/D6T26 with hydroxy-terminated soft segments. If mesophase-like ordering can be made to exist in the hard domains, these polyurethanes may exhibit unusual properties. No examples of segmented polyurethanes with liquid-crystalline hard segments have yet been reported.

BIBLIOGRAPHY

- Alderman, N. J., Mackley, M. R. *Faraday Discuss. Chem. Soc.* **1985**, *79*, 149.
- Arnold, H. Z. *Phys. Chem. (Leipzig)* **1964**, *226*, 146.
- Asrar, J., Toriumi, H., Watanabe, J., Krigbaum, W. R., Ciferri, A., Preston, J. J. *J. Polym. Sci., Polym. Phys. Ed.* **1983**, *21*, 1119.
- Avrami, M. J. *J. Chem. Phys.* **1939**, *7*, 1103.
- Avrami, M. J. *J. Chem. Phys.* **1941**, *9*, 177.
- Avrami, M. J. *J. Chem. Phys.* **1941**, *8*, 212.
- Azaroff, L. V. *Mol. Cryst. Liq. Cryst.* **1980**, *60*, 73.
- Azaroff, L. V. *Proc. Natl. Acad. Sci. U.S.A.* **1980**, *77*, 1252.
- Azaroff, L. V. *Mol. Cryst. Liq. Cryst.* **1987**, *145*, 31.
- Azaroff, L. V., Schuman, C. A. *Mol. Cryst. Liq. Cryst.* **1985**, *122*, 309.
- Ballauff, M. *Angew. Chem.* **1988**, *100*, 775.
- Barrall, E. M. In *Liquid Crystals: The Fourth State of Matter*; F. D. Saeva, Ed.; Marcel Dekker: New York, 1979.
- Barrall II, E. M., Johnson, J. F., Porter, R. S. In *Thermal Analysis*; R. F. Schwenker Jr. and P. D. Gain, Ed.; Academic Press: New York, 1969; Vol. 1; pp 555.
- Bassett, D. C. *Principles of Polymer Morphology*; Cambridge University Press: Cambridge, 1981.
- Bawden, F. C., Pirie, N. W. *Proc. R. Soc. London, Ser. B* **1937**, *123*, 274.
- Bechtoldt, H., Wendorff, J. H., Zimmerman, H. J. *Makromol. Chem.* **1987**, *188*, 651.
- Berry, G. C., Cotts, P. M., Chu, S.-G. *Br. Polym. J.* **1981**, *13*, 47.
- Bhattacharya, S. K., Lenz, R. W. Submitted for publication.
- Bickel, A., Shaw, M. T., Samulski, E. T. *J. Rheol. (N.Y.)* **1984**, *28*, 647.

- Biswas, A., Blackwell, J. *Macromolecules* **1988**, *21*, 3146.
- Biswas, A., Blackwell, J. *Macromolecules* **1988**, *21*, 3152.
- Biswas, A., Blackwell, J. *Macromolecules* **1988**, *21*, 3158.
- Blackwell, J., Biswas, A., Gutierrez, G. A., Chivers, R. A. *Faraday Discuss. Chem. Soc.* **1985**, *79*, 73.
- Blackwell, J., Gutierrez, G. A., Chivers, R. A. *Macromolecules* **1984**, *17*, 1219.
- Blumstein, A., Sivaramakrishnan, K. N., Clough, S. B., Blumstein, R. B. *Mol. Cryst. Liq. Cryst.* **1979**, *49*, 255.
- Blumstein, A., Thomas, O., Asrar, J., Makris, P., Clough, S. B., Blumstein, R. B. *J. Polym. Sci., Polym. Lett. Ed.* **1984**, *22*, 13.
- Blumstein, A., Vilasagar, S., Ponrathnam, S., Clough, S. B., Blumstein, R. B., Maret, G. *J. Polym. Sci., Polym. Phys. Ed.* **1982**, *20*, 877.
- Blumstein, R. B., Stickles, E. M. *Mol. Cryst. Liq. Cryst.* **1982**, *82*, 151.
- Blumstein, R. B., Stickles, E. M., Blumstein, A. *Mol. Cryst. Liq. Cryst.* **1982**, *82*, 205.
- Blumstein, R. B., Stickles, E. M., Gauthier, M. M., Blumstein, A., Volino, F. *Macromolecules* **1984**, *17*, 177.
- Bormuth, F.-J., Haase, W. *Mol. Cryst. Liq. Cryst.* **1987**, *148*, 1.
- Brunette, C. M., Hsu, S. L., MacKnight, W. J. *Macromolecules* **1982**, *15*, 71.
- Butzbach, G. D., Wendorff, J. H., Zimmermann, H. J. *Polymer* **1986**, *27*, 1337.
- Chandrasekhar, S. *Liquid Crystals*; Cambridge University Press: Cambridge (U.K.), 1977.
- Chandrasekhar, S. *Philos. Trans. R. Soc. London, A* **1983**, *309*, 93.
- Chandrasekhar, S., Sadashiva, B. K., Suresh, K. A. *Pramana* **1977**, *9*, 471.
- Cheng, S. Z. D. *Macromolecules* **1988**, *21*, 2475.

- Cheng, S. Z. D., Wunderlich, B. *Macromolecules* **1988**, *21*, 3327.
- Chistyakov, I. G., Chaikowsky, W. M. *Mol. Cryst. Liq. Cryst.* **1969**, *7*, 269.
- Chivers, R. A., Blackwell, J., Gutierrez, G. A. *Polymer* **1984**, *25*, 435.
- Ciferri, A., Krigbaum, W. R., Meyer, R. B. *Polymer Liquid Crystals*; Academic Press: New York, 1982.
- Cogswell, F. N. *Br. Polym. J.* **1980**, *12*, 170.
- Costa, G., Nora, A., Trefiletti, V., Valenti, B. *Mol. Cryst. Liq. Cryst.* **1988**, *157*, 79.
- Davis, G. J., Porter, R. S. *Mol. Cryst. Liq. Cryst.* **1970**, *6*, 377.
- de Gennes, P. C. *R. Acad. Sci. Paris, Ser. B* **1975**, *281*, 101.
- de Gennes, P. G. *The Physics of Liquid Crystals*; Clarendon Press: Oxford (U.K.), 1974.
- de Vries, A. *Mol. Cryst. Liq. Cryst.* **1970**, *10*, 219.
- de Vries, A. *J. Chem. Phys.* **1972**, *56*, 4489.
- de Vries, A. *Mol. Cryst. Liq. Cryst.* **1985**, *131*, 125.
- Demus, D., Diele, S., Klapperstück, M., Link, V., Zschke, H. *Mol. Cryst. Liq. Cryst.* **1971**, *15*, 161.
- Demus, D., Richter, L. *Textures of Liquid Crystals*; Verlag Chemie: Weinheim, 1978.
- Destrade, C., Foucher, P., Gasparoux, H., Tinh, N. H. *Mol. Cryst. Liq. Cryst.* **1984**, *106*, 121.
- Elliot, A., Ambrose, E. J. *Faraday Discuss. Chem. Soc.* **1950**, *9*, 246.
- Ennulat, R. D. In *Analytical Calorimetry*; R. S. Porter and J. F. Johnson, Ed.; Plenum Press: New York, 1968; pp 219.
- Ennulat, R. D. *Mol. Cryst. Liq. Cryst.* **1969**, *8*, 247.
- Fatou, J. G. *Makromol. Chem. Suppl.* **1984**, *7*, 131.

- Feijoo, J. L., Ungar, G., Owen, A. J., Keller, A., Percec, V. *Mol. Cryst. Liq. Cryst.* **1988**, *155*, 487.
- Finkelmann, H. In *Thermotropic Liquid Crystals*; G. W. Gray, Ed.; John Wiley & Sons: Chichester, 1987; pp 145.
- Finkelmann, H., Rehage, G. *Makromol. Chem., Rapid Commun.* **1980**, *1*, 31.
- Flory, P. J. *Proc. R. Soc. (London)* **1956**, *A234*, 73.
- Flory, P. J. *Proc. R. Soc. (London)* **1956**, *A234*, 60.
- Flory, P. J. *Adv. Polym. Sci.* **1984**, *59*, 1.
- Flory, P. J., Abe, A. *Macromolecules* **1978**, *11*, 1119.
- Freidel, E. *C. R. Acad. Sci.* **1925**, *180*, 269.
- Frosini, V., de Petris, S., Chiellini, E., Galli, G., Lenz, R. W. *Mol. Cryst. Liq. Cryst.* **1983**, *98*, 223.
- Galli, G., Benedetti, E., Chiellini, E., Ober, C., Lenz, R. W. *Polym. Bull.* **1981**, *5*, 497.
- Ghanem, A. M., Dickinson, L. C., Porter, R. S., Zachariades, A. E. *J. Polym. Sci., Polym. Phys. Ed.* **1990**, *28*, 1891.
- Gray, G. W. In *Liquid Crystals and Ordered Fluids*; J. F. Johnson and R. S. Porter, Ed.; Plenum: 1974; Vol. 2; pp 617.
- Grebowicz, J., Wunderlich, B. *J. Polym. Sci., Polym. Phys. Ed.* **1983**, *21*, 141.
- Griffin, A. C., Havens, S. J. *Mol. Cryst. Liq. Cryst.* **1979**, *49*, 239.
- Griffin, A. C., Havens, S. J. *J. Polym. Sci., Polym. Phys. Ed.* **1981**, *19*, 951.
- Gutierrez, G. A., Chivers, R. A., Blackwell, J., Stamatoff, J. B., Yoon, H. *Polymer* **1983**, *24*, 937.
- Hartshorne, N. H. *The Microscopy of Liquid Crystals*; Microscope Publications Ltd.: London, 1974.
- Hemsley, D. A. *The Light Microscopy of Synthetic Polymers*; Oxford University Press: New York, 1984.

- Hessel, F., Finkelmann, H. *Polym. Bull.* **1986**, *15*, 349.
- Hessel, F., Herr, R.-P., Finkelmann, H. *Makromol. Chem.* **1987**, *188*, 1597.
- Hoffman, J. D., Weeks, J. J. *J. Res. Natl. Bur. Stand.* **1962**, *66A*, 13.
- Holdsworth, P. J., Turner-Jones, A. *Polymer* **1971**, *12*, 195.
- Hong, S. K., Blackwell, J. *Polymer* **1989**, *30*, 225.
- Hughes, A. J., Daley, R. *Mol. Cryst. Liq. Cryst.* **1987**, *148*, 163.
- Iannelli, P., Roviello, A., Sirigu, A. *Eur. Polym. J.* **1982**, *18*, 745.
- Iannelli, P., Roviello, A., Sirigu, A. *Eur. Polym. J.* **1982**, *18*, 753.
- Iimura, K., Koide, N., Tanabe, H., Takeda, M. *Makromol. Chem.* **1981**, *182*, 2569.
- Iizuka, E., Inoue, S., Hanabusa, K., Shirai, H. *Mol. Cryst. Liq. Cryst.* **1987**, *149*, 61.
- Jackson, W. J., Jr., Kuhfuss, H. F. *J. Polym. Sci., Polym. Chem. Ed.* **1976**, *14*, 2043.
- Jadhav, J. Y., Kantor, S. W. Submitted for publication.
- Jerman, R. E. *J. Rheol. (N.Y.)* **1981**, *25*, 275.
- Jungbauer, D., Wendorff, J. H. *Mol. Cryst. Liq. Cryst.* **1989**, *170*, 159.
- Keller, P. *Macromolecules* **1984**, *17*, 2937.
- Koide, N. *Mol. Cryst. Liq. Cryst.* **1986**, *139*, 47.
- Kricheldorf, H. R., Awe, J. *Makromol. Chem., Rapid Commun.* **1988**, *9*, 681.
- Kricheldorf, H. R., Awe, J. *Makromol. Chem.* **1989**, *190*, 2579.
- Kricheldorf, H. R., Awe, J. *Makromol. Chem.* **1989**, *190*, 2597.
- Krigbaum, W. R., Asrar, J., Toriumi, H., Ciferri, A., Preston, J. J. *Polym. Sci., Polym. Lett. Ed.* **1982**, *20*, 109.
- Lawson, K. D., Flautt, T. J. *J. Am. Chem. Soc.* **1967**, *89*, 5489.

- Leadbetter, A. J. In *Thermotropic Liquid Crystals*; G. W. Gray, Ed.; John Wiley and Sons: Chichester, 1987; pp 1.
- Leadbetter, A. J., Norris, E. K. *Mol. Phys.* **1979**, *38*, 669.
- Leclerc, M., Billard, J., Jacques, J. *Compt. Rend.* **1967**, *264*, 1789.
- Lei, L. *Mol. Cryst. Liq. Cryst.* **1987**, *146*, 41.
- Lemmon, T. J., Hanna, S., Windle, A. H. *Polym. Commun.* **1989**, *30*, 2.
- Leung, K. M., Lei, L. *Mol. Cryst. Liq. Cryst.* **1987**, *146*, 71.
- Levelut, A. M. *J. Chim. Phys.* **1983**, *80*, 149.
- Levelut, A. M., Malthete, J., Collet, A. *J. Phys. (Paris)* **1986**, *47*, 351.
- Lin, Y. G., Winter, H. H. *Macromolecules* **1988**, *21*, 2439.
- Liu, X., Hu, S., Shi, L., Xu, M., Zhou, Q., Duan, X. *Polymer* **1989**, *30*, 273.
- Mackley, M. R., Pinaud, F., Siekmann, G. *Polymer* **1981**, *22*, 437.
- MacKnight, W. J., Yang, M. *J. Polym. Sci., Polym. Symp.* **1973**, *42*, 817.
- Magill, J. H. *Polym. Lett.* **1968**, *6*, 853.
- Majnusz, J., Catala, J. M., Lenz, R. W. *Eur. Polym. J.* **1983**, *10/11*, 1043.
- Malthete, J., Collet, A. *Nouv. J. de Chemie* **1985**, *9*, 151.
- Mandelkern, L. *Crystallization in Polymers*; McGraw-Hill: New York, 1964.
- Maret, G., Blumstein, A. *Mol. Cryst. Liq. Cryst.* **1982**, *88*, 295.
- Martins, A. F., Ferriera, J. B., Volino, F., Blumstein, A., Blumstein, R. *B. Macromolecules* **1983**, *16*, 279.
- McMillan, W. L. *Phys. Rev.* **1972**, *A6*, 936.
- Menczel, J., Wunderlich, B. *Polymer* **1981**, *22*, 778.
- Merret, W. G., Cole, G. D., Walker, W. W. *Mol. Cryst. Liq. Cryst.* **1971**, *15*, 105.

- Meurisse, P., Noel, C., Monnerie, L., Fayolle, B. *Br. Polym. J.* **1981**, *13*, 55.
- Morgan, P. W. *Macromolecules* **1977**, *10*, 1381.
- Mormann, W. *Polym. Prepr.* **1989**, *30(1)*, 291.
- Mormann, W., Baharifar, A. *Polym. Bull.* **1990**, *24*, 413.
- Mormann, W., Brahm, M. *Makromol. Chem.* **1989**, *190*, 631.
- Mormann, W., Brahm, M. *Macromolecules* **1991**, *24*, 1096.
- Mueller, K., Hisgen, B., Ringsdorf, H., Lenz, R. W., Kothe, G. In ; L. Chapoy, Ed.; Elsevier: London, 1984.
- Noel, C. In *Recent Advances in Liquid Crystalline Polymers*; L. L. Chapoy, Ed.; Elsevier Applied Science Publishers: New York, 1985.
- Noel, C., Friedrich, C., Bosio, L., Strazielle, C. *Polymer* **1984**, *25*, 1281.
- Noel, C., Laupretre, F., Friedrich, C., Fayolle, B., Bosio, L. *Polymer* **1984**, *25*, 808.
- Ober, C., Jin, J.-I., Lenz, R. W. *Polym. J.* **1982**, *14*, 9.
- Ober, C., Lenz, R. W., Galli, G., Chiellini, E. *Macromolecules* **1983**, *16*, 1034.
- Panar, M., Beste, L. F. *Macromolecules* **1977**, *10*, 1401.
- Papadimitrakopoulos, F., Hsu, S. L., MacKnight, W. J. Submitted for publication.
- Papadimitrakopoulos, F., Stenhouse, P. J., MacKnight, W. J. to be submitted.
- Papkov, V. S., Svistunov, V. S., Godovsky, Y. K., Zhdanov, A. A. *J. Polym. Sci., Polym. Phys. Ed.* **1987**, *25*, 1859.
- Percec, V., Tomazos, D., Pugh, C. *Macromolecules* **1989**, *22*, 3259.
- Percec, V., Yourd, R. *Macromolecules* **1989**, *22*, 3229.
- Percec, V., Yourd, R. *Macromolecules* **1989**, *22*, 524.

- Pollack, S. K., Shen, D. Y., Wang, Q., Stidham, H. D., Hsu, S. L. *Macromolecules* **1989**, *22*, 551.
- Pollack, S. K., Smyth, G., Hsu, S. L., MacKnight, W. J. *Macromolecules* Submitted for publication.
- Porter, R. S., Johnson, J. F. In *Rheology*; F. R. Eirich, Ed.; Academic Press: New York, 1967.
- Prasadarao, M., Pearce, E. M., Han, C. D. *J. Appl. Polym. Sci.* **1982**, *27*, 1343.
- Reck, B., Ringsdorf, H. *Makromol. Chem., Rapid Commun.* **1985**, *6*, 691.
- Reck, B., Ringsdorf, H. *Makromol. Chem., Rapid Commun.* **1985**, *6*, 291.
- Reck, B., Ringsdorf, H. *Makromol. Chem., Rapid Commun.* **1987**, *7*, 389.
- Reddy, C. R., Rao, K. K., Jin, J.-I., Lenz, R. W. *J. Polym. Sci., Polym. Chem. Ed.* **1990**, *28*, 2269.
- Reitnitzer, F. *Monatsh. Chem.* **1888**, *9*, 421.
- Ringsdorf, H., Portugal, M., Happ, M., Finkelmann, H. *Makromol. Chem.* **1978**, *179*, 2541.
- Ringsdorf, H., Schneller, A. *Br. Polym. J.* **1981**, *13*, 43.
- Robinson, C. *Trans. Faraday Soc.* **1956**, *52*, 571.
- Robinson, C., Ward, J. C., Beevers, R. B. *Discuss. Faraday Soc.* **1958**, *25*, 29.
- Roviello, A., Sirigu, A. *J. Polym. Sci., Polym. Lett. Ed.* **1975**, *13*, 455.
- Roviello, A., Sirigu, A. *Eur. Polym. J.* **1979**, *15*, 61.
- Roviello, A., Sirigu, A. *Makromol. Chem.* **1982**, *183*, 409.
- Sagane, T., Lenz, R. W. *Macromolecules* **1989**, *22*, 3763.
- Sartirana, M. L., Marsano, E., Bianchi, E., Ciferri, A. *Macromolecules* **1986**, *19*, 1176.
- Sato, M., Jadhav, J. Y., Mallon, J. J., Kantor, S. W. Submitted for publication.

- Sato, M., Nakatsuchi, K., Ohkatsu, Y. *Makromol. Chem., Rapid Commun.* **1986**, 7, 231.
- Seurin, M. J., Gilli, J. M., Ten Bosch, A., Sixou, P. *Polymer* **1984**, 25, 1073.
- Shaffer, T. D., Jamaludin, M., Percec, V. *J. Polym. Sci., Polym. Chem. Ed.* **1985**, 23, 2913.
- Shaffer, T. D., Percec, V. *J. Polym. Sci., Polym. Lett. Ed.* **1985**, 23, 185.
- Shaffer, T. D., Percec, V. *Makromol. Chem.* **1986**, 187, 111.
- Shen, D. Y., Pollack, S. K., Hsu, S. L. *Macromolecules* **1989**, 22, 2565.
- Shibaev, V. P., Platé, N. A., Smolyansky, A. L., Voloskov, A. Y. *Makromol. Chem.* **1980**, 181, 1393.
- Shilov, V. V., Tsukruk, V. V., Lipatov, Y. S. *J. Polym. Sci., Polym. Phys. Ed.* **1984**, 22, 41.
- Small, D. M., Bourgis, M. *Mol. Cryst.* **1966**, 1, 541.
- Smyth, G., Grebowicz, J., Stenhouse, P. J., MacKnight, W. J., Kantor, S. W. *Proceedings of the Seventeenth North American Thermal Analysis Society Conference*; C. M. Earnest, Ed.; 1988, Vol. II, p 424.
- Smyth, G., Pollack, S. K., MacKnight, W. J., Hsu, S. L. *Liq. Cryst.* **1990**, 7, 839.
- Smyth, G., Vallés, E. M., Pollack, S. K., Grebowicz, J., Stenhouse, P. J., Hsu, S. L., MacKnight, W. J. *Macromolecules* **1990**, 23, 3389.
- Sorai, M., Suga, H. *Mol. Cryst. Liq. Cryst.* **1981**, 73, 47.
- Sorai, M., Tsuji, K., Suga, H., Seki, S. *Mol. Cryst. Liq. Cryst.* **1980**, 80, 33.
- Sorai, M., Yoshioka, H., Suga, H. *Mol. Cryst. Liq. Cryst.* **1982**, 84, 39.
- Stenhouse, P. J., MacKnight, W. J., Kantor, S. W. *Bulletin of the American Physical Society*; 1990, Vol. 35(3), p 653.
- Stenhouse, P. J., Vallés, E. M., Kantor, S. W., MacKnight, W. J. *Macromolecules* **1989**, 22, 1467.

- Sugiyama, H., Lewis, D. N., White, J. L., Fellers, J. F. *J. Appl. Polym. Sci.* **1985**, *30*, 2329.
- Sun, T., Bhattacharya, S. K., Lenz, R. W., Porter, R. S. *J. Polym. Sci., Polym. Phys. Ed.* **1990**, *28*, 1677.
- Tanaka, M., Nakaya, T. *Makromol. Chem.* **1984**, *185*, 1915.
- Tanaka, M., Nakaya, T. *Kobunshi Ronbunshu* **1986**, *43*, 311.
- Tanaka, M., Nakaya, T. *J. Macromol. Sci., Chem.* **1987**, *A24*, 777.
- Tanaka, M., Nakaya, T. *Makromol. Chem.* **1988**, *189*, 771.
- Taylor, T. R., Arora, S. L., Ferguson, J. L. *Phys. Rev. Lett.* **1970**, *25*, 722.
- Tinh, N. H., Foucher, P., Destrade, C., Levelut, A. M., Malthete, J. *Mol. Cryst. Liq. Cryst.* **1984**, *111*, 277.
- Tipton, A. J. Ph.D. Thesis, University of Massachusetts, 1988.
- Van Luyen, D., Strzelecki, L. *Eur. Polym. J.* **1980**, *16*, 303.
- Varshney, S. K. *JMS-Rev. Macromol. Chem. Phys.* **1986**, *C26*, 551.
- Viney, C., Mitchell, G. R., Windle, A. H. *Mol. Cryst. Liq. Cryst.* **1985**, *129*, 75.
- Viney, C., Windle, A. H. *J. Mater. Sci.* **1982**, *17*, 2661.
- Vogel, M. J., Barrall II, E. M., Mignosa, C. P. *Mol. Cryst. Liq. Cryst.* **1971**, *15*, 49.
- Vorländer, D. *Z. Phys. Chem.* **1927**, *A126*, 449.
- Warner, S. B., Jaffe, M. *J. Cryst. Growth* **1980**, *48*, 184.
- Wendorff, J. H., Frick, G., Zimmerman, H. *Mol. Cryst. Liq. Cryst.* **1988**, *157*, 455.
- Windle, A. H., Viney, C., Golombok, R., Donald, A. M., Mitchell, G. R. *Faraday Discuss. Chem. Soc.* **1985**, *79*, 55.
- Wissbrun, K. F. *Br. Polym. J.* **1980**, *12*, 163.
- Wissbrun, K. F. *J. Rheol. (N.Y.)* **1981**, *25*, 619.

- Wissbrun, K. F., Griffin, A. C. *J. Polym. Sci., Polym. Phys. Ed.* **1982**, *20*, 1835.
- Wong, C. P., Ohnuma, H., Berry, G. C. *J. Polym. Sci., Polym. Symp.* **1978**, *65*, 173.
- Wunderlich, B. *Macromolecular Physics*; Academic Press: New York, 1973; Vol. 1.
- Wunderlich, B. *Macromolecular Physics*; Academic Press: New York, 1976; Vol. 2.
- Wunderlich, B. *Macromolecular Physics*; Academic Press: New York, 1980; Vol. 3.
- Wunderlich, B., Grebowicz, J. *Adv. Polym. Sci.* **1984**, *60/61*, 1.
- Yoo, Y. D., Kim, S. C. *Polym. J.* **1988**, *20*, 1117.
- Zhou, Q.-F., Jin, J.-I., Lenz, R. W. *Can. J. Chem.* **1985**, *63*, 181.
- Zhou, Q.-F., Lenz, R. W. *J. Polym. Sci., Polym. Chem. Ed.* **1983**, *21*, 3313.
- Zhou, Q. F., Duan, X. L., Liu, Y. L. *Macromolecules* **1986**, *19*, 247.
- Zimmermann, H., Poupko, R., Luz, Z., Billard, J. Z. *Naturforsch* **1985**, *40a*, 149.

